Geological Survey of Israel

Ministry of Enrgy

The Elat and Timna areas, southern Israel, as a field school for geology

Michael Beyth and Ran Calvo

Report GSI/11/2022

Jerusalem, June 2022

© Published by the Geological Survey of Israel
32 Yeshayahu Leibowitz St. Jerusalem 9692100, Israel

Cover photo: Block rotation due to bed-parallel, horizontal shear, base Gerofit Fm.

Mt. Hizkyahu. Coord. 188311/395672

Design: Bat Sheva Cohen

Geological Survey of Israel

Ministry of Energy

The Elat and Timna areas, southern Israel, as a field school for geology

Michael Beyth[1] and Ran Calvo[1]

1. Geological Survey of Israel, 32 Yeshayahu Leibowitz, Jerusalem 9371234, Israel

Report GSI/11/2022 Jerusalem, June 2022

Table of contents

Introduction……1

Brief geological background……3

A few examples……6

The Roded and Elat Neoproterozoic blocks……..6

The Amram Block and Amir Syncline……10

The Timna Valley……16

Themed Fault and the Raham Syncline……..20

The Shelomo and Yotam grabens……..23

Elat Sabkha , Avrona Playa and the young recent faults……..28

Conclusion……31

References……31

Appendix I: Location map of figures……..38

II: Location of photos (Excel table) ……39

Supplementary

I: The Geology of the Elat Sheet, Explanatory Notes

II: The Timna Valley as a Geological Park (poster)

Introduction

The stratigraphy and structure of the well-exposed rocks in the extreme arid desert climate of the Elat/Timna area (Fig. 1) document the evolution of three major processes from Neoproterozoic to the Holocene, thus making the geology of this area quite unique. The extensive research done in the Elat and Timna area and it's uniqueness has turned this region into a field laboratory for geoscience students (see references) similarly to the Interuniversity Institute for Marine Sciences in Elat. For many years this area has been used as a field school for students mainly from the Institute of Earth Sciences at the Hebrew University, Jerusalem and the Department of Geology and Environmental Science, Ben Gurion University of the Negev.
This is more so after the publication by the Geological Survey of Israel of the Be'er Ora and Elat sheets geological maps which cover this area (Figs. 2, 3, 4), as part of the 1:50,000 scale geological mapping project of the country and which was based on and have updated previous maps by additional field work. This very detailed mapping was carried out on a 1:10,000 average scale using GIS and orthophotos as the base maps (Beyth et al., 1999a., updated 2021; Beyth et al., 2012 updated 2021) with explanatory notes attached (Beyth et al., 2011 updated 2013; Beyth et al., 2018). In order to make these maps more accessible and easier to disseminate geological concepts and ideas of this area a series of reports (in Hebrew, English abstract) focusing on especially attractive tracks, partly along the Israel National Trail were published. The geological maps, the explanatory notes (supplementary) and the reports (PDF) are available from the library of the Geological Survey of Israel and the web-site www.gsi.gov.il. In addition to the unique geology the area is attractive as geological field school, since necessary logistic are relatively easy with an international airport nearby (Fig. 1) and numerous accommodation facilities.

In this text the abbreviate N. and W. are used for Nahal and Wadi, ephemeral river in Hebrew and Arabic and Mt. for mountain; Fm. for Formation; Mb. for Member; and Coord. for coordinate in the Israel grid, ITM (Appendix). For the detailed stratigraphy and structure the Be'er Ora and Elat sheets are attached (figs. 2, 3 and 4). Names used and available walking trails mapped are from the Field Trips of the Elat Mountains 1:50,000 map, Sheet #20 (in Hebrew) Israel Mapping Center.

Figure 1: General location map.

Brief geological background

The three major geological processes which controlled the geological and geomorphological evolution of the Elat/Timna area are: 1) The creation of the Arabian-Nubian Shield (ANS) during the Neoproterozoic as part of and the East African Orogen during the closing of the Mozambique Ocean between the east and west Gondwana plates (Stern, 1994; Miller and Stern, 2021); 2) Accumulation of the Cambrian to Eocene sedimentary sequence on the Arabian Plate at the southeast margins of the paleo-Tethys and Tethys Seas; 3) The Miocene to Recent evolution of the Dead Sea Transform (DST), a sinistral fault, which is an active plate boundary between the Arabian Plate to the east and the African Plate to the west (Beyth et al., 2017 and references therein).

Consequently that the Elat/Timna area comprises of three major rock sequences: 1) The Neoproterozoic, metamorphic and magmatic basement of the ANS with few Cadomian mafic dykes on its northern edge (Abbo et al., 2020); 2) the sedimentary rocks from Cambrian to Eocene and 3) the young clastic and playa deposits accreted during the evolution of the Dead Sea Transform since the Miocene (see legend Beyth et al., 1999a; Beyth et al., 2012). An Early Cambrian peneplain separates between the first two sequences (Beyth and Heimann, 1999b) and an Oligocene erosion surface between the second and the third sequences (Avni et al., 2012; Avni, 2016).

The structures of the Elat and Be'er Ora Sheets were classified into three types: 1) The ancient metamorphic/magmatic structures, 2) the structures related to the Themed east-west dextral fault system and 3) Younger structures which are related to the Dead Sea Transform and its margins. The ancient structures of Neoproterozoic to early Cambrian age are expressed in the metamorphic fabric or the dyke directions (Katzir et al., 2006 and 2007), which are all parts of the evolution of the East African Orogen and the development of the Arabian-Nubian Shield. This tectonic event was terminated by extension, exhumation and peneplanation (Beyth et al., 2014a and references therein).

The dextral Themed Fault which is part of the Sinai-Negev Shear Zone (Bartov, 1967, 1974) strikes west-northeast and extends from Nahal Shani at the west to Be'er Ora at the Arava at the east. The major activity of this fault was from late Oligocene to early Miocene, 22-27 million years ago (Weinberger et al., 2020).

The young faults, which are the dominant structures in the Elat/Timna area, and controll its geomorphology, were developed as a result of the young tectonic activity associated with the rifting component of the Dead Sea Transform. These structures are the Gulf of Elat/Aqaba, the Elat Sabkha, Avrona Playa and the Yotam and Shelomo grabens. The grabens and the step faulting along the margins of the rift are controlled by north-northeast sinistral faults which also have a vertical component. The sinistral marginal faults begun to be active at the Miocene, 22-~18 million years ago (Nuriel et al., 2017) while the more recent major transform faults along the Arava Valley are the focus of historical and recent earthquakes. The most accurate estimate of the sinistral displacement along the Arava/Araba segment of the Dead Sea Transform at the southern Arava/Aqaba is 109 km (Beyth et al., 2017).

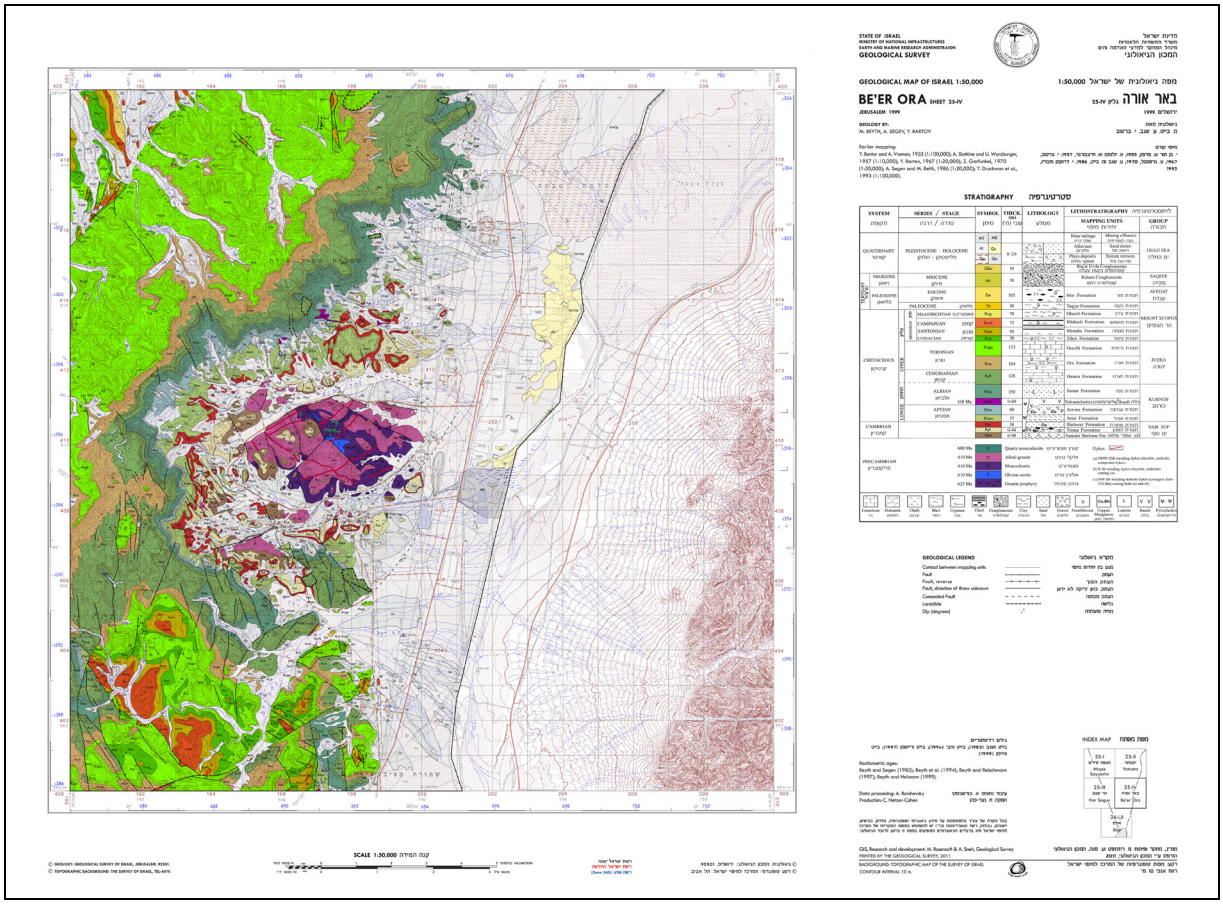

Figure 2: Be'er Ora 1:50,000 geological map.

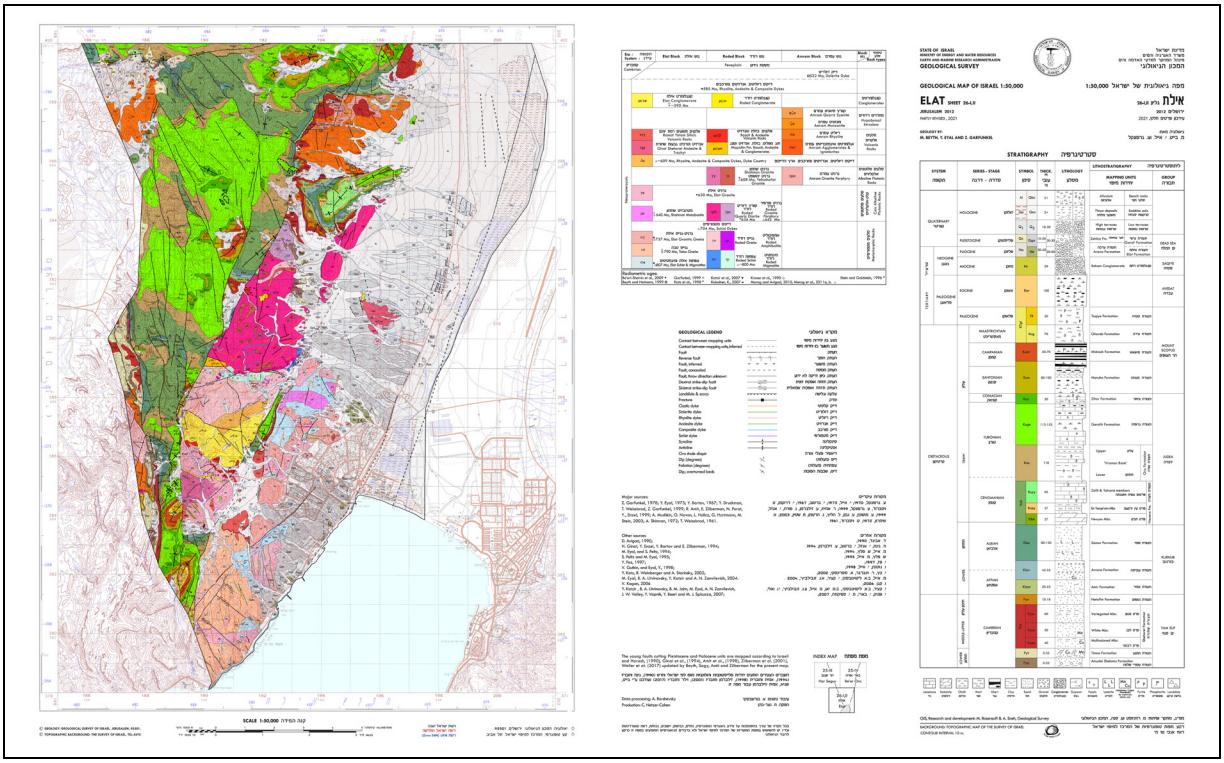

Figure 3: Elat 1:50,000 geological map.

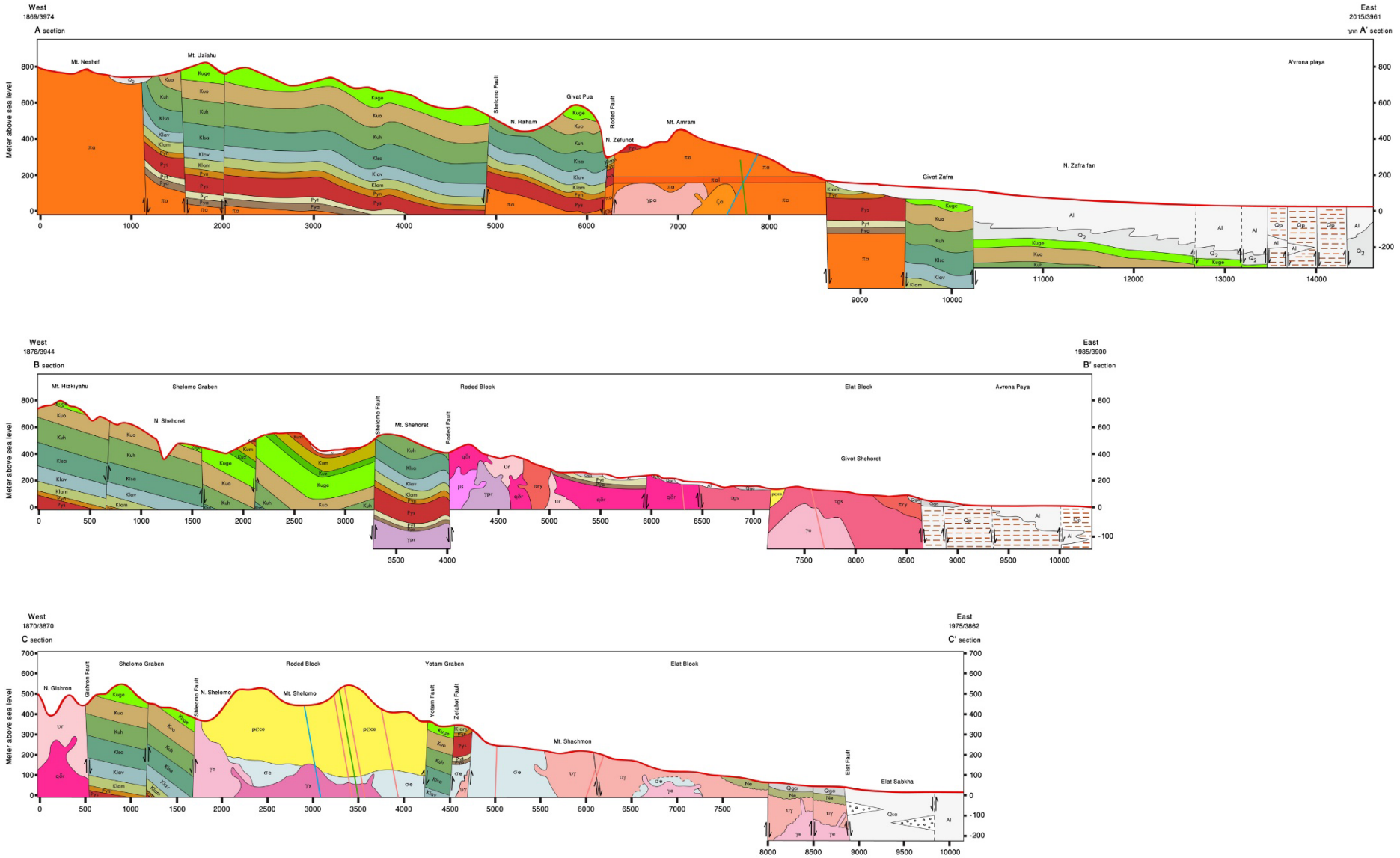

Fig. 4: Geological cross sections, Elat sheet.

A few examples

The idea behind the presentation of six areas with a short text, maps and photos is to show the unique opportunity to study geology in the Elat/Timna areas. This manuscript does not intend to cover the complete geology but rather to let the reader a glimpse of its uniqueness. The legend of each geological map from these areas is the one attached to figures 2 and 3. The detailed geology regarding special topics is available through the reference list attached and the explanatory notes (Supplementary-Beyth et al., 2011 and Beyth et al., 2018). Explanatory notes of the 1996, 2001 and 2010 field trips of the Israel Geological Society in the Elat/Timna area are available from the Israel Geological Society web- site www.igs.org.il.

The Roded and Elat Neoproterozoic Blocks (Figs. 5-6) - The Roded Block consists of a north-northeast striking block of metamorphic and igneous rocks (Weissbrod, 1961, 1965) cut at the west by the Shelomo and Roded sinistral faults and at the east by the Tzefahot and Yotam faults (Eyal, 1973). The Elat Block is a north-east striking block of Neoproterozoic consists of metamorphic and plutonic rocks that are cut on the west by the Tzefahot and Yotam sinistral faults and on the east by the Elat fault (Frieslander, 2000). The Neoproterozoic metamorphic rocks of the Roded and Elat blocks appear to be the result of an event which consist of subduction, formation of island arcs, erosion of the arcs, deposition of the erosion products and their metamorphism into schists, gneiss and migmatite. The metamorphic rocks of the Elat block consist of the metapelitic and metapsammitic Elat Schist, with an age of their provenance 800-813 Ma (Kroner et al., 1990; Eyal et al., 1991). The metamorphic minerals in the schist are biotite, garnet, staurolite, cordierite, andalusite and silimenite (Shimron, 1972). Those schists were intruded by early quartz dioritic, 780-790 Ma, and granitic, 740-744 Ma, plutons after a first metamorphic event and were intensely deformed by a second event to Roded Gneiss, Taba Gneiss and Elat Granitic Gneiss (Kroner et al., 1990; Eyal et al., 1991; Kolodner, 2007). Later large calc alkaline intrusions such as the Roded Quartz Diorite, 612-634, and the Elat Granite, 630-636 Ma, (Stein and Goldstein, 1996; Katz et al., 1998; Be'eri-Shelvin et al., 2009: Morag et al., 2011a) mark the cratonization phase of the orogeny. Metamorphic conditions reached amphibolitic facies and peaked at 660-700º C and 4-5 Kbar (Matthews et al., 1989; Katz et al., 1998; Anenburg and Katzir, 2014; Vapnik, 1993). Morag and Avigad (2010) suggested two metamorphic phases, one characterized by an amphibolite facies at about 720 Ma and a second one of amphibolite-greenschist facies younger then ~700 (considering the age obtained for the schist dykes of Elat block that cut older metamorphic structures). Garfunkel (1980, 1999) suggested that they indicate the existence of two orogenic phases separated by 50 million years. Elisha et al., (2017; 2019) suggested that peak thermal conditions prevailed from 620 to 610 Ma in Elat area, as in nearby Abu-Barqa (SW Jordan) and Taba-Nuweiba (Sinai, Egypt) areas. The volcano-conglomeratic event, following a late alkali granitic phase, 608 Ma (Morag et al., 2011a, 2012; Be'eri-Shelvin et al., 2009), is the final, major event in the Elat area, and is represented by basalts, andesits and the Elat Conglomerate, Roded Conglomerates and the Mapalim Formation in the Roded block (Paz, 1997; Weissbrod; 1961, 1965). Outside of the Roded block, this event is represented by andesites and trachytes in Gevaot Shehoret (Fig. 5) (Peltz and Eyal, 1995) and acid volcanic rocks in the Ramat Yotam Caldera (Eyal and Peltz, 1994, Fig. 5) and at the Amram Block (Mushkin et al., 2003). These conglomerates, dated to about 590 Ma (Katzir et al., 2007; Morag et al., 2011a), are the products of a major erosion phase in which 12,000 m of the section were removed (Garfunkel, 1999; Avigad and Gvitzman, 2009).

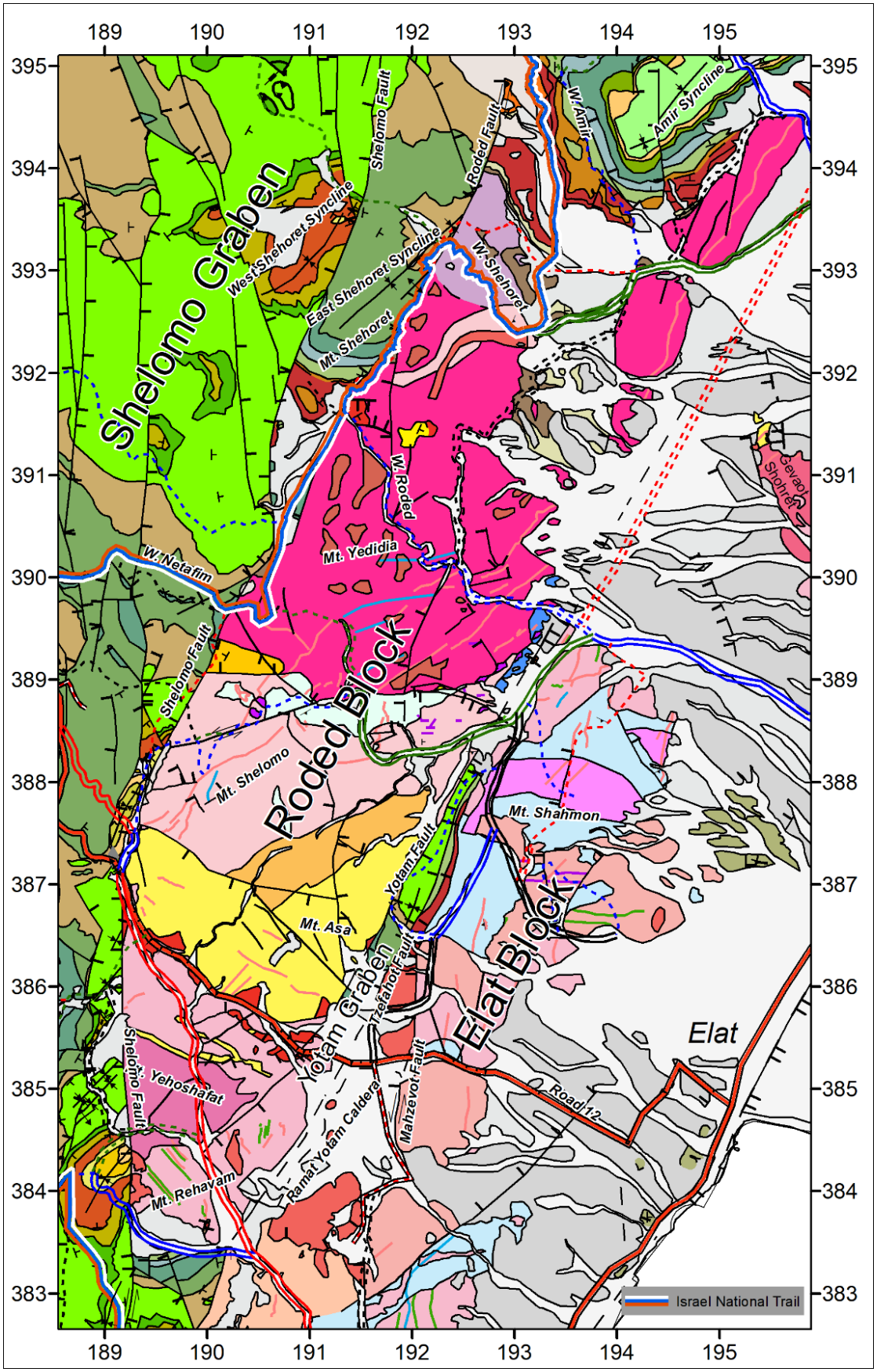

Figure 5: Geological map of the Roded and Elat Neoproterozoic blocks.

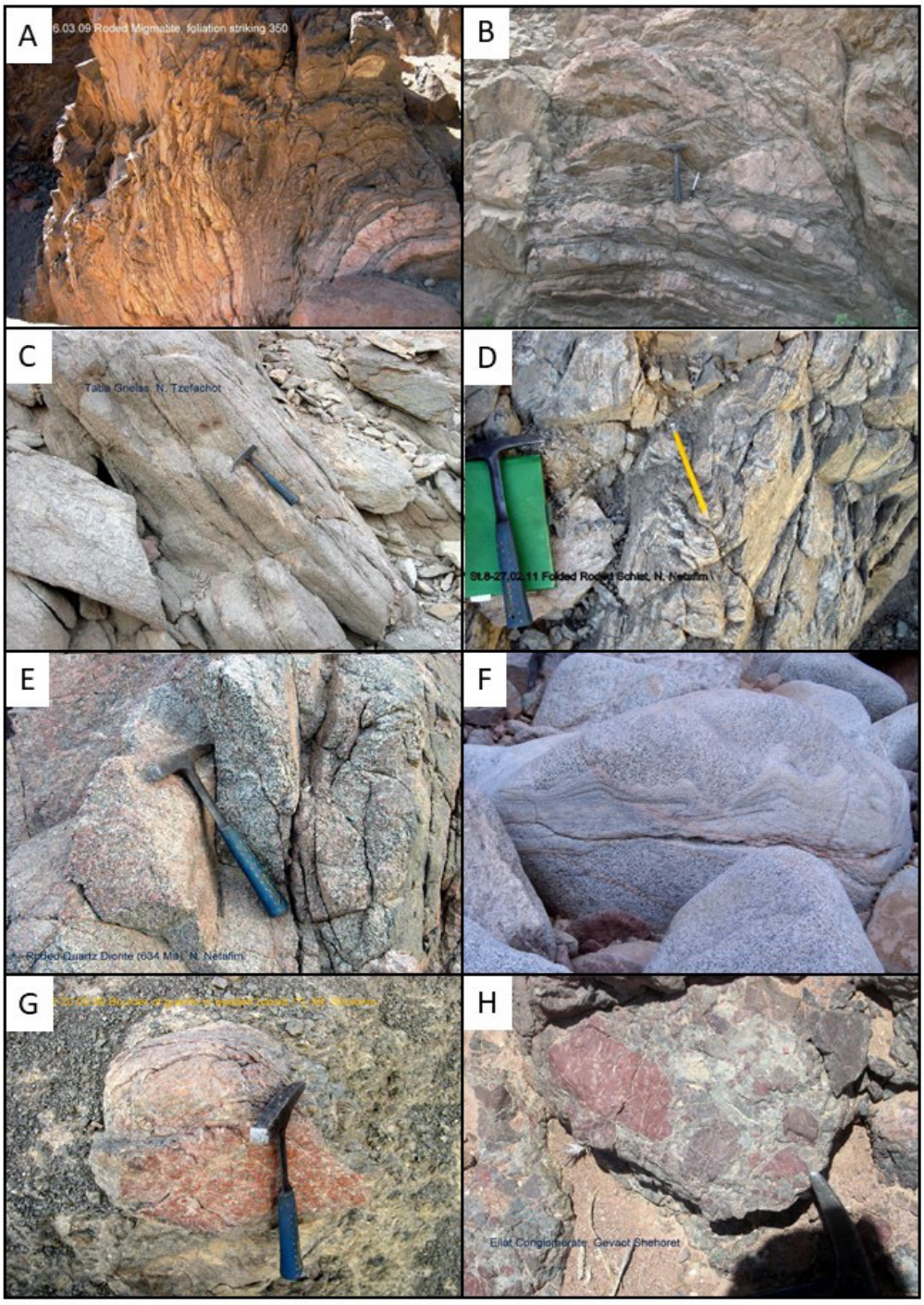

Figure 6: a&b Roded Migmatite, foliation striking 350º azimuth, Mt. Shelomo. Coord. 190612/388773 c. Taba Gneiss, foliation dip 70º/055º. N. Tzefachot. Coord. 190565/381197 d. Folded Roded Schist, N. Netafim. Coord. 191992/388413 e. Roded Quartz Diorite, N. Netafim. Coord. 191335/389543. f. Boulder of Roded Quartz Diorite partly folded. N. Gishron. Coord. 188038/386217 g. Neoproterozoic boulder of Elat Granite in bedded "basalt", Mt. Shelomo. Coord.189533/386406 h. Neoproterozoic Elat Conglomerate, Gevaot Shehoret. Coord. 195356/391548.

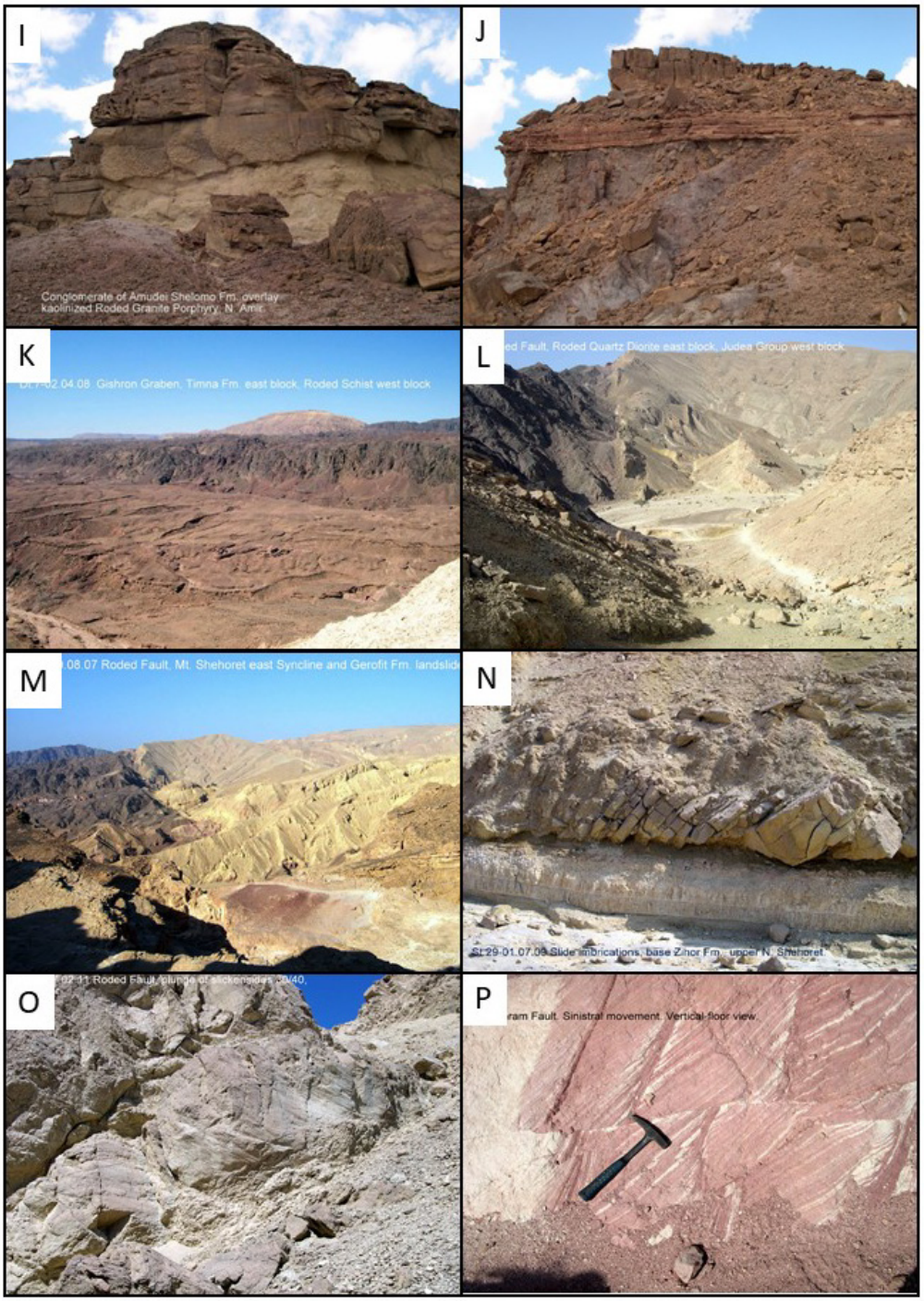

Figure 6 (cont.): i. Conglomerate of base Amudei Shelomo Fm. overlying pedogenesis weathered Roded Granite Porphyry to kaolinite, Early Cambrian peneplain (Sandler et al., 2011; Angerer et al., 2011). Coord. 193120/392880. J. Early Cambrian peneplain developed on Roded Quartz Diorite, Roded Gneiss (El-Hura Gneiss, Eyal et al., 2017) and Amram Rhyolite intruded by andesite and rhyolite dykes. N, Gishron. Coord. 188108/385088. k. View from east, from Male Gishron (Gishron Climb in Hebrew) Coord. 188669/384127, to Gishron Fault zone, east block Timna Fm. west uplifted block Roded Schist, at the background Hazera Fm. at the top of Gebel Umm Vatat, Sinai (Egypt) l. View southward from the Israel National Trail, at the western margins of Mt. Amir, to Roded Fault striking 30º azimuth, east block Roded Quartz Diorite and Roded Granite Porphyry, west block syncline and anticline of Judea Group limestones and dolomites of Mt. Shehoret. Coord. 192320/393256. m. View southward from the Israel National Trail, at the western margins of Mt. Amir Coord. 193148/396227. A landslide of a "yellow" block of Gerofit Fm. limestone sliding from west to east above the purple lubricant shales of the Ora Fm. across the Roded Fault. The Israel National Trail seen on the purple shales of the Ora Fm. n. Landslide imbrications at base of Zihor Fm. Coord. 190541/394974. o. Sub-horizontal slickensides plunging 30º/040º, Roded Fault plane. N. Shehoret Coord. 192855/394580. p. Vertical view. Sinistral fault in the Amram Fault shear zone, Shehoret Fm. N. Amram, Coord. 195361/395588.

The Amram Block and Amir Syncline (Figs. 7-11) - The Amir Syncline is a Miocene(?) structure formed between the Neoproterozoic igneous Roded and Amram blocks in response to local compressional forces associated with sinistral movement along the Dead Sea Transform (Katz et al., 2002; Beyth et al., 2017). The Cambrian sedimentary Amudei Shelomo, Timna, Shehoret and Netafim formations (Weissbrod, 1969, 1980, 2005) onlap on the igneous rocks and from the base of the Amir Syncline sedimentary section. This syncline is build of Amir, Avrona and Samar sandstones formations and Hazera, Ora, Grofit, Zihor, Menuha and Mishash limestones, marls, shales and chert formations of the Cretaceous age (Bartov et al., 1972). The Amram Rhyolite, dated 606 Ma (Be'eri-Shlevin, 2008), which forms major parts of the Amram block mark the volcano-conglomeratic event, that is the final major Neoproterozoic magmatic event in the Elat/Timna area. The direction of the Amram Block is east-west while the Elat and Roded blocks are elongated in a north-north-east direction. The boundary faults of the Amram Block are: The Elat Fault to the east, the Roded Fault to the west, Avrona Fault to the north and Amram Fault to the south. In the center it is separated into two sub-blocks by the Zefunot Fault (Mushkin et al., 2003). Shirman et al., (2015) suggested a dextral displacement of ~500 m. of the deep monzonite pluton along the Zefunot fault using magnetic and gravity data. Arava and Roded faults are sinistral faults striking north-east and Avrona, Amram and Zefunot faults are dextral faults striking east-west. These east-west striking faults like the Amram and Zefunot faults are shear zones consisting of numerous fault segments. The Avrona Fault is cut at the northwest corner of Mt. Amram by a north-south trending fault with a sinistral displacement of 120 meters (Fig. 8). Some of these faults like the Zefunot fault, where the north block of Amram Granite Porphyry faces the Amram Rhyolite south block below the Early Cambrian peneplain, are reactivated Neoproterozoic faults (Garfunkel, 1970). From Pleistocene to Holocene, changes in the flow direction and depositional characteristics of the fluvial units adjacent to the Dead Sea Transform, indicate that the Amir Syncline, the Amram and the Roded blocks continued to response to compressional forces at least to the Middle Holocene (Gellman, 2018).

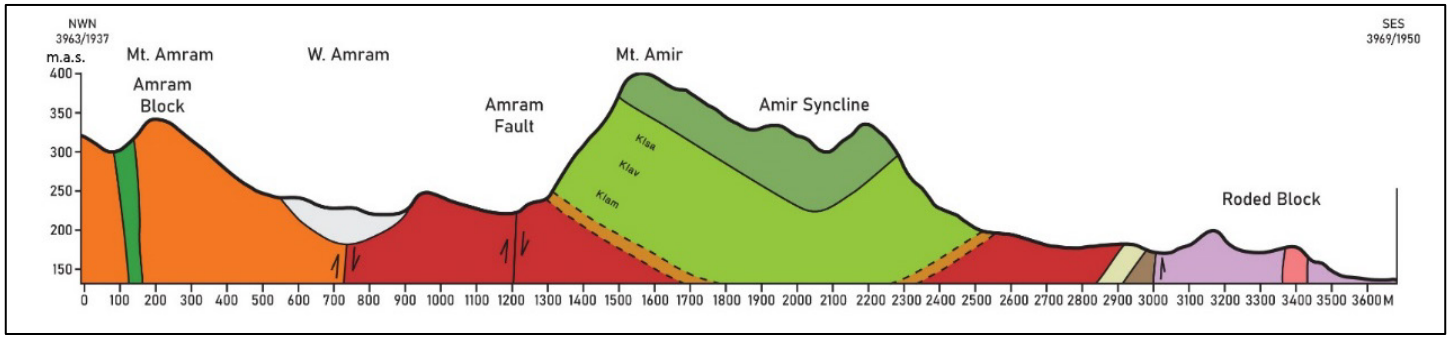

Fig. 7: Schematic cross section west Amir Syncline.

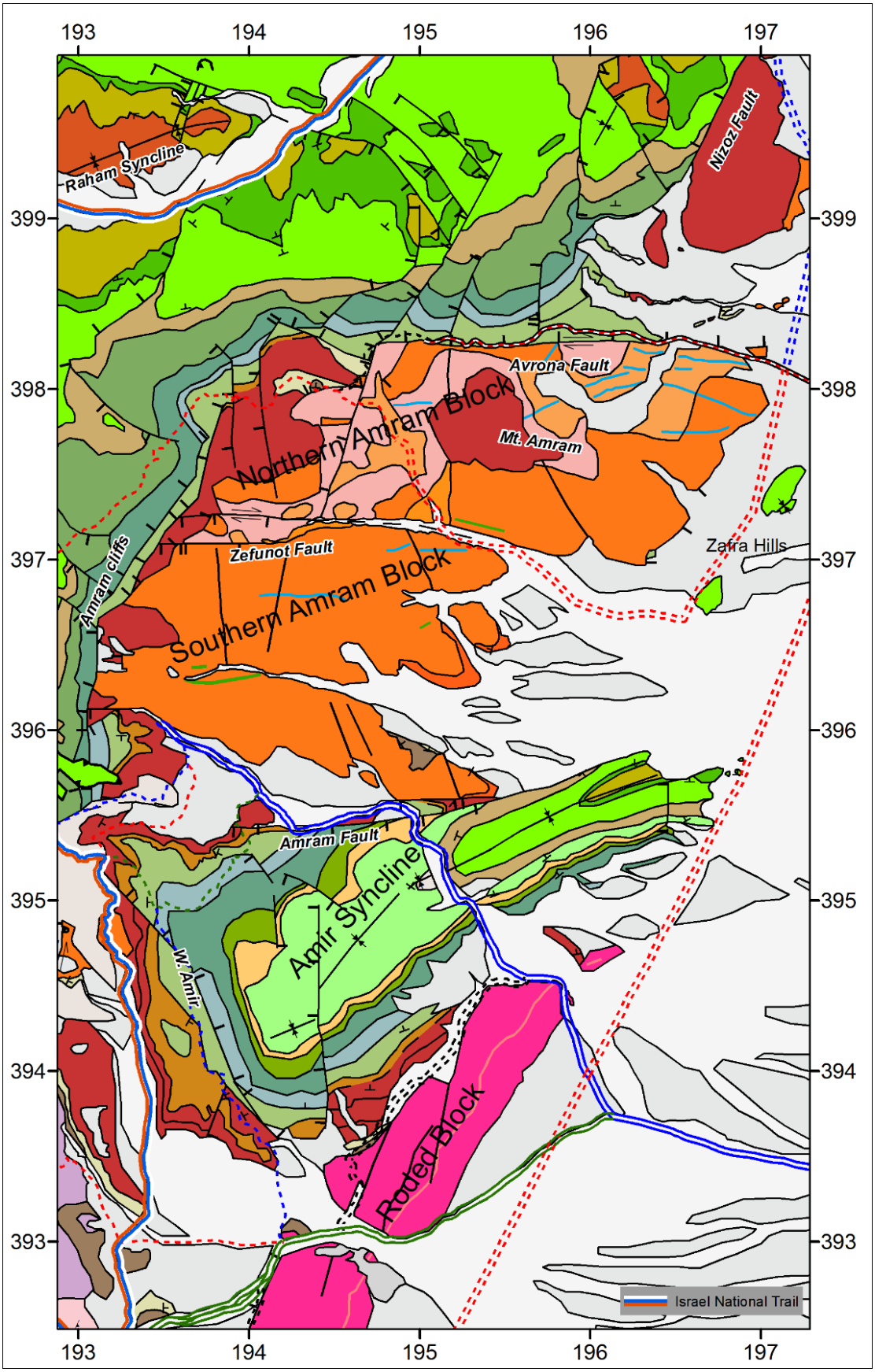

Figure 8: Geological map of the Amram Block and Amir Syncline.

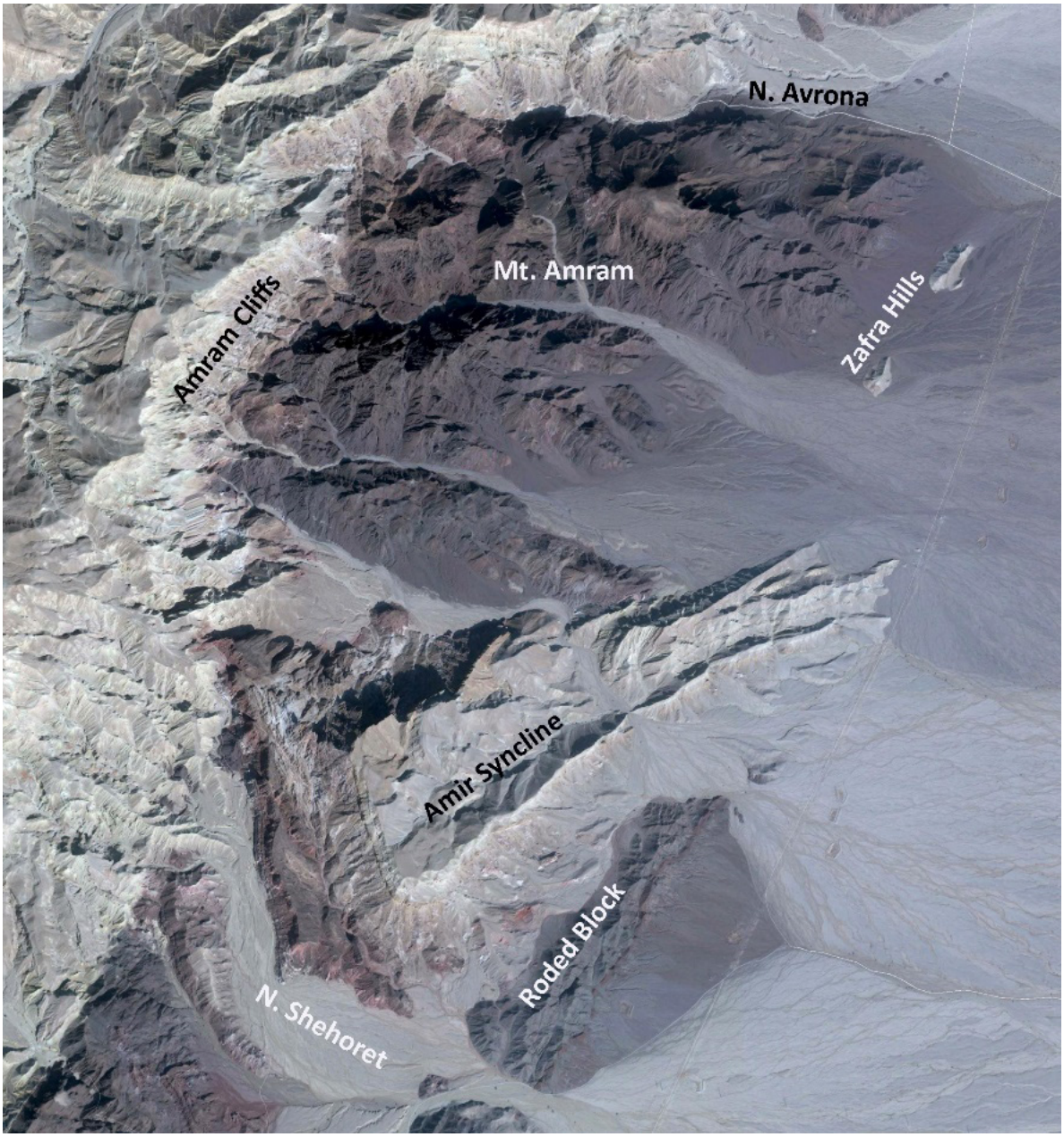

Figure 9: Orthophoto of the northern edge of the Roded Block, north-east plunging Amir Syncline south of Mt. Amram and the Amram cliffs west of Mt. Amram. The Zafra Hills at the east margins of Mt. Amram and the alluvial fans of N. Shehoret and N. Avrona are the west margins of the Arava, of the Dead Sea Transform.

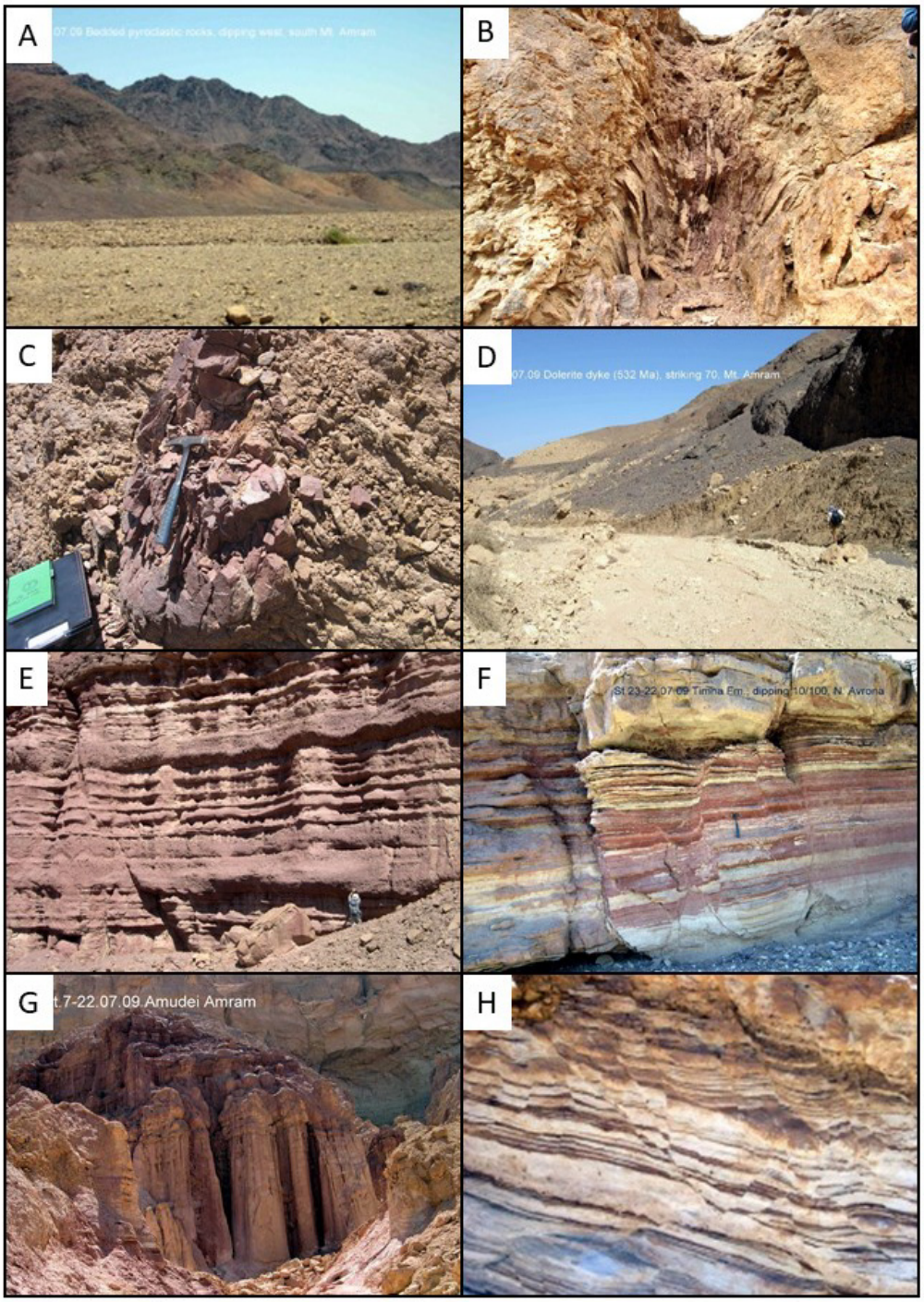

Figure 10: a. View from south-east, pyroclastic beds of the Southern Amram Block. Coord. 195399/396444; b. Volcanic feeder vent Amram Rhyolite. 3 m. wide. Vents are vertical at the base and horizontal at the top. N. Amram. (Wurtzburger, 1959). Coord. 194726/395794; c. Xenolith of rhyolite in the Amram Quartz Syenite. Coord. 195056/397448; d. Dolerite dyke (532 Ma) striking 70^{o} azimuth. Coord. 193810/396275; e. Sub-arkosic sandstones of Amudei Shelomo Fm. "Hidden Valley" ("Emeq Neelam" in Hebrew), north-west corner of Mt. Amram. Coord. 194582/ 398020; f. Sandstones, silts and shales of the Sasgon Mb. Timna Fm., N. Avrona. Coord. 196802/398473; g. View from east to Amram Pillars ("Amudei Amram" in Hebrew), which are ~20m high and build of white sandstone of the White Mb. of the Shehoret Fm. Coord. 193095/396106. h. Multicolored Mb. Shehoret Fm., cut by the faults of the shear zone of the east-west striking Amram Fault.

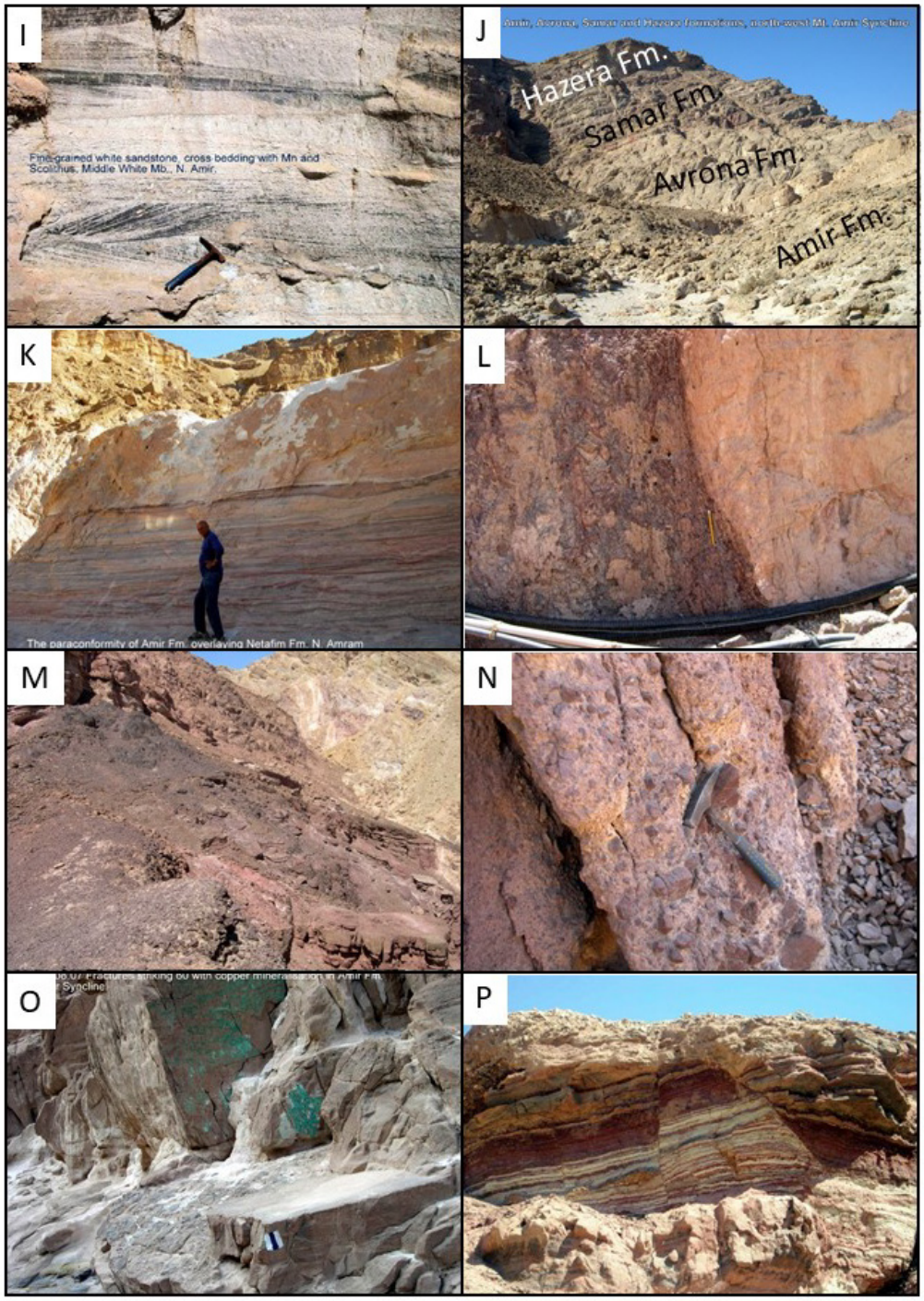

Figure 10 (cont.): i. fine grained white sandstone, cross bedding with manganese and *Skolithus*, White Mb., Shehoret Fm. N. Amir. Coord. 193502/393637. j&k Coord 194263/395406. J. Amir, Avrona, Samar and Hazera formations, north Amir Syncline, N. Amram. k. The paraconformity between the Netafim Cambrian Fm. overlaying by the Amir Aptian Fm. (see also Fig. 11). l&m. Coord. 195023/398288. l. Seismographic underground station. m. View from west to the Avrona east-west striking fault, Amram Rhyolite and Timna Fm. left, south block, white sandstones of the Amir Fm. north block, N. Avrona. n. Breccia of Amram Rhyolite along a north-south fault plane. The Avrona fault is displaced 120 m. sinistraly by the N-S fault. Coord. 194722/398184. o. Copper mineralization along 60^{o} striking fractures, Amir Fm. N. Amir. Coord. 193580/394694. p. Faulted sandstone, silt and clay of the Hakhlil and Sasgon members of the Timna Fm. (Segev, 1984) N. Shehoret. Coord. 193487/392163.

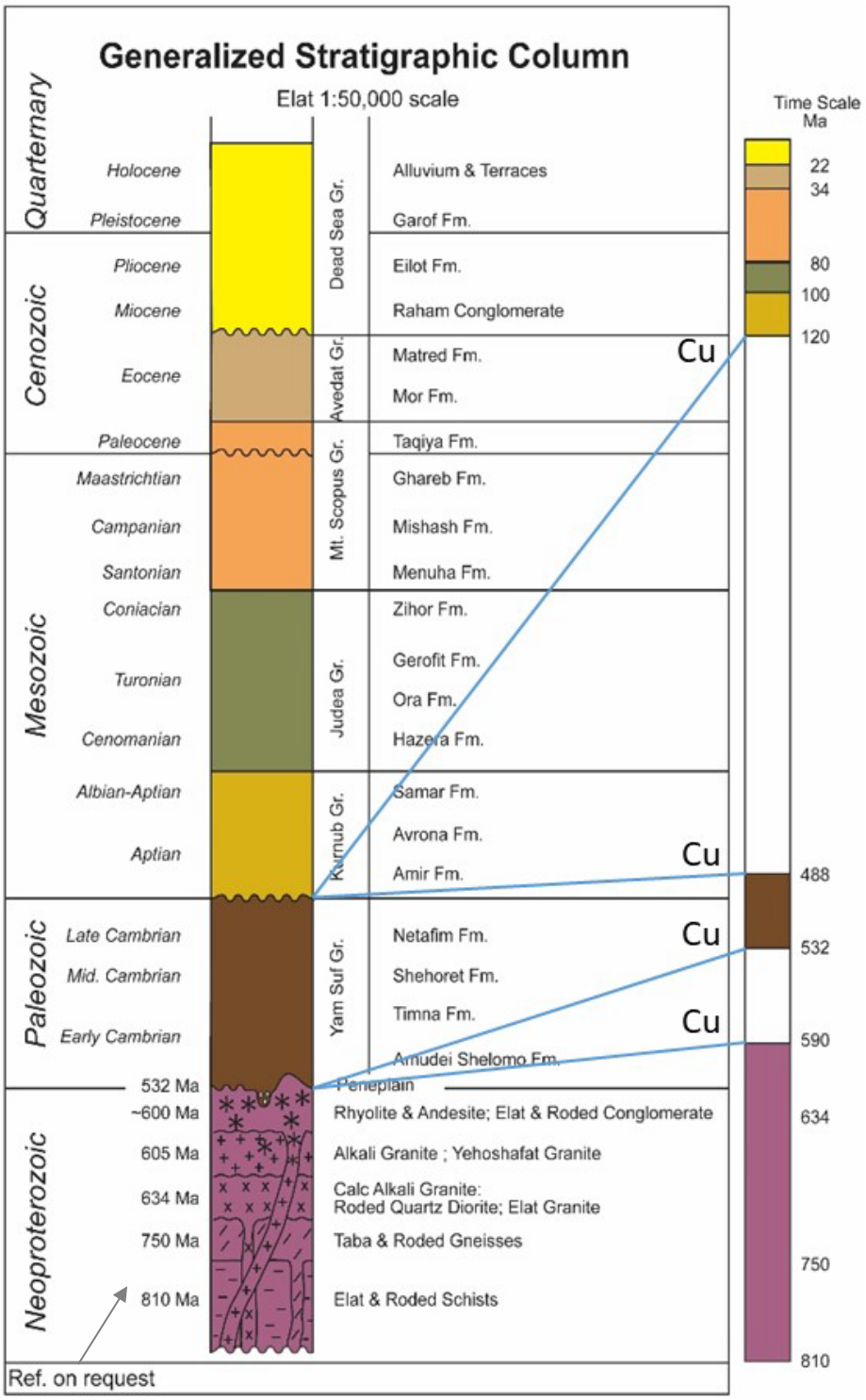

Figure 11: Two significant gaps-hiatus in the geological history of Elat/Timna area and the Copper (Cu) mineralization. Ref. for Neoproterozoic ages: Beyth and Heimann, 1999; Katzir et al., 2007; Beeri et al., 2009; Katz et al., 1998; Kroner et al., 1990.

Timna Valley (Figs. 12-14, supplementaryII) -The Timna Valley, 9 x 10 sq km in size, is a semi-circular shaped valley, truncated to the east by the Dead Sea Transform and surrounded other edges by 500-m-high cliffs of very well exposed Cambrian to Cretaceous sedimentary rocks. The core of the Timna Valley which is a structural dome, is Mt. Timna, 5x3 sq km in size, 453 m pick above sea level, which is the highest topographic feature in the Timna Valley (Beyth et al., 2018a). Mt. Timna and Mt. Amram that is 12 km south of it are both the most northern blocks of the exposed Arabian-Nubian Shield west of the Dead Sea Transform. The Cambrian Amudei Shelomo, Timna and Shehoret formations onlap on the Mt. Amram and Mt. Timna igneous complexes indicating that Mt. Amram, like Mt. Timna, are Neogene-Quarternary rejuvenated, ancient, Cambrian structures (Karcz and Key, 1966; Garfunkel, 1980). Both blocks were exposed by Neogene-Quaternary uplift along the margins of the Dead Sea Transform (Beyth and Mushkin, 2010). The Amram Igneous Complex consists of volcanic Amram Rhyolite and was dated to 606 Ma. (Be'eri- Shelvin, 2008) with minor hypabyssal intrusions while the Timna Igneous Complex consists of a wide variety of plutonic rocks. Both complexes are intruded by rhyolite, andesite and composite dykes. The Timna and Amram igneous complexes are older than 580 Ma except for unique dolerite dykes, which intrude both complexes in an~E-W orientation. They are pre-peneplain and are dated to 532 Ma, Early Cambrian (Beyth and Heiman, 1999b). Two magmatic cycles were suggested for the rocks of the Amram Igneous Complex (Mushkin et al., 2003). The older cycles consist of the Amram Granites and the Amram Rhyolites. The Timna Igneous Complex is characterized by a quasi- stratified magmatic cell, with a wide variety of plutonic rocks from olivine-norite to A-type alkali granite, formed 610 Ma ago in an old I type 625 Ma granitic crust (Beyth et al., 1994). Both complexes were later during the younger cycle intruded by younger 600 Ma quartz-monzodiorites (Beyth et al., 1997). Intensive pre-peneplain uplifting due to faulting along the Themed Fault and deeper erosion of the Timna Igneous Complex may explain the missing Amram Rhyolite and the exposure of the magmatic cell and granite porphyry in the Mt. Timna. Both the Timna Valley and N. Amram are also very interesting because of the Early Bronze and Early Iron ages of "King Solomon" copper mines which were and are extensively studied and a lot of recent archaeological studies combined with studies in Faynan, in SW Hashemite Kingdom of Jordan, on the eastern margins of the Dead Sea Transform are available (Ben-Yosef, 2018, 2016; Avner et al., 2018). The Timna Valley as a geological park was described by Beyth and Calvo (2014b and supplementary II).

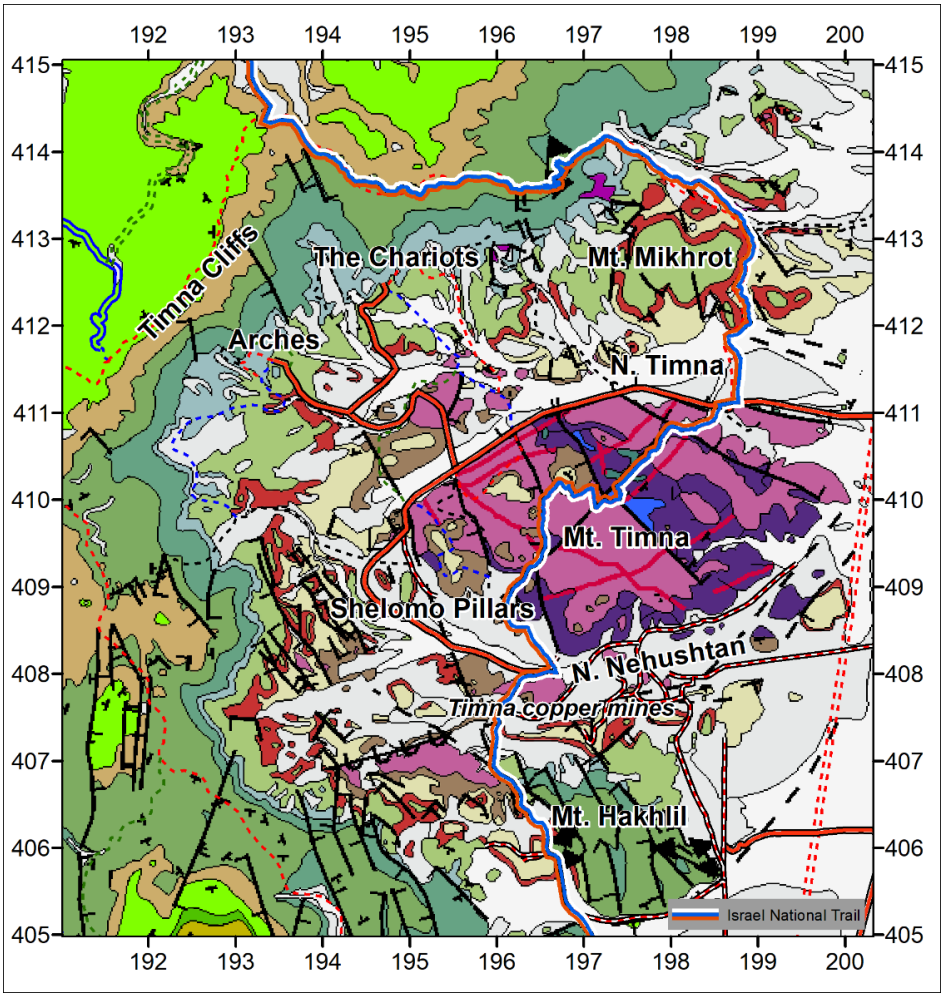

Fig. 12 Geological map of Timna Valley.

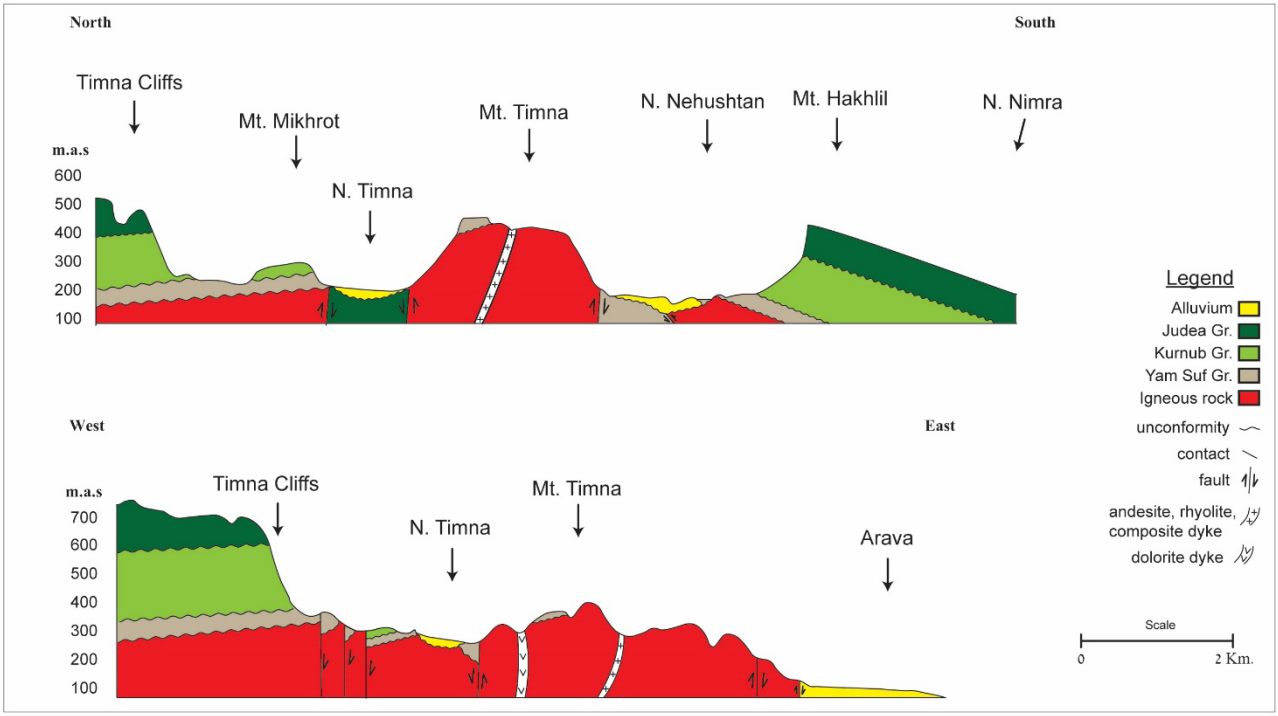

Fig. 13: Timna Valley cross sections.

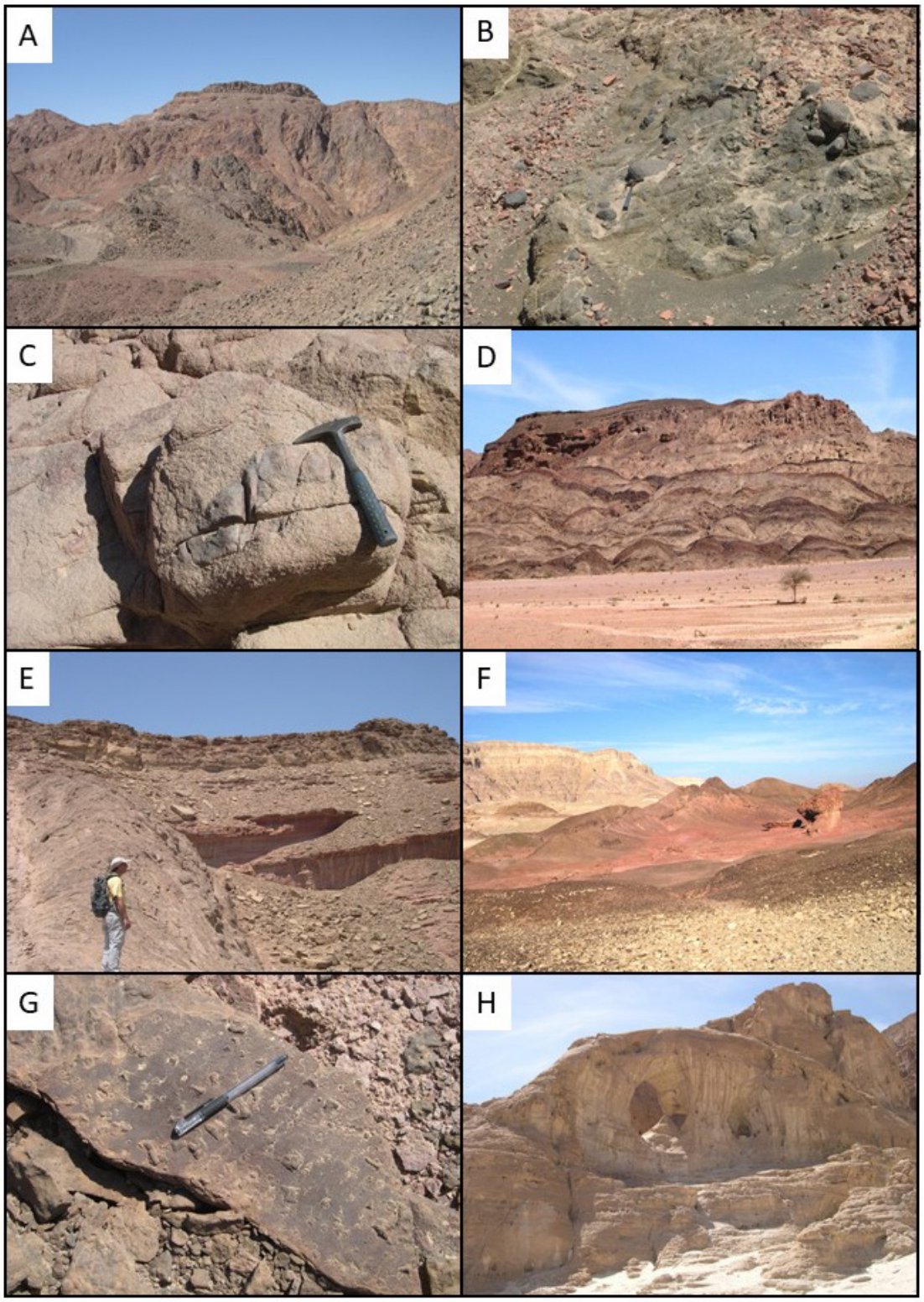

Figure 14: a. View from south, Amudei Shelomo and Timna formations at the top of Mt. Timna above the alkali granite (610 Ma) Coord. 196858/410212. b. Partly altered olivine norite (610 Ma) Coord. 197473/410073. c. A rhyolite xenolith in quartz monsodiorite (600 Ma) the youngest magmatic intrusion in the Timna Igneous Complex. Coord. 197517/410317 d. Dyke swarm of rhyolite, andesite and composite dykes, striking east-west, north margins of Mt. Timna. Coord. 195858/410297 e. Onlap of Amudie Shelomo and Timna formations on the Early Cambrian peneplain. Coord. 196681/410171. f. Quartzitic pebble conglomerate and sandstones of Amudei Shelomo Fm. covering the Early Cambrian peneplain at the "Petria" (mushroom in Hebrew). Timna Cliffs at the background. Coord. 195250/411257. g. Halite pseudomorphs in the sandy dolomite of Timna Fm., west Timna valley. Coord. 193820/408140. h. The arch in Avrona Fm. Coord. 193168/411563.

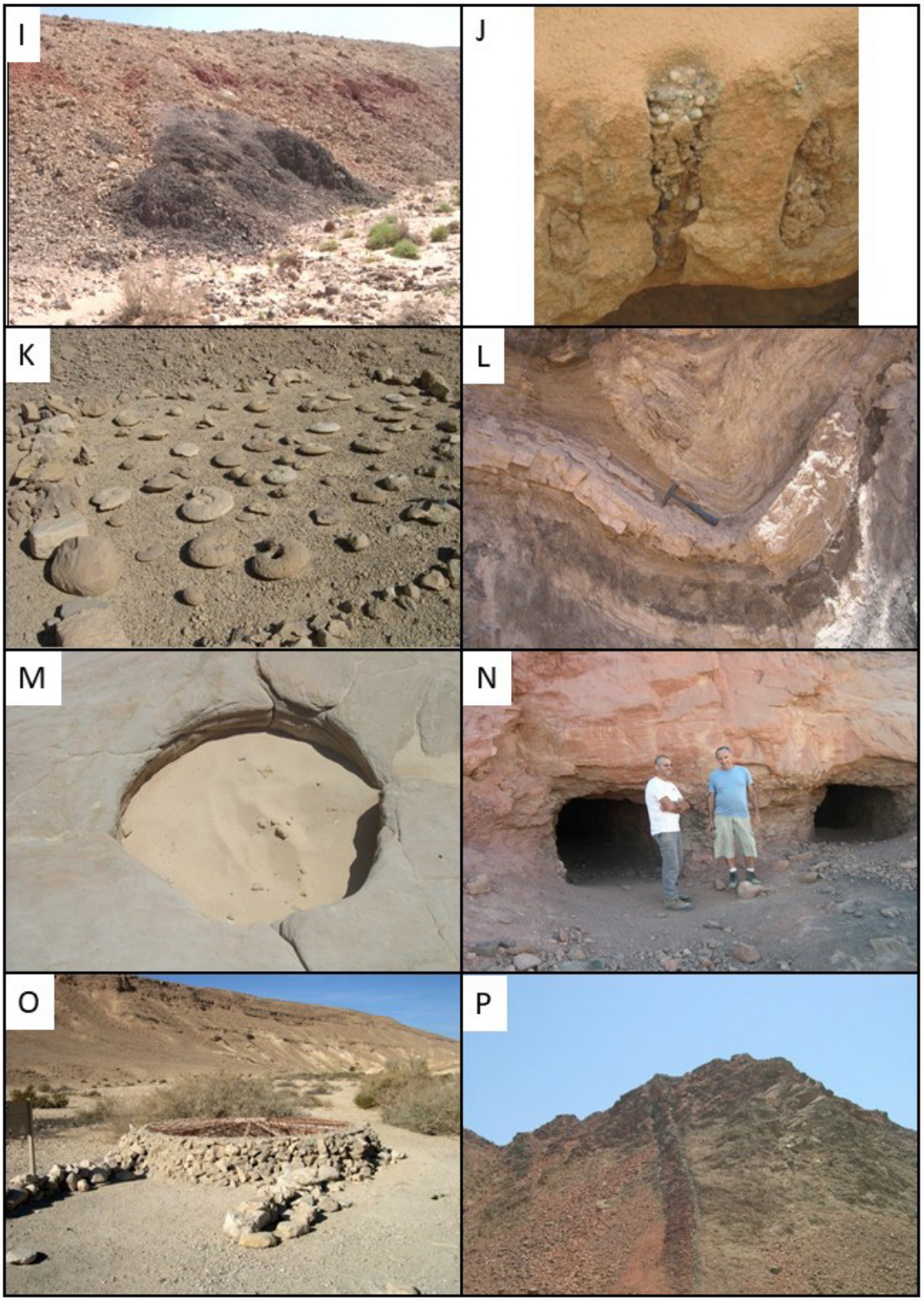

Figure 14 (cont.) i. Lower Cretaceous basaltic plug (90-100 Ma), ~10 m surface diameter, N. Mangan (Beyth and Segev, 1983; Segev et al., 1995). Coord. 199704/413036. j. Borrows, top Amir Fm. with pebbles from the Avrona Fm. surrounded by tidal channels (Weissbrod and Sneh, 1997) Coord. 193399/411503. k. Ammonites mainly *Choffaticeras* and *Vascoceras* from Ora Fm. Turonian index fossils (Freund 1961). N. Milhan. Coord. 193655/414335. l. Folded beds in Timna Fm. formed along a north striking manganese strip by epigenetic Holocene dissolution (karstification) of the dolomite by circulating of thermal brines along faults and fractures formed along the margins of the Dead Sea Transform. Coord. 194093/406957. m. A shaft, a remnant of an ancient copper mine (~11 BC). Coord. 193168/411563. n. Manganese prospection caves from, N. Mangan. Coord. 198664/413121. o. Hand dug brackish water well in an aquifer of Gerofit Fm. limestone above the aquiclude of the Ora Fm. shales. N. Milhan. Coord. 192284/416040. p. Composite dyke (~593 Ma, Katzir et al., 2007) striking 060°-070° azimuth, center 7 m. thick rhyolite (72% SiO_2) both margins, ~2 m. thick, andesite (56% SiO_2). Coord. 196358/408530.

Themed Fault and the Raham Syncline (Figs. 15-16) - The dextral Themed Fault which is part of the Sinai-Negev Shear Zone (Bartov, 1967, 1974) strikes west-northeast and extends in the Elat/Timna area from Nahal Shani on the west to Be'er Ora on eastern edge of the the Arava (Elat and Be'er Ora Sheets). The continuation of this fault at the east is the Dana Fault at the south-west Hashemite Kingdom of Jordan on the eastern margins of the Dead Sea Transform with a left lateral offset of 109 km. Garfunkel (1970) suggested that the Themed Fault is a reactivated pre-rift marginal Neoproterozoic fault. The Themed Fault in the Elat area is accompanied by marginal grabens with blocks of Zihor, Menuha and Mishash formations and synclines and anticlines parallel to the main fault, each few hundred meters in size. Faults striking north-south like the Nizoz Fault on the east or Neshef Fault on the west are cut by the Themed Fault. The Late Pleistocene Zhiha Formation in Nahal Shani is not affected by the Themed Fault. The major activity of this fault was from late Oligocene to early Miocene, 22-27 Ma (Weinberger et al., 2020). The east-northeast striking Nahal Raham Syncline (Bartov, 1967) is one of the biggest synclines mapped in the area. Its southern limb is adjacent to the Amram Block and its northern limb to the Themed Fault. The formations exposed in the syncline are Ora through Mishash (Steinitz et al., 1967, 1970). Lances of sandstone are exposed in the Menuha Formation and the white chalk of the Mishash Formation was dated as early Late Campanian by *ostracods* of biozone S-5a (Lifshitz et al., 1985).

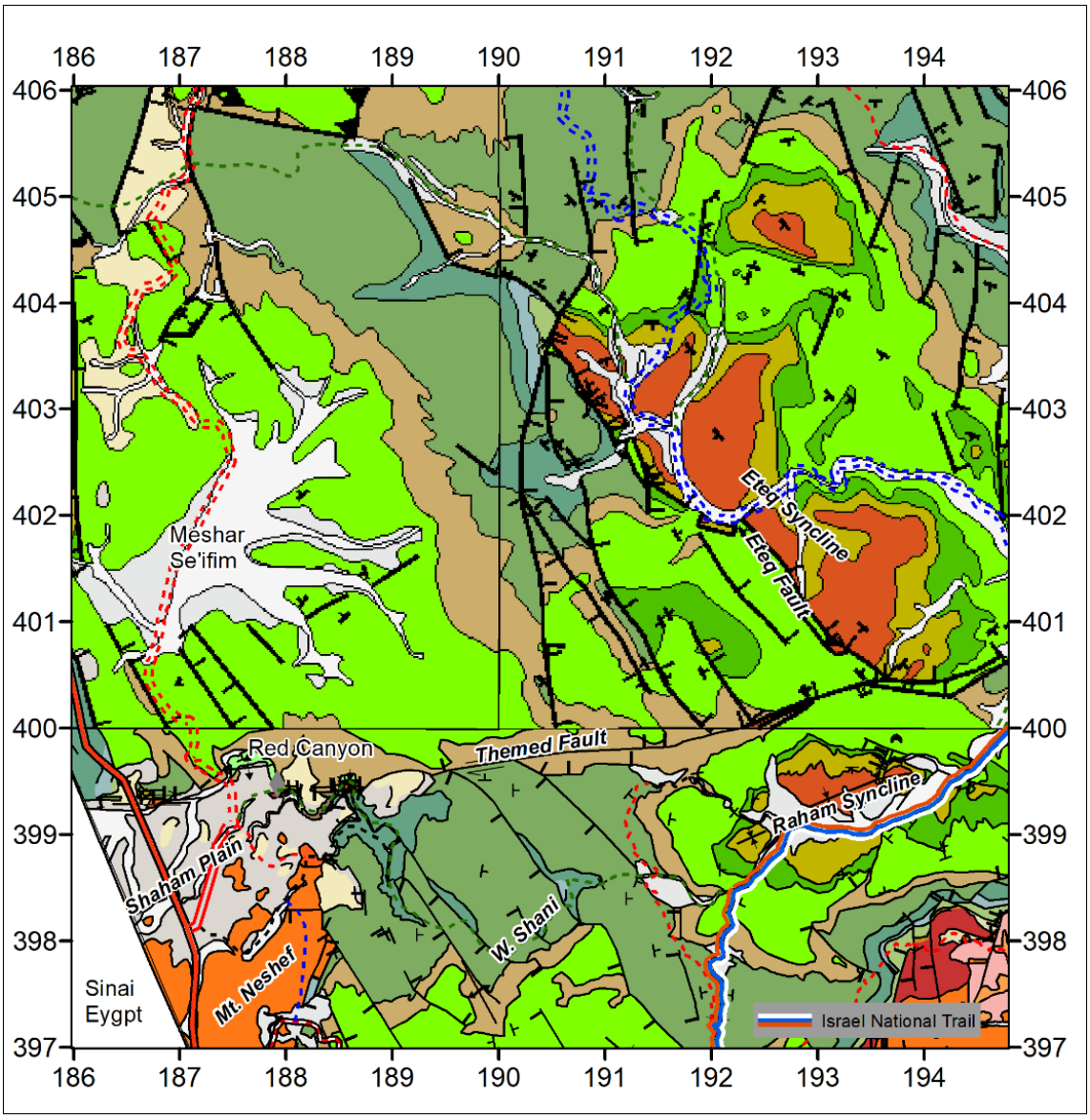

Figure 15: Themed Fault and Raham Syncline.

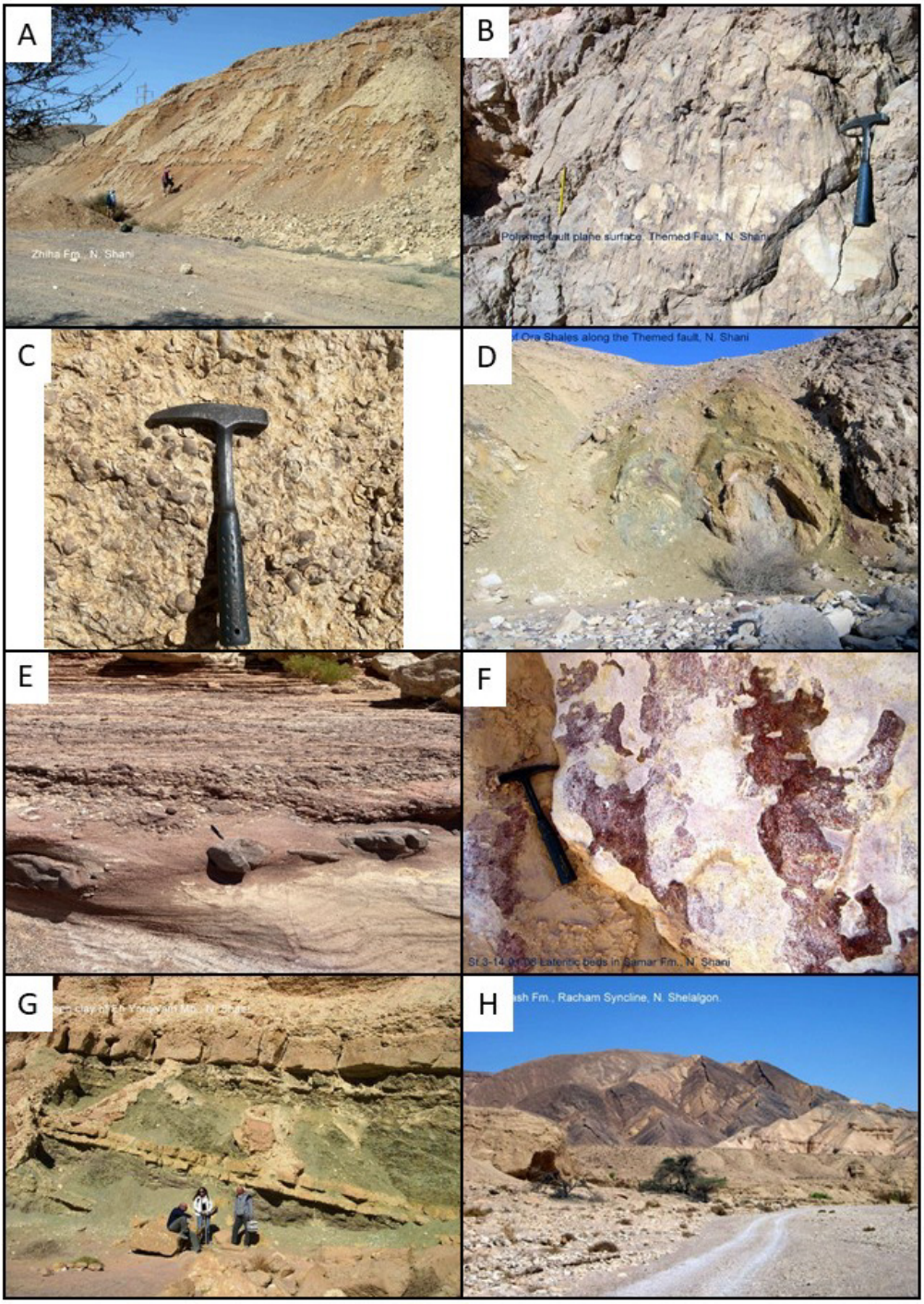

Figure 16: a. Silts and shales of the Pleistocene Zehiha Fm. (Ginat et al., 2001) N. Shani. Coord. 186347/399260. b. 70º/175º dip of a polished fault plane with vertical slickensides and fault breccia, north accessary of the Themed Fault, N. Shani. Coord. 186669/399408. c. Limestone of Yotvata Mb. with *mussel*. N. Shani. Coord. 187550/399750. d. Folded shales of Ora fm. along a north accessary fault of the Themed Fault. N. Shani. Coord. 187985/399464. e. Well bedded sandstones of Amudie Shelomo Fm. with Neoproterozoic angular boulders at the base, quartzitic pebble conglomerate at the middle and well bedded silt of Timna Fm. at the very top of the photo. Red Canyon. coord. 188122/399228. f. Laterite bed in the Samar Fm. N. Shani. Coord, 189010/398872. g. Green marl with limestone beds of En Yorqe'am Mb. N. Shani. Coord. 189238/398225. h. View from N. Raham at Coord. 192668/399082 to the Zihor, Mishash and Menuha formations diping ~30º southward at the northern limb of the Raham Syncline Coord. 192793/399375.

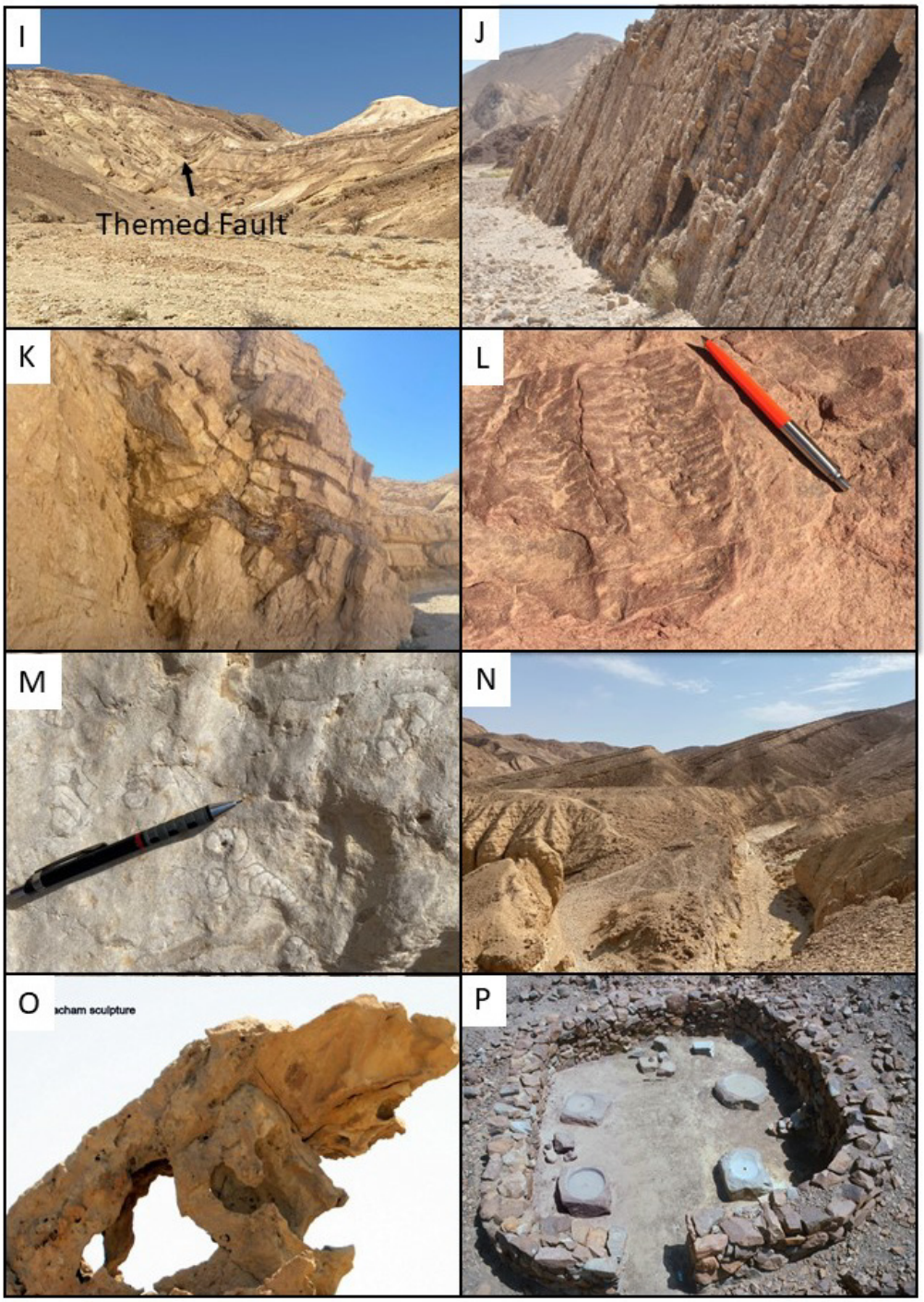

Figure 16 (cont.): i&j. N. Raham. Coord. 194977/400820. View westward to the Themed Fault. A syncline in the limestone of Grofit Fm. attached to the southern block of the Themed fault. j. View eastward, brown reddish dolomite of Hazera Fm. along the Themed fault plane dipping 60º/324º. k. Disharmonic folds in a small graben striking NW, base Gerofit Fm. N. Raham. Coord. 195575/401897. ("Yad Hazatan" Bartov, 1967). l. Traces of *Trilobite* in Cambrian shale in a collapse boulder. N. Shehoret. Coord. 193120/392880. Cambrian *Trilobite* was described from the Timna Fm. by Parnes (1971) and trilobite associations of the lower-Middle Cambrian from the Burj Fm., east of the Dead Sea, SW Jordan by Elicki and Geyer (2013). m&n. N. Uziyahu Coord. 191695/397896. m. *Nerinea,* a gastropod, index fossil, in the limestone of Zafit Mb. Hazera Fm. n. Sinistral Displacement of N. Uziyahu by ~100 m. along a sinistral fault with sub-horizontal slickensides plunging ~ 45º south and ~10 m. of vertical displacement. o. A sculpture created by weathering at the surface of the alluvial river terrace of N. Raham. Coord. 190422/395350. p. Gold millstones from the early Moslem period (between the 7 and the 10 centuries AC) in W. Tavachin south tributary of N. Roded; Coord. 192129/389527 (Avner and Shirav, 2001).

The Shelomo and Yotam grabens (Figs. 17-19) - were formed at the western margins of the Dead Sea Transform between the Neoproterozoic Sinai (Eyal et al., 2017), Roded and Elat blocks with their boundary faults generally striking north-south (Eyal,Y., 1967; 1973). The Shelomo Graben is 1 km wide at its south end at the Gulf of Aqaba/Elat and 5 km wide at its northern end. In its northern end adjacent to the Themed Fault where the graben cut the Amram Rhyolite of Mt. Amram at the east from the Amram Rhyolite of Mt. Neshef at the west (Fig. 4). A nice overview of the Shelomo Graben, Roded Block, Sinai (Taba) block and the Gulf of Aqaba/Elat is from Mt. Yoash 734 m.a.s.l. From here it is recommended to take the N. Gishron geological track (Beyth et al., 2018b) along the Israel National Trail running along the Gishron Fault (Fig. 9) all the way to the Red Sea. The core of this track are the metamorphic Neoproterozoic Taba and Roded Gneisses, Amram Rhyolite and Mapalim (?) Formation. The sediments are the Amudei Shehlomo, Timna and Shehoret Cambrian formations overlaid at the top by the Eocene Avedat Group most probably Mor Fm. covered by the Raham Conglomerate. The younger formations are mainly preserved in the synclines like Rehavam, Taba and Shelomo along the Shelomo and Roded Faults (Fig. 5). The vertical displacement along the Shelomo Fault at the Shelomo Syncline is about 1,600 m., where the Eocene Mor Fm. on the west block is opposite to the Roded Gneiss of the east block (Eyal, 1967) and the total sinistral displacement is about 6 km. (Garfunkel, 1970). N. Roded is changing its course abruptly southward at the junction with the Roded Fault suggesting a sinistral displacement of ~ 1 km. along the fault. The Yehoshafat Fault (Ayadin and Eyal, 2002) with its accessory faults (Fig. 18) at the Zafra Pass where the large alluvial terrace of Nahal Gishron Q_2 and the old terraces, Q_1, with the diorite boulders are of special geomorphological interest suggesting the "capturing" of ancient N. Gishron by the younger N. Yehoshafat.

The Yotam Graben is a small steeply folded graben-syncline, plunging northward and terminating at N. Netafim and N. Roded. Its boundary faults are Yotam on the west and Tzefahot and Mahzevot on the east and they coalesce northward in the subsurface to the north-east Elat Fault (Frieslender, 2000). The shear zone of this faults at N. Roded cut through Pleistocene alluvial formations (Beyth et al., 2012; Wieler et al., 2017. Fig.21f). The horizontal or sub-horizontal slickensides on the fault planes (Fig. 6,o) and the folds oblique to the Shelomo Fault like Taba, Rehavam, Yehoshafat, Shelomo and West Shehoret folds and to the Roded fault like east Shehoret fold and Amir synclines all indicate sinistral displacement along these faults. The calculated amount of the sinistral movements of the Elat and Roded blocks in respect to the Gishron Block (supplementary I Fig. 6) west of the Gishron Fault is 8 and 2.5 kilometers respectively (Garfunkel, 1970).

The Israel National Trail and the most southern part of the recently constructed security Fence presents a unique opportunity to study the geology of the Gishron Fault zone (Fig. 19a&p).

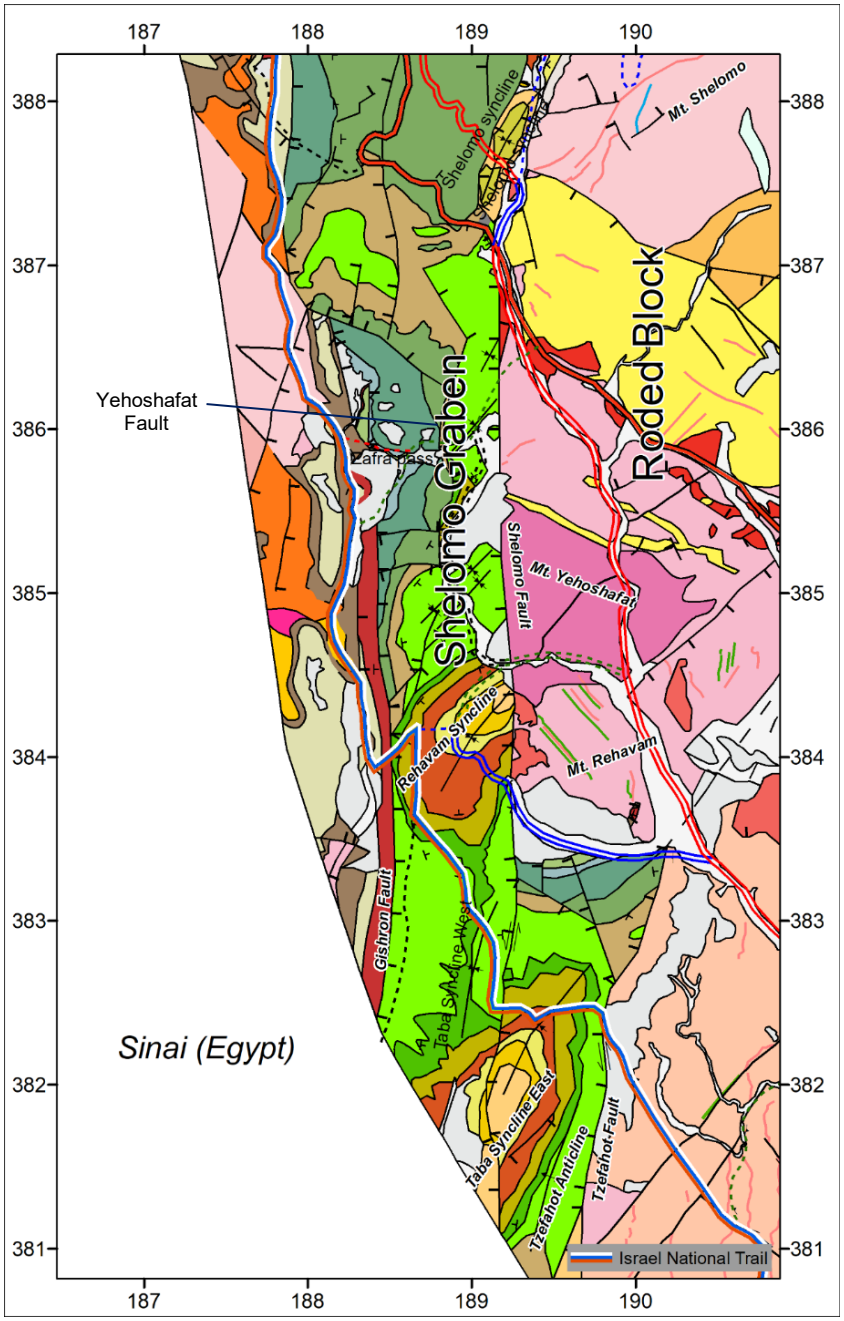

Figure 17: South Shelomo Graben geological map.

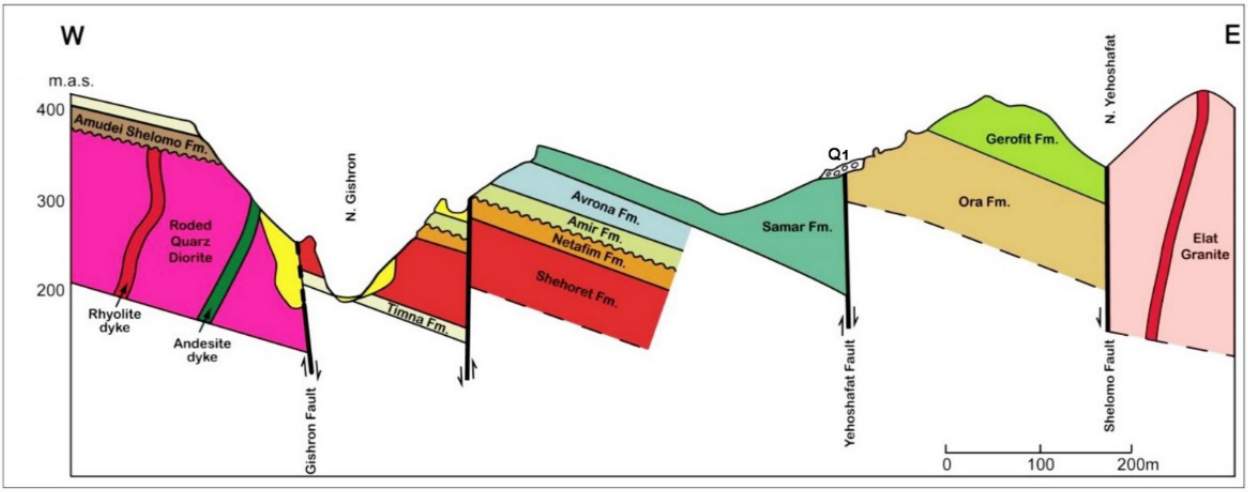

Figure 18: Generalized cross section, N. Gishron to N. Yehoshafat at Zafra Pass.

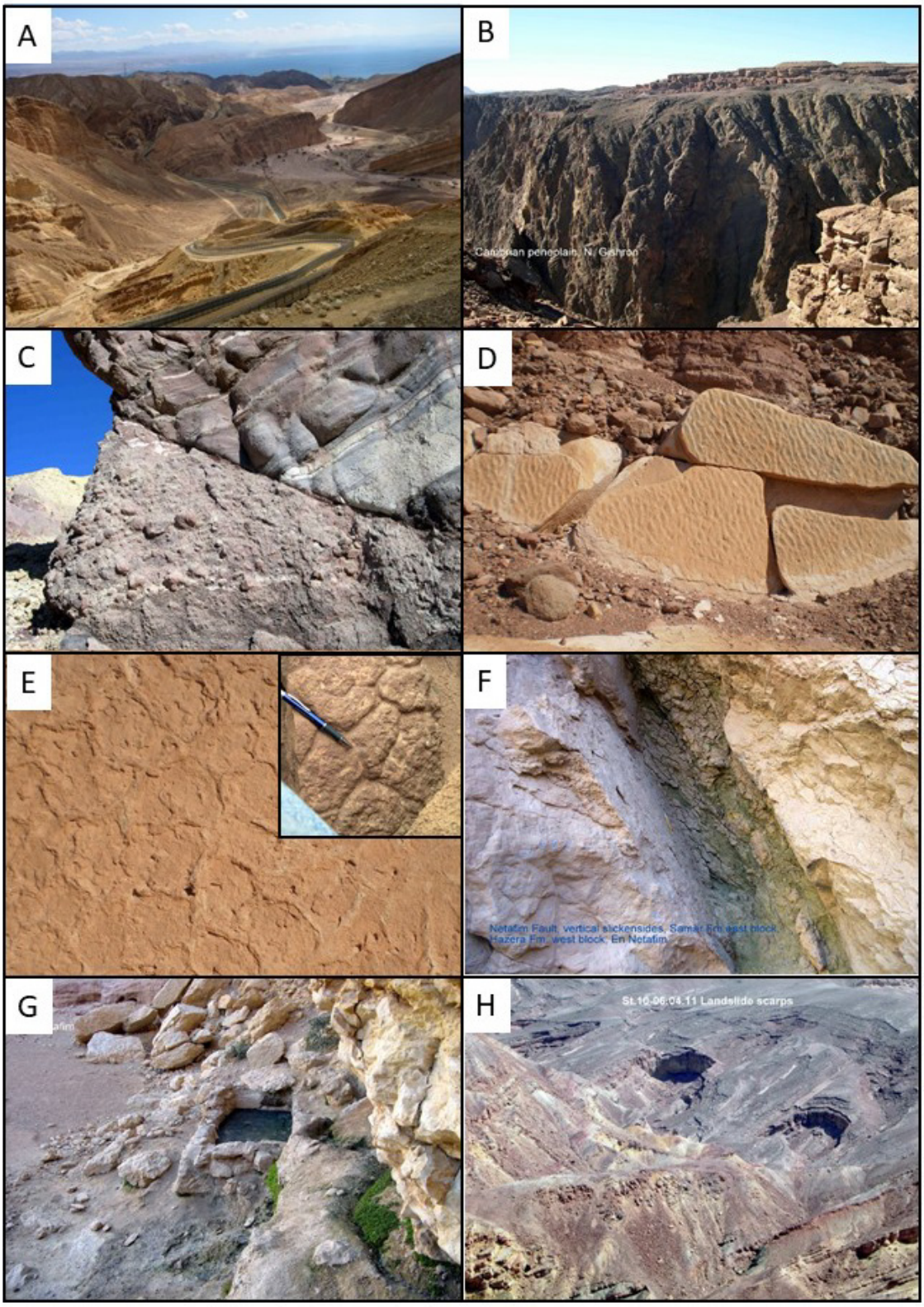

Figure 19: a. View from Coord. 188537/382330 to the road and the security Fence along N. Gishron through the junction with W. Taba to the Gulf of Elat/Aqaba. b. View south from Coord. 187634/387849 to the gorge of N. Gishron and the Early Cambrian peneplain on top of the ridge of ~700 m.a.s.l high. c. Sub-horizontal, listric fault between Amudei Shelomo bedded sandstone and the base conglomerate, adjacent to the Roded and Shelomo faults. Coord. 190479/390018. d&e. Mud cracks and ripple marks, White Mb., Shehoret Fm. Coord. 188291/385496. f&g. Netafim Fault and Ein Netafim spring. Coord. 188184/389947. f. View from north on Netafim Fault plane dipping 70º/235º with smear of green shale and vertical slickensides. East block sandstone of Samar Fm. west block limestone of Hevyon Mb., Hazera Fm. g. Ein Netafim a spring at the N. Netafim river bed. h. Three crescent scarps of embryonic tributaries at the Yotvata Mb. top of Hazera Fm. below the shales of the Ora Fm. Coord. 192394/397688.

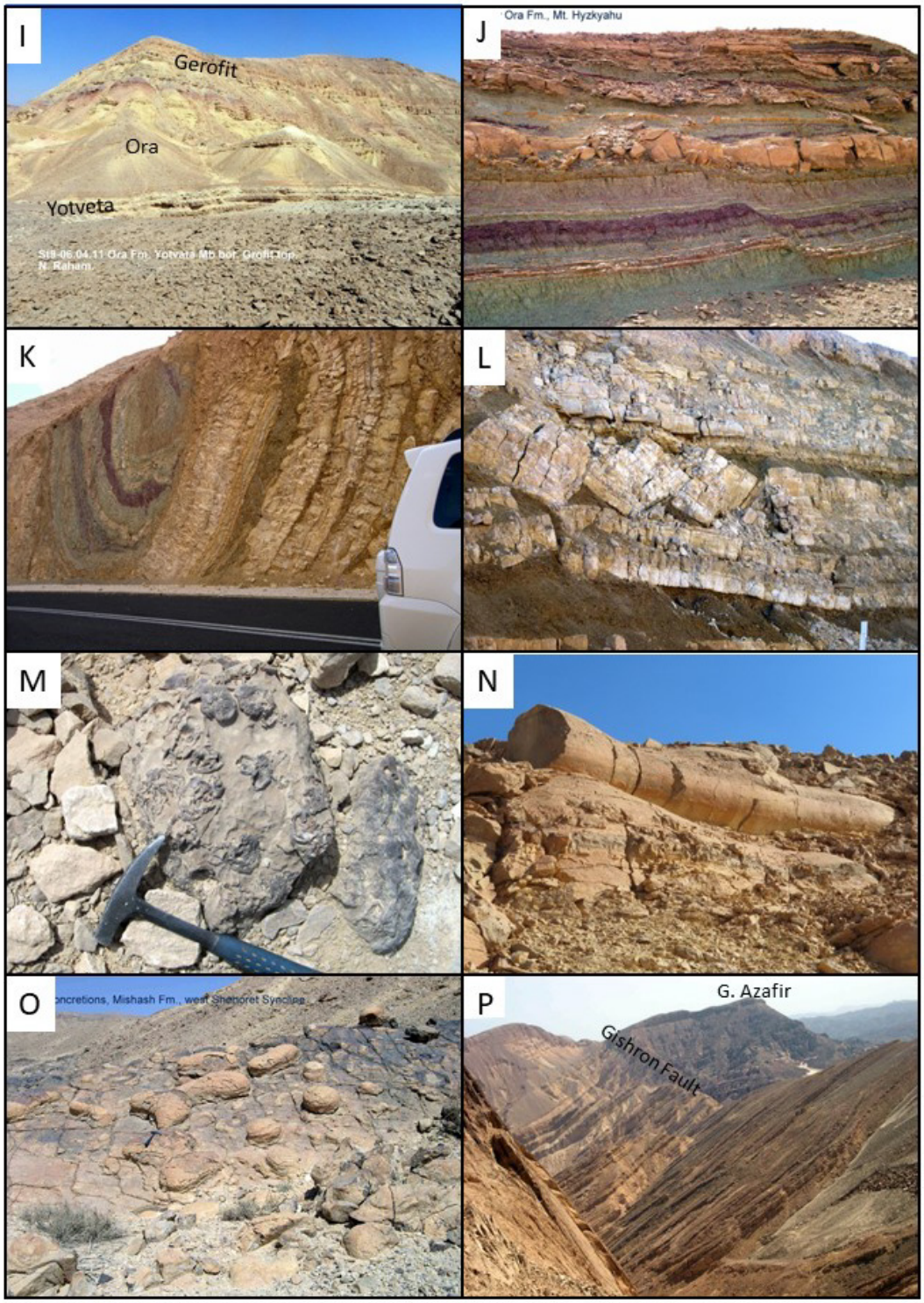

Figure 19 (cont.): i. Yotvata Mb. top Hazeva Fm. at the bottom cliff to the upper limestone cliffs of Grofit Fm. N. Shelalgon. Coord. 191250/399034. J. Green and purple shales, dolostone, limestone beds and gypsum of upper Ora Fm. Coord.188055/394533. Fossil flora from Late Cretaceous the earliest fully angiospermous flora found in this sequence in the Gerofit Valley 30 km north of the Timna Valley (Krassilov, et al., 2005). k. Fold of the upper Ora Fm. at the contact with base Gerofit Fm. in a folded area between the Gishron and Shelomo faults (Fig. 3). Coord. 188677/384847. l. Block rotation, due to bed-parallel horizontal shear, base Gerofit Fm. Mt. Hizkyahu. Coord. 188311/395672. m. *Hippurites* at top Grofit Fm. a Rudist index fossil for top Turonian. Coord. 190432/394359. n. Elongated chert 15 m.(?) concretion base Mishash Fm. Coord. 189833/420194. o. Carbonate concretions (Sass and Kolodny, 1972), Mishash Fm. N. Shehoret. Coord. 190742/393645. p. Axis of Taba West syncline plunging southward along the gully. North-south striking Gishron Fault, G. Azafir west block consist of Samar and Hazera formations, east block Taba east syncline consist of Ghareb, Taqiya formations and Avedat group on top, Coord. 189021/382921.

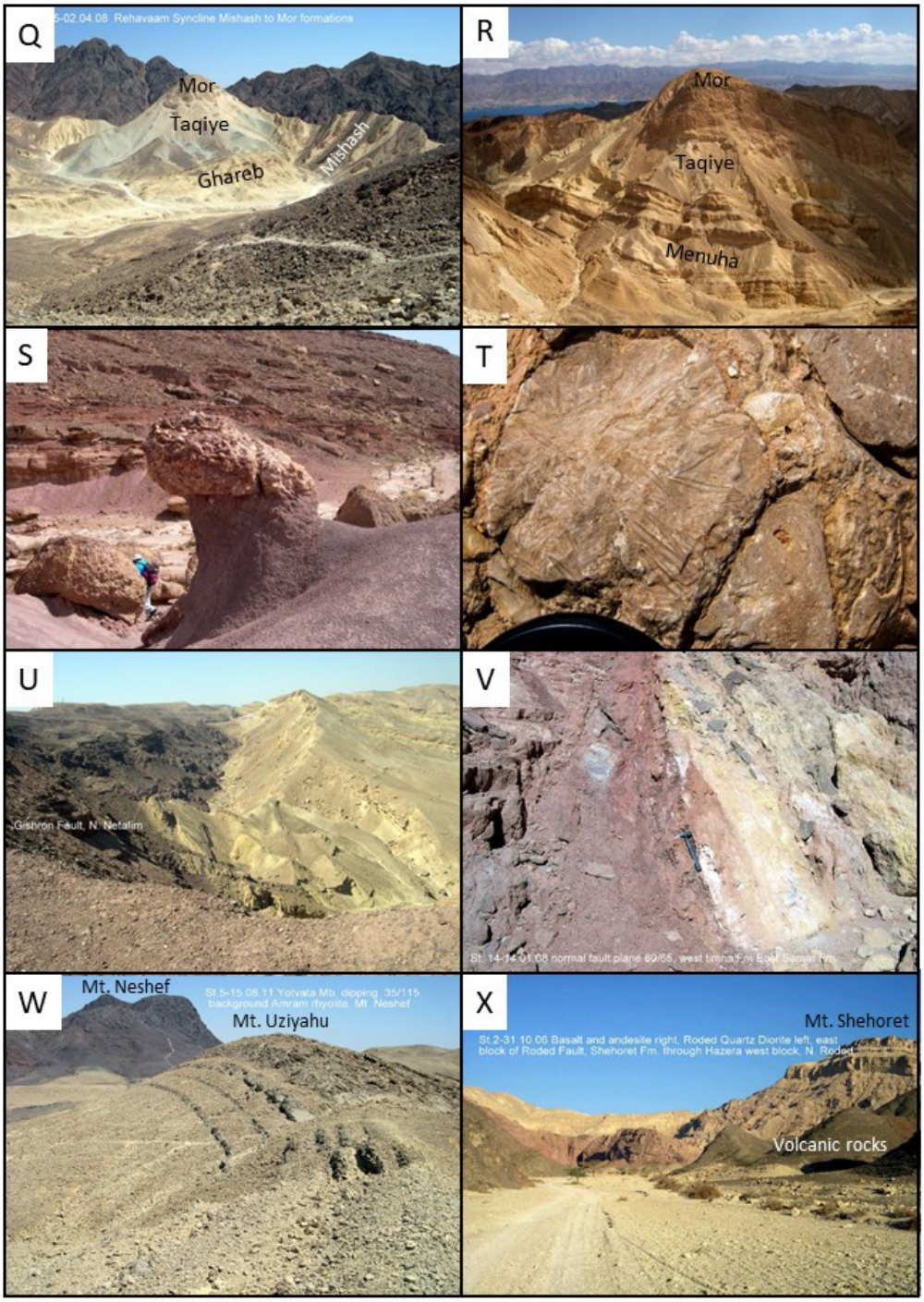

Figure 19 (cont.): q. Rehavaam Syncline, Mishash to Mor formations, at the background Mt. Yehoshafat and Mt. Rehavaam of the Roded Block. Coord. 188979/384005. r. Menuha, Mishash, Ghareb, Taqiye and Mor formations at the west limb of the Taba East Syncline. Gulf of Aqaba and Edom mountains at the background. Coord, 3819/1892. s. Conglomerate of base Amudei Shalomo Fm. overlay laterite formed by Early Cambrian pedogenesis of Amram Rhyolite, N. Gishron. Coord. 187592/388257. t. Nummulite, Eocene index fossil, boulder, Shelomo Syncline. Coord. 189406/388060. u. View from Road 12 northward to the Gishron Fault at upper N. Netafim. East block limestone and dolomite of Hazera Fm. west block Amudei Shelomo and Timna formations. Coord. 187500/389500. v. View northward at the Gishron fault plane dipping 80º/065º, west block Timna Fm., east block Samar Fm. N. Gishron. Coord. 187831/387448. w. View from south, from Mt. Uziyahu bedded limestone of Yotvata Mb. dipping 35º/115º to the Amram Rhyolite of Mt. Neshef, along the Neshef/Gishron Fault shear zone. Coord. 188236/397599. x. View from east, from N. Roded, across the Roded Fault, from the Roded Block to the Shelomo Graben. (Fig. 5&6,o) Coord. 191330/391605.

Elat Sabkha, Avrona Playa and the young recent faults (Figs. 20-22) - The eastern part of the Elat geological map consists of up-to 1,000 meters deep structural basins of the southern Arava (Frieslander, 2000) and the Gulf of Aqaba/Elat with a water depth of up to 1,500 m (Sade et al., 2008). On land the geomorphological expression of these depressions are the Avrona playa, Elat Sabkha and the alluvial fans of the ephemeral rivers draining eastward and partly cut by recent faults. Major young tectonic activity was documented at the N. Roded and N. Shehoret alluvial fans (Wieler et al., 2017; Zilberman et al., 2001). The general pattern of the active faults along the Dead Sea Transform cross the Arava alluvial fans, the Avrona Playa and the Elat Sabkha was presented by Garfunkel et al. (1981) and Wieler et al. (2017). Amit et al. (1999, 1996) suggested that at the Avrona Playa there were at least six earthquake events of magnitude 6 or larger, during the last 14,000 years. During the last 1,000 years a relief inversion occurred in the Avrona Playa as a result of an uplift by 1 meter due to a 6.1 magnitude earthquake. This event opened the previously closed drainage system and the Avrona Playa is now drained by N. Avrona to the Elat Sabkha. The young recent faults displace the Pliocene-Pleistocene Elot and Garof formations (Ginat et al., 1994) and were partly active during the last 10,000 years. In the city of Elat the young Shahamon Fault was mapped in detail and has been shown to have a fault plane of ~80^0/300^o and a vertical down throw of 7-10 meters of its western block (Israeli and Harash, 1990). Changes of stream direction as at Mt. Amram (Beyth and Mushkin, 2010), the N. Shehoret (Gellman et al., 2018) and Roded rivers (Weissbrod and Sneh, 1990) and the "capture" of the Gishron by the Yehoshafat River (Aydin and Eyal, 2002) which were controlled by the young Pliocene, Pleistocene and Holocene tectonic activity of the Dead Sea Transform are all documented at the Elat/Timna areas.

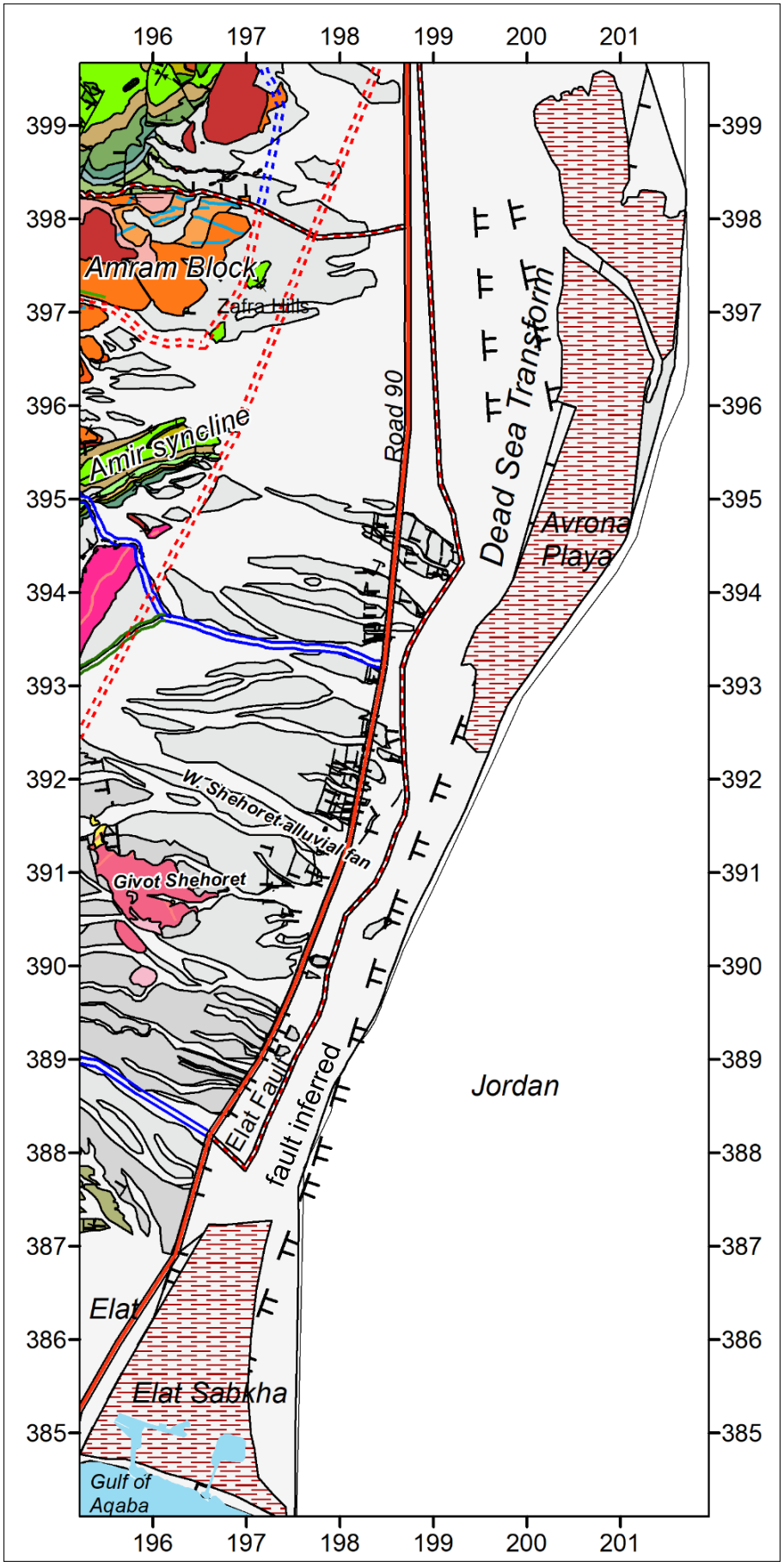

Figure 20: The geological map of the Elat Sabkha, Avrona Playa and the young recent faults.

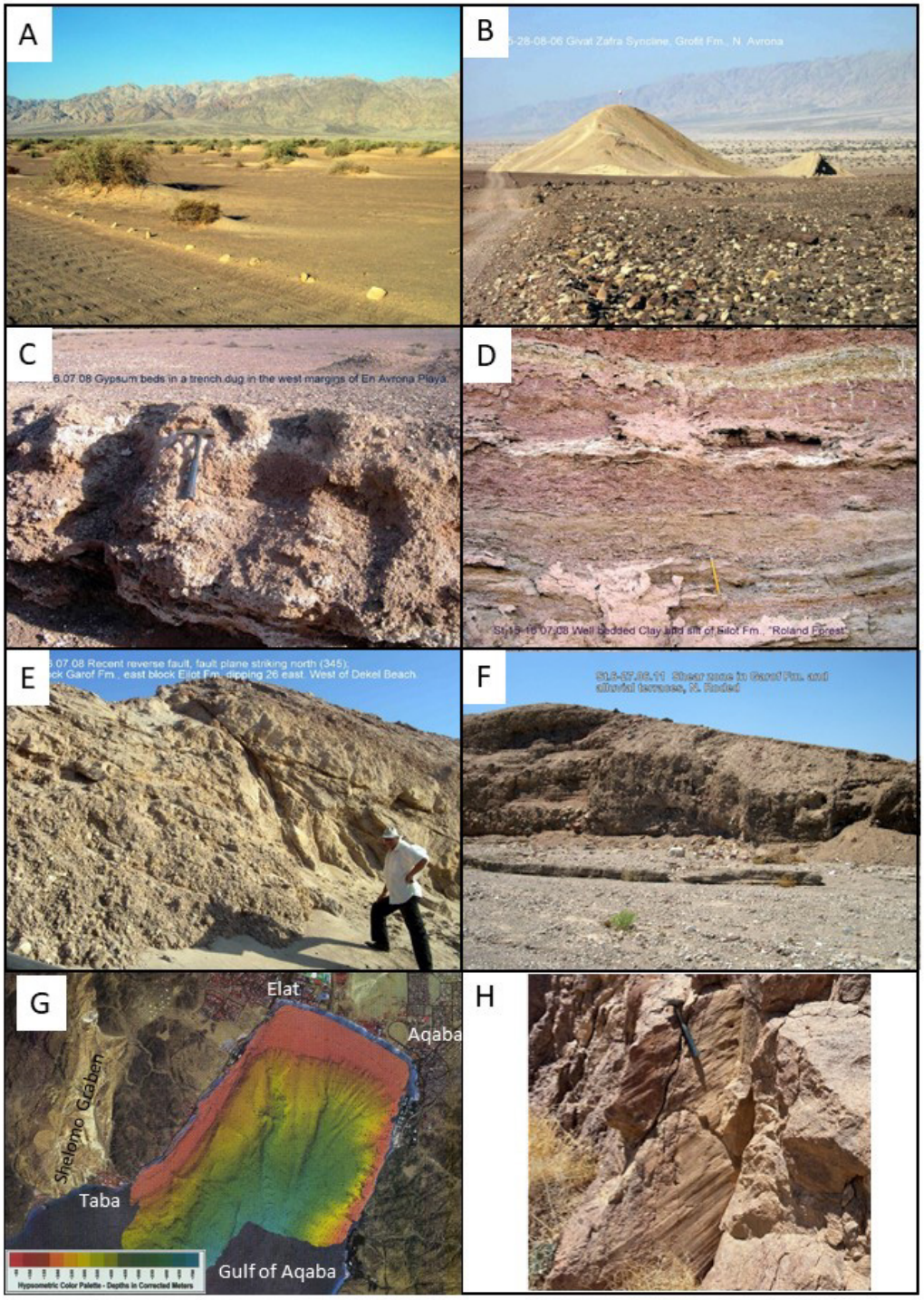

Figure 21: a. View eastward from Avrona Playa across the Arava/Araba, the rift of the Dead Sea Transform, to the Edom Mountains in south-west Jordan. b. Zafra Hills (Fig. 9) a Grofit limestone syncline plunging north-east, east of Mt. Amram in the Arava rift, Dead Sea Transform. Coord. 197090/397357. c&d. Gypsum beds in a trench dug in the Arava Playa. Coord. 199527/395581. e. View from south. A recent fault striking 345º azimuth between the boulders and sandstones of the Garuf Fm. west block and silt and shales of the Eilot Fm. dipping 26º east, east block. Coord. 194295/383567 f. View from south. Recent faults of the NE plunging Yotam Graben/Syncline in Pleistocene alluvial fans, N. Roded, west margins of the Arava, Dead Sea Transform. Coord. 193492/389721. g. Bathymetric map of the northern tip of the Gulf of Aqaba/Elat (Sade et al., 2008). Beach rocks and coral reefs terraces which indicate tectonic movements and sea level changes, are mapped along the south-west (Israel) and south-east (Jordan) head of the Gulf (Bar, 2014). h. A fault plane in Amram Rhyolite with sub-horizontal slickensides plunging 36º/223º, Mt. Neshef. Coord. 187840/397311.

Conclusions

The present crust in the Elat and Timna areas is telling the history of Planet Earth during 800 million years in this location and present a unique opportunity to be exposed to a large variety of rock types and structures not only for students but also for amateur geologists and tourists. This study present the variable and extremely well preserved outcrops and is based on up- to-date research, including both recent field studies as well as analytical geochemistry like isotope geology and and computer technic like GIS. The stratigraphy and structure of this area show its evolution from the Neproterozoic East African Orogen and the enclosure of the Mozambique Ocean through the accumulation of Cambrian to Eocene sedimentary sequence and up to the Miocene to recent evolution of the active plate boundary of the Dead Sea Transform. It is also possible to follow in this area some of the evolution of biota and flora during this evolution up to the Holocene Early Bronze copper mines when archaeology matches the geology. This story indicate the complexity and the time scale of this evolution and how precious and sensitive is our planet.

Acknowledgments

Yair Rotstein, Navot Morag and Ram Weinberger for editing the manuscript and the constructive comments.

References

Abbo, A., Avigad, D., Gerdes, A., Morag, N. and Vainer, S., 2020, Cadomian (Ca. 550 Ma) magmatic and thermal imprint on the North Arabian-Nubian Shield (south and central Israel): New age and isotopic constraints. Precambrian Research 346 (2020) 105804.

Amit, R., Zilberman, E., Enzel, Y. and Porat, N., 1996, Recent faults and characteristic earthquake in the Elat area-a field trip to the faults of Nalal Shehoret and Avrona Playa. Isr. Geol. Soc. Annual meeting, Elat, field trip guidebook p. 1-21 (in Hebrew).

Amit, R., Zilberman, E., Porat, N. and Enzel, Y., 1999, Relief Inversion in the Avrona playa as evidence of large-magnitude historical earthquakes, southern Arava Valley, Dead Sea Rift: Qurternary Research 52:76-91.

Anenburg, M. and Katzir, Y., 2014, Muscovite dehydration melting in Si-rich metapelites: microstructural evidence from Trondhjemitic migmatites. Roded, Southern Israel. Miner. Petrol. 108:137-152.

Angerer, T., Greilling, R. O. and Avigad, D., 2011, Fabric development in the weathering profile at a basement-cover interface, the sub-Cambrian peneplain, Israel: Implications for decollement tectonics: J. Structural Geol. 33:819-832.

Avigad, D., 1984. The deformation and metamorphism of the schistose dikes in the Elat area (NE Sinai). M.Sc. thesis, Hebrew University, Jerusalem, 85 pp.

Avigad, D., 1990, Geological map of the east-central part of the Roded area, 1:2500: Geol. Surv. Isr.

Avigad, D., Sandler, A., Kolodner, K., Stern, R. J., McWilliams, M., Miller, N. and Beyth, M., 2005, Mass-production of Cambro-Ordovician quartz-rich sandstone as a consequence of chemical weathering of Pan-African terranes: Environmental implications: Earth Planet Sci. Lett. 240:818-826.

Avigad, D. and Gvirtzman, Z., 2009, Late Neoproterozoic rise and fall of the northern Arabian-Nubian shield: The role of lithospheric mantle delamination and subsequent thermal subsidence: Tectonophysics 477:217-228.

Avner, U., Ginat, H., Shalev, S., Shilstine, S., Langford, B., Frumkin, A., Shem-Tov, R., Filin, S., Arav, R., Basson, U. Shemir, O., and Scott-Cummings, L., 2018, Ancient copper mines at Nahal Amram, Southern Arabah. Mining for ancient copper ed. E. Ben-Yosef Institute of Archaeology Tel Aviv University, Monograph Series 37:147-177.

Avner, U. and Shirav, M., 2001, Geo-archaeology of the Elat area -field trip. Isr. Geol. Soc. Ann. Meeting Elat. 71-79 pp.

Avni, Y., 2016, The new concept on the tectonics of the Elat region. Isr. Geol. Soc. Ann. Meeting Elat, 64-84 pp.

Avni, Y., Segev, A. and Ginat, H., 2012. Oligocene regional denudation of the northern Afar dome: pre- and syn-breakup stages of the Afro-Arabian plate. GSA Bulletin, 124:1871-1857.

Aydin, A, and Eyal, Y., 2002, Anatomy of a normal fault with shale smear: implications for fault seal. AAPG Bulletin, 36:1367-1381.

Bar, N., 2014, Tectonic movements and sea-level changes from coral reefs terraces along the north-east Gulf of Aqaba. Geol. Sur. Isr. Report No. GSI/14/2014. 79 pp (in Hebrew English abstract).

Bartov,Y., 1967, The geology of Beer Ora area, unpublished M.Sc. thesis, Hebrew University, Jerusalem (in Hebrew), 39 pp.

Bartov, J., Eyal, Y., Garfunkel, Z. and Steinitz, 1972, Late Cretaceous and Tertiary stratigraphy and paleogeography of southern Israel: Isr. J. Earth Sci. 21:69-97.

Bartov, Y., 1974, A Structural and Paleogeographical Study of the Central Sinai Faults and Domes. Ph.D Thesis submitted to the Hebrew University. 143 pp. (in Hebrew English abstract).

Be`eri-Shlevin, Y., 2008, The origin and evolution of Neoproterozoic magmatism in the northern Arabian-Nubian Shield (Sinai Peninsula, Egypt and southern Israel) evidence from stable and radiogenic isotope record. Ph.D. thesis, Ben-Gurion University, Israel. 134 pp.

Be`eri-Shlevin, Y., Katzir, Y. and Whitehouse, M., 2009, Post collisional tectonomagmatic evolution in the northern Arabian-Nubian Shield: time constraints from ion-probe U-Pb dating of zircon: J. Geol. Soc. 166:71-85.

Ben-Yosef, E., 2016, Back to the Solomon's Era: Results of the First Excavations at Slaves' Hill (Site 34, Timna, Israel). Bulletin of the American Schools of Oriental Research 376: 169-198.

Ben-Yosef, E., 2018, The Central Timna Valley Project: Research design and preliminary results. Mining for ancient copper ed. E. Ben-Yosef Institute of Archaeology Tel Aviv University, Monograph Series 37:28-63.

Beyth, M. and Segev, a., 1983, Lower Cretaceous Basaltic Plug in the Timna valley. Isr. J. Earth Sciences 32:165-166.

Beyth, M., Stern, R., J., Altherr, R. and Kroner, A., 1994, The Late Precambrian Timna Igneous Complex, southern Israel: Evidence for comagmatic type Sanukitoid monsodiorite and alkali granite magma: Lithos 31:103-124.

Beyth, M. and Reischmann, T., 1997, The age of the Quartz Monzodiorite, the Youngest Plutonic Intrusion in the Timna Igneous Complex. Isr. J., Earth Sciences 45: 223-226.

Beyth, M., Segev, a. and Bartov, Y., 1999a (updated 2021), Geological map of Israel 1:50,000, Be'er Ora Sheet, Geological Survey of Israel.

Beyth, M. and Heimann, A., 1999b, The youngest igneous event in the crystalline basement of the Arabian-Nubian Shield, Timna igneous complex: Isr. J. Earth Sci.: 48:113-120.

Beyth, M. and Mushkin, A., 2010, Mt. Amram, an E-W striking Neogene-Quarternary rejuvenated Early Cambrian structure. Isr. Geol. Soc. Ann. Meeting, Elot p. 37 (abstract).

Beyth, M., Eyal, y. and Garfunkel, z., 2011 (updated 2013), The geology of the Elat Sheet-explanatory notes. Geol. Surv. Isr. Report No. GSI/22/2011 updated March 2013, 59 pp.

Beyth, M., Eyal, Y. and Garfunkel, Z., 2012 (updated 2021), Geological Map of Israel 1:50,000, Elat Sheet. Geol. Surv. Isr.

Beyth, M., Eyal, Y. and Garfunkel, Z., 2014a, The Geology of the northern tip of the Arabian-Nubian Shield. J. African Earth Sci. 99:332-341.

Beyth, M. and Calvo, R., 2014b, The Timna Valley as a geological park. Geol. Surv. Isr., Report GSI/09/2014, 69 pp. (in Habrew).

Beyth, M. and Calvo, R., 2015, The Elat area as a field school for geology. Geol. Surv. Isr., Report GSI/10/2014, 86 pp. (in Hebrew, English abstract)

Beyth, M., Sagi, A., Hajazi, H., Alkhraisha, S., Mushkin, A. and Ginat, H., 2017, New evidence on the accurate displacement along the Arava/Araba segment of the Dead Sea Transform. Int. J. Earth Sci., ISSN 1437-3254.

Beyth, M., Segev, A. and Ginat, H., 2018a, Stratigraphy and structure of the Timna Valley and adjacent ancient mining areas. Mining for ancient copper ed. E. Ben-Yosef Institute of Archaeology Tel Aviv University, Monograph Series 37: 3-20 p.

Beyth. M., Calvo, R. and Eyal, Y., 1918b, Nahal Gishron Geological Track, Elat area. Geological Survey of Israel Report GSI/29/2018. 56 pp. (in Hebrew English abstract).

Beyth, M., Mushkin, A., Calvo, R. and Eyal. Y., 2020a, Disemination of the geology of the Amram Block and Amir Syncline, Elat Reservation, south Israel. Geological Survey of Israel Report GSI/02/2020. 60 pp. (in Hebrew English abstract).

Beyth, M., Calvo, R., Katz, O. and Morag, N., 2020b, Dissemination of the geology of Mt. Yedidia, north Roded Block and Shelomo Graben along the Netafim, Roded and Shehoret rivers. Geological Survey of Israel Report GSI/34/2020. 52 pp. (in Hebrew, English abstract).

Dafni, J., 2010, Eilat's Mountains. Ye'ela Publishers 192 pp. (in Hebrew).

Elicki, O. and Geyer, A., 2013, The Cambrian trilobites of Jordan-taxonomy, systematic and stratigraphic significance. Acta Geological Polonica, 63:1-56.

Elisha, B., Katzir, Y., & Kylander-Clark, A. (2017). Ediacaran (~620 Ma) high-grade regional metamorphism in the northern Arabian Nubian Shield: U-Th-Pb monazite ages of the Elat schist. Precambrian Research, 295, 172-186.

Elisha, B., Katzir, Y., Kylander-Clark, A., R., C., Golan. T., Coble, M., A., 2019, The timing of the migmatization in the northern Arabian-Nubian Shield: Evidence for a juvenile sedimentary component in collision-related batholiths. J. Metamorph Geol. 37:591-610.

Eyal, M. and Peltz, S., 1994, The structure of Ramat Yotam Caldera, southern Israel: A deeply eroded Late Precambrian ash-flow caldera: Isr. J. Earth Sci.: 43:81-90.

Eyal, M., Litvinovsky, B.A., Katzir, Y. and Zanvilevich, A N., 2004, The Pan-African high- K calc-alkaline peraluminous Elat Granite from southern Israel: geology, geochemistry and petrogenesis: J. Afric. Earth Sci. 40:115-136.

Eyal, Y., 1967, The geology of the sedimentary rocks at Nahal Shelomo-Nahal Netafim region, M.Sc. thesis, Hebrew University, Jerusalem, 38 pp. (in Hebrew).

Eyal, Y., 1973, The tectonics of the Shelomo and Yotam grabens, Elat, Israel: Isr. J. Earth Sci.: 22:165-184.

Eyal, Y., 1980, The geological history of the Precambrian metamorphic rocks between Wadi Twaiba and Wadi Um-Mara, NE Sinai: Isr. J. Earth Sci., 29:53-66.

Eyal, Y., Eyal, M. and Kroner, A., 1991, Geochronology of the Elat terrain, metamorphic basement and its implication for crustal evolution of the NE part of the Arabian-Nubian Shield: Isr. J. Earth Sci. 40:5-16.

Eyal, Y., Eyal, M., Calvo, R., Hall, J. K., Rosensaft, M., 2017, Geological map of the Elat metamorphic belt, Taba area, NE Sinai, Egypt, 1:50,000. Ben Gurion University of the Negev and the Geological Survey of Israel.

Freund, R., 1961, Distribution of Lower Turonian ammonites in Israel and the neighboring countries. Bull. Res. Council Isr. 10:79-100.

Garfunkel, Z., 1970, The tectonics of the western margin of the southern Arava: Ph.D. thesis, Hebrew University, Jerusalem, 204 pp. (In Hebrew, English abstract)

Garfunkel, Z., 1980, Contribution to the geology of the Precambrian of the Elat area; Is. J. Earth Sci. 20:25-40.

Garfunkel, Z., 1999, History and paleogeography during the Pan-African orogen to stable platform transition: Reappraisal of the evidence from the Elat area and the northern Arabian-Nubian Shield: Isr. J. Earth Sci.: 48:135-157.

Gellman, Y., Matmon, A., Mushkin, A. and Porat, N., 2018, Drainage system reorganization and late Quaternary tectonic deformation along the southern Dead Sea Transform. Quaternary Research 53:1-14.

Ginat, H., 1997, The geology and landscape evolution of the Hiyyon and Zihor valleys: Ph.D thesis, Hebrew University, Jerusalem, 115 pp. (in Hebrew, English abstract).

Ginat, H., Zilberman, E. and Amit, R., 2001, Red sedimentary unit as indicators for Early Pleistocene tectonic activity in the southern Negev desert, Israel. Geomorphology 1146: 127-146. .

Gutkin, V. and Eyal, Y., 1998, Geology and evolution of Precambrian rocks, Mt. Shelomo, Elat area: Isr. J. Earth Sci.: 47:1-17.

Israeli, A. and Harash, A., 1990, Shahmon area, Eilat, a geotechnical report for the master plane; Tahal Engineering, Rep. 04/90/10, 20 pp. (in Hebrew, an English appendix)

Karcz, I. and Key, C. A., 1966, Note on the pre-Paleozoic morphology of the basement in the Timna area (southern Israel): Isr. J. Earth Sci. 15:47-56.

Karcz, I., Weiler, Y. and Key, C.A., 1971, Lithology and environment of deposition of the Amudei Shelomo Sandstone ("NSP") in Nahal Shani, Elat. Isr. J. Earth Sci. 20:119-124.

Katz, O, Beyth, M., Miller, N., Stern, R., Avigad, D., Basu, A. and Anbar, A., 2004, Late Neoproterozoic (~630 Ma) high-magnesium andesite suit from southern Israel: implications for consolidation of Gondwanaland: Earth Planet Sci. Lett. 218:475-490.

Katz, O., Avigad, D., Matthews, A. and Heimann, A., 1998, Precambrian metamorphic evolution of the Arabian-Nubian Shield in the Roded area, southern Israel: Isr. J. Earth Sci.:47:93-110.

Katz, Y., Weinberger, R., and Starinsky, A. 2002. Faulting in porous sandstones, Amir Mountain, southern Israel. Isr. Geol. Surv. Isr. Current Res. 13:59-63.

Katzir, Y., Litvinovsky, B., Eyal, M., Zanvilevich, A. and Vapnik, y., 2006, Four successive episodes of Late Pan-African dikes in the central Elat area, southern Israel. Isr. J. Earth Sci.; 55:69-93.

Katzir, Y., Litvinovsky, B.A., Jahn, B. M., Eyal, M., Zanvilevich, A.N., Valley, J. W., Vapnik, Ye., Beeri, Y. and Spicuzza, M.J., 2007, Interrelations between coeval mafic and A-type silicic magmas from composite dykes in a bimodal suite of southern Israel, northernmost Arabian-Nubian Shield: Geochemical and isotope constraints: Lithos, 97:336-364.

Kessel, R., Stein, M. and Navon, O., 1998, Petrogenesis of Late Neoproterozoic dikes in the northern Arabian-Nubian Shield. Implications for the origin of A-type granites. Precambrian Res. 92:195-213.

Kohn, B. P., Eyal, M. and Feinstein, S., 1992, A major Late Devonian-Early Carboniferous (Hercynian) thermotectonic event at the NW margin of the Arabian-Nubian Shield: Evidence from zircon fission-track dating . Tectonics 11:1018-1027.

Kolodner, K., 2007, The provenance of the siliciclastic section in Israel and Jordan: U-Pb dating of detrital zircons. Ph.D. thesis, Hebrew University, Jerusalem, 133 pp.

Krassilov, V., Lewy, Z., Nevo, E. and Silantieva, 2005, Late Cretaceous (Turonian) flora of southern Negev, Israel. Pensoft Pablishers. 252 pp.

Kroner, A., Eyal, M. and Eyal, Y., 1990, Early Pan-African evolution of the basement around Elat, Israel, and the Sinai Peninsula revealed by single-zircon evaporation dating, and implications for crustal accretion rates: Geology 18:545-548.

Lifshitz, A., Honigstein, A., Livnat, A., Roded, R. and Flexer, A., 1985, The Sayyarim Formation, Nahal Ya'alon area, southern Arava Valley: Lithostratigraphy, Ostracode biostratigraphy and paleoenvironmental implications: Isr. J. Earth Sci. 34:193-204.

Matthews, A., Reymer, A. P. S., Avigad, D., Cochin, J. and Marco, S., 1989, Pressures and temperatures of Pan-African high-grade metamorphism in Elat Association, NE Sinai: Isr. J. Earth Sci. 38:1-17.

Miller, N., R. and Stern, R., J., 2021, Evolution of the Arabian Nubian Shield and Snowball Earth. Edi. Hamimi, Z., Fowler, A-R,. Liegeois, J-P., Collins, A., Abdelsalam., H. G. and El-Wahed. M. A. The Geology of the Arabian Nubian Shield. SpringerLink. pp. 153-194.

Morag, N. and Avigad, D., 2010, Crustal evolution of the continental crust in the Arabian Nubian Shield in the Elat Area: Isr. Geol. Soc. Ann. Meeting, Eilot, Field Trip. pp. 49-57 (in Hebrew).

Morag, N., Avigad, D., Gerdes, A., Belousova, E. and Harlavan, Y., 2011a, Crustal evolution and recycling in the northern Arabian-Nubian Shield: new perspectives from zircon Lu-Hf and U-Pb systematics, Precambrian Res. 186:101-116..

Morag, N., Avigad, D., Gerdes, A. and Harlavan, Y., 2011b, Crustal evolution in the northern Arabian-Nubian Shield revealed by the Elat Conglomerate detrital zircon archive. Isr. Geol. Soc. Ann Meet. Mitzpe Ramon, abstract p. 111.

Morag, N., Avigad, D., Gerdes, A., Belousova, E. and Harlavan, Y., 2011c, Detrital zircon Hf isotopic composition indicates long-distance transport of North Gondwana Cambrian-Ordovician sandstones: Geology 39/955-958.

Morag, N., Avigad, D., Gerdes, A. and Harlavan, Y., 2012, 1000-580 Ma crustal evolution in the northern Arabian-Nubian Shield revealed by U-Pb-Hf of detrital zircons from Late Neoproterozoic sediments: Precambrian Res. 197-212.

Mushkin, A., Navon, O., Halicz, L., Hartmann, G. and Stein, M., 2003, The petrogenesis of A-type magmas from the Amram Massif, southern Israel. J. Petrol.: 44:815-832.

Nuriel, P., Weinberger, Kylandar-Clark, A. R. C., Hacker, B. R., Craddock, J. P., 2017, The onset of the Dead Sea transform based on calcite age-strain analyses. Geology 45(7):587-590.

Parnes, A., 1971, Late Lower Cambrian trilobites from the Timna area and Har Amram (southern Negev, Israel): Isr. J. Earth Sci. 20:179-205.

Paz, Y., 1997, The geology and the stratigraphy of the volcano-sedimentary units in Nahal Netafim and Nahal Roded in the Elat area: Implications for the history of the Late Precambrian in the Elat region: Unpubl. M.Sc. thesis, Ben Gurion University (in Hebrew, English abstract): 121 pp.

Peltz, S. and Eyal, M., 1995, Lithology and volcanic stratigraphy of Givot Shehoret, Elat region, 1995, Geol. Sur. Isr. Rep. GSI/10/95, 16 pp.

Porat, N., Amit, R., Enzel, Y., Zilberman, E., Avni, Y., Ginat, H. and Gluck, D., 2010, Abandonment ages of alluvial landforms in the hyperarid Negev determined by luminescence dating. J. Arid Environ., 74:861-869.

Sade, A.R., Hall, J., K., Tibor, G., Niemi, T., M., Ben-Avraham, Z., Hartman, G., Akawwi, F., Alueladas, A. and Amit, G., 2008, Multibeam bathymetry of the northern Gulf of Aqaba/Elat. Geol. Surv. Isr. Rep. GSI/03/2008.

Sandler, A., Teutsch, N. and Avigad, D., 2011, A sub-Cambrian pedogenesis recorded in weathering profiles of the Arabian-Nubian Shield: Sedimentology 50:1305-1320.

Sass, E. and Kolodny, Y., 1972, Stable isotopes, chemistry and petrology of carbonate concretions (Mishash Formation, Israel). Chemical Geology 261-286.

Segev, A., 1984, Lithostratigraphy and Paleogeography of the marine Cambrian sequence in southern Israel and southwestern Jordan: Isr. J. Earth Sci. 33:26-33.

Segev, A., Rybakov, M., Weissbrod, T. and Beyth, M., 1995, Lower Cretaceous gabbroic intrusion at shallow depth in the Timna Valley, southern Israel. Isr. J. Earth Sci. 44:137-148.

Shimron, A.E., 1972, The Precambrian Structural and Metamorphic History of the Elat Area: Ph.D. Thesis, Hebrew University, Jerusalem: 244 pp.

Shirman, b., Ribakov, M., Beyth, M., Mushkin, A. and Ginat, H., 2015, Deep structure of Mount Amram igneous complex, interpretation of magmatic and gravity data, Geophysical Journal International, 200:1362-1373.

Stein, M. and Goldstein, S.L., 1996, From plum head to continental lithosphere in the Arabian-Nubian Shield: Nature 382:773-778.

Steinitz, G., 1967, Petrological problems in the Mishash Formation, Southern Negev. M.Sc. Thesis submitted to the Hebrew University, Jerusalem. 57 pp. (in Hebrew).

Steinitz, G., 1970, Chert “dike” structures in Senonian chert beds, Southern Negev, Israel. J. Sediment. Petrol., 40:1241-1254.

Stern, R., J., 1994. The Assembly and Continental Collision in the Neoproterozoic East African Orogeny Implications for the Consolidation of Gondwanaland. Ann. Rev. Earth. Planet. Sci. 22:319-351.

Vapnik, Y., 1993, Fluid inclusions in metamorphic rocks of the Elat area. Isr. J. Earth Sci. 42:71-84.

Weinberger, R., Nuriel, P., Kylander-Clark, A. R. C. Craddock, J., P., 2020, Temporal and spatial relations between large-scale fault systems: Evidence from the Sinai-Negev shear zone and the Dead Sea Fault. Earth-Science Reviews 211 (2020) 103377.

Weissbrod, T., 1961, The geology and petrography of the Roded Massif: unpubl. M.Sc. thesis Hebrew University, Jerusalem (in Hebrew), 64 pp.

Weissbrod, T., 1965, Precambrian volcanism at Roded Massif, Elat area: Isr. Geol. Soc. Ann Meet., abstract p. 11 (in Hebrew).

Weissbrod, T., 1969, The Paleozoic of Israel and adjacent countries, part II. Geol. Surv. Isr. Bull. 48, 32 pp.

Weissbrod, T., 1980, The Paleozoic of Israel and adjacent countries (lithospheric study). unpubl. Ph.D. thesis, Hebrew University, Jerusalem, 275 pp. (In Hebrew, English abstract).

Weissbrod, T. and Sneh, A., 1990, Capturing of streams in the Roded area- an indication for young tectonic activity along the rift margins: Isr. Geol. Soc. Ann. Meet., Field Trip, Elat, p. 25-26 (in Hebrew).

Weissbrod, T. and Sneh, A., 1997, Stratigraphy and sedimentology of the Lower Cretaceous Amir Formation in Israel and Sinai: A marine clastic deposit with tidal channels. Isr. J. Earth Sci. 46:79-93.

Weissbrod, T., 2005, The Paleozoic in Israel and Environs. In: Hall et al., (Eds), Geological Framework of the Levant Volume II: The Levantine Basin and Israel, Historical Production Hall, p. 283-316.

Wieler, N., Avni, Y., Ginat, H. and Rosensaft, M., 2017, Quatenary map of the Eilat Region on a scale of 1:10,000 with explanatory notes. Geol. Surv. Isr. Rep. GSI/37/2016. 18 pp. (in Hebrew with English abstract).

Wurtzburger, U., 1959, The geology and petrography of the Amram mountains: M. Sc. Thesis, Hebrew university, Jerusalem (in Hebrew).

Zilberman, E., Amit, R. and Nachmias, Y. 2001, Mapping fault systems around Nahal Roded and Gevaot Shehoret : Israel Geol. Surv. Isr. Rep. GSI/25/2001, 14 pp. (in Hebrew).

Appendix I: Location map of figures.

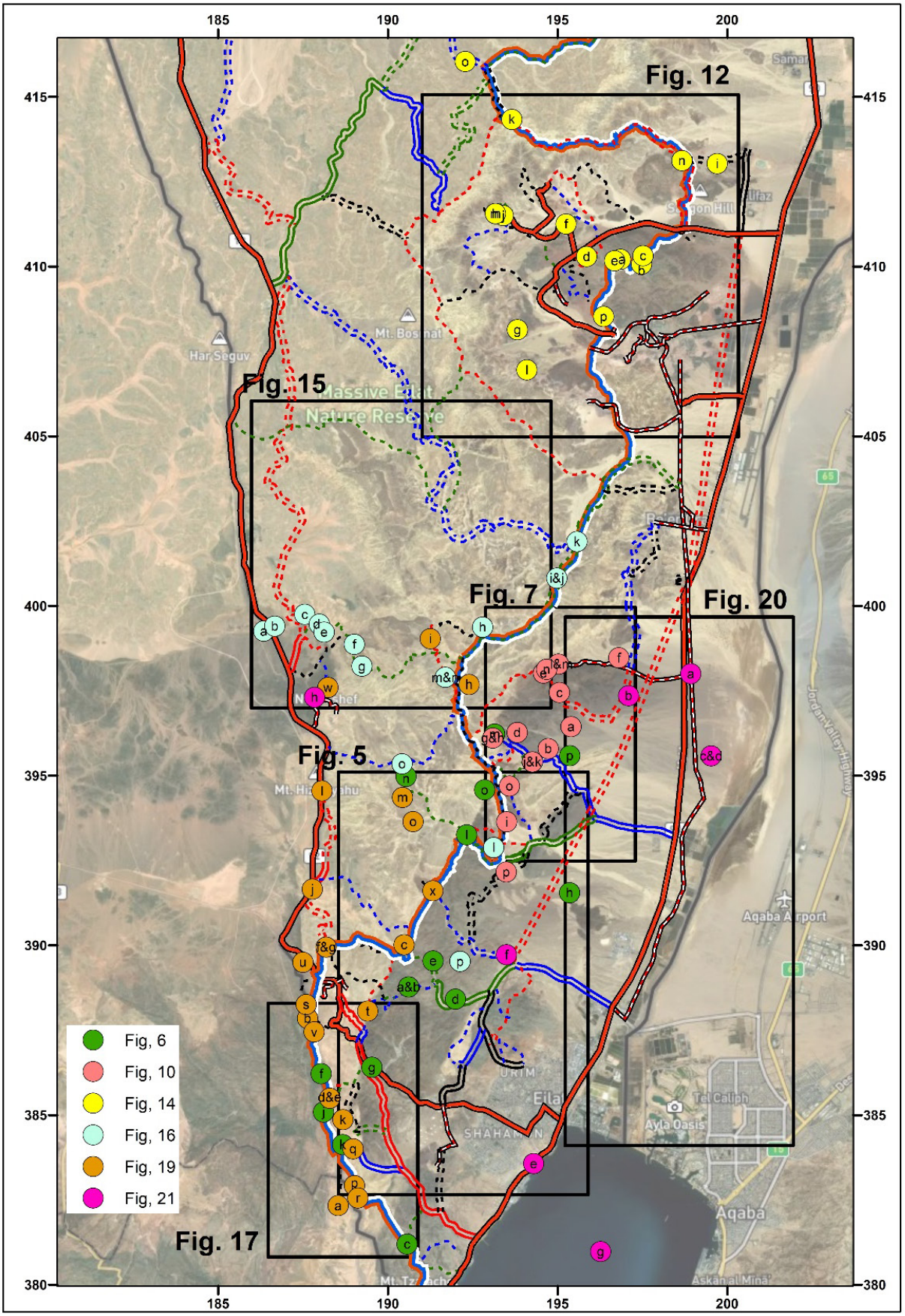

Appendix II: Location of photos.

Figure #	Israel grid ITM		Report chapter
	E. coord.	N. Coord.	
6a&b	190612	388773	Roded & Elat blocks
6c	190565	381197	
6d	191992	388413	
6e	191335	389543	
6f	188038	386217	
6g	189533	386406	
6m	193148	396227	
6n	190541	394974	
6o	192855	394580	
6p	195361	395588	
10a	195399	396444	Amram Block & Amir Syncline
10b	194726	395794	
10c	195056	397448	
10d	193810	396275	
10e	194582	398020	
10f	196802	398473	
10g&h	193095	396106	
10i	193502	393637	
10j&k	194263	395406	
10l&m	195023	398288	
10n	19470	398184	
10o	193580	394694	
10p	193487	392163	
14a	196858	410212	Timna Valley
14b	197473	410073	
14c	197517	410317	
14d	195858	410297	
14e	196681	410171	
14f	195250	411257	
14g	193820	408140	
14h	193168	411563	
14i	199704	413036	
14j	193399	411503	
14k	193655	414335	
14l	194093	406957	
14m	193168	411563	
14n	198664	413121	
14o	192284	416040	
14p	196358	408530	
16a	186347	399260	Themed Fault & Raham Syncline
16b	186669	399408	
16c	187550	399750	
16d	187985	399464	

16e	188122	399228	
16f	189010	398872	
16g	189238	398225	
16h	192793	399375	
16i&j	194977	400820	
16k	195800	402200	
16l	193120	392880	
16m&n	191695	397896	
16o	190422	395350	
16p	192129	389527	
19a	188537	382330	Shelomo & Yotam Grabens
19b	187634	387849	
19c	190479	390018	
19d&e	188291	385496	
19f&g	188184	389947	
19h	192394	397688	
19i	191250	399034	
19j	188677	384847	
19l	188311	395672	
19m	190432	394359	
19n	189833	420194	
19o	190742	393645	
19p	189021	382921	
19q	188979	384005	
19r	382532	189142	
19s	187592	388257	
19t	189406	388060	
19u	187500	389500	
19v	187831	387448	
19w	188236	397599	
19x	191330	391605	
21a	198570	398210	Elat Sabkha & Avrona Playa
21b	197090	397357	
21c&d	199527	395581	
21e	194295	383567	
21f	193492	389721	
21g	196500	381600	
21h	187840	397311	

Supplementary

I

THE MINISTRY OF NATIONAL INFRASTRUCTURES
GEOLOGICAL SURVEY OF ISRAEL

The Geology of the Elat Sheet
Explanatory Notes

Beyth, M.,[(1)] Eyal, Y.[(2)] and Garfunkel Z.[(3)]

(1) The Geological Survey of Israel
(2) The Department of Geology and Environmental Sciences, Ben- Gurion University
(3) Earth Sciences Institute, the Hebrew University, Jerusalem

Report No. GSI/22/2011

Jerusalem, October, 2011
Updated March 2013

This map is dedicated to our teacher Prof. Yakov Bentor a pioneer in the geological study of the Elat area.

List of Contents

1. Introduction……1
2. Geomorphology……1
3. Stratigraphy……...2
4. Structure……..9
5. Landslides and rock collapse……11
6. Economic aspects……12
7. Previous studies ……..12
8. Acknowledgment……..13
9. References……13

1. Introduction

Three major processes controlled the geological and geomorphological evolution of the Elat area (Fig. 1): 1) The creation of the Arabian-Nubian Shield during the Neoproterozoic as part of the East African Orogen and the enclosure of the Mozambique Ocean between the east and west Gondwana plates; 2) Accumulation of the Cambrian to Eocene sedimentary sequence on the Arabian Plate at the southeast margins of the paleo-Tethys and Tethys Sea; 3) The Miocene to Recent evolution of the Dead Sea Transform, a sinistral fault, which is the plate boundary between the Arabian Plate to the east and the African Plate to the west (Fig. 2).
The stratigraphy and structure of the well-exposed rocks in the extreme arid climate of the Elat area document these three processes and thus make the geology of the Elat Sheet so unique.
Therefore the extensive research done in the Elat area has turned this region into a field laboratory for geoscience students. The Elat Sheet geological map was prepared as part of the 1: 50,000 scale geological mapping project of the Geological Survey of Israel and is based on previous maps updated by the present study. This most recent effort of very detailed mapping was carried out on a 1:10,000 average scale using GIS and orthophoto as the base map.

2. Geomorphology

The eastern part of the Elat Sheet consists of up-to 1,000 meters deep structural basins of the southern Arava (Frieslander, 2000) and the Gulf of Aqaba/Elat with a water depth of up to 1,500 m (Sade et al., 2008). On land the geomorphological expression of these depressions are the Avrona playa, Elat sabkha and the alluvial fans of the ephemeral rivers (wadis) draining eastward. These rivers (wadis), which drain into the southern Arava and the gulf are from south to north: Taba and it's tributary Gishron, Shelomo, Garof, Shahmon, Netafim, Roded with its tributary Yael, Shehoret, Amram, Zefunot, Avrona with its tributary Nizoz, and Raham with it's tributaries Shelalgon, Shani and Uziahu. On the west, most of these rivers incise on their upper parts, the sedimentary rocks of the Shelomo Graben. To the southeast they incise the metamorphic-magmatic rocks of the Roded and Elat blocks and to the north the Amram Block. The topographic elevation in the eastern part of the Elat Sheet, at the Avrona playa, ranges from sea level to +40 m. The elevation in the western part ranges from 700 m. at Mt. Shelomo to more than 800 m. above sea level at Mt. Hizkiyahu and Mt. Neshef. This sharp difference in the east-west relief, which occurs over less than 15 km is the major reason for the canyon morphology of most of these ephemeral rivers. Changes of stream direction as at Mt. Amram (Beyth and Mushkin, 2010), of the Shehoret and Roded rivers (Weissbrod and Sneh, 1990) and the "capture" of the Gishron by the Yehoshafat River (Eyal, 1967) were all the result of the young Pliocene, Pleistocene and Holocene tectonic activity of the Dead Sea Transform and its margins. Garfunkel (1970) presented a detailed study of the evolution of the rift margins in the southern Arava.

3. Stratigraphy

The Elat area consists of three major rock sequences: 1) The Neoproterozoic metamorphic and magmatic basement; 2) the sedimentary rocks from Cambrian to Eocene and 3) The clastics and playa deposits accreted during the evolution of the Dead Sea Transform since the Miocene. An Early Cambrian peneplain separates between the first two sequences (Beyth and Heimann, 1999) and an Oligocene erosion surface between the second and the third sequences (Avni et al., 2011a, b).

3.1 The metamorphic and magmatic rocks were mapped at the Elat, Roded and Amram blocks as part of the northern margins of the Arabian-Nubian Shield (Bentor, 1961; Garfunkel, 1980, Fig. 3). These rocks formed during more than 300 milion years of the Neoproterozoic crustal evolution (Be'eri-Shlevin et al., 2009; Kolodner, 2007; Kroner et al., 1990; Morag et al., 2011a, b). The oldest rock association was mapped at the Roded and Elat blocks and the youngest at Mt. Amram (Mushkin et al., 2003). The U-Pb dating and Hf isotopic analysis of single detrital zircons from the Late Neoproterozoic Elat Conglomerate bear evidence for two major magmatic cycles, island-arc magmatism peaking at ~800 Ma and post-collisional granitoids and volcanics, which invented the amalgamated arc crust peaking at 610-630 Ma. The results of the Hf isotopic analysis are in line with the overall juvenile character of the Arabian-Nubian Shield with some contamination of older crust (Morag et al., 2012; Fig. 4).

3.1.1 The metamorphic rocks of the Elat block consist of the metapelitic and metapsammitic Elat Schist, 800-813 Ma of age (Kroner et al., 1990). The metamorphic minerals in the schist are biotite, garnet, staurolite, cordierite, andalusite and silimenite (Shimron, 1972). The Elat Schist is intruded by the quartz-diorite Taba Gneiss, with an age of 782-790 Ma (Morag et al, 2011a; Kroner et al., 1990) and by the Elat Granitic Gneiss, 740-744 Ma of age (Kolodner, 2007; Kroner et al., 1990). Garfunkel (1980, 1999) suggested the existence of two orogenic phases separated by 50 million years. Two metamorphic phases are distinguished in the Elat metamorphic association, the medium to high temperature amphibolitic and the low pressure amphibolite-greenschist facies (Morag and Avigad, 2010). The mineralogic association suggests temperatures of 580 to 660 C^0 and pressures between 4.6 to 3.8 Kbar (Matthews et al., 1989).

The metamorphic rocks of the Roded block are the Roded Migmatites and Roded Schists, 800 Ma old (Morag et al., 2011a). The metamorphic amphibolitic facies suggests temperatures up to 650 C^0 and pressure between 4 to 5 Kbar. The peak of the metamorphic event was pre-750 Ma (Katz et al., 1998).The Roded Migmatites of Mt. Shelomo developed from the Roded Schist by metamorphic segregation while the protolite of the Roded Gneiss was probably magmatic (Gutkin and Eyal, 1998). At Nahal Netafim the metamorphic rocks encircle the east and south margins of the younger plutonic rocks of the Roded Quartz Diorite.

The metamorphic rocks of the Elat and Roded blocks represent an event of subduction, formation of island arcs, erosion of the arcs, deposition of the erosion products and metamorphism of these sediments. This event took place between ~800 Ma (the age of the zircons in the schists), to 780-790 Ma (the age of the zircons in the Taba Gneiss; Eyal et al., 1991). The schists were intruded by quartz dioritic and granitic plutons after the first metamorphic event and metamorphosed to form rocks such as the Elat Granitic Gneiss. The andesitic magnesium-rich schist dykes (Garfunkel, 1970; Shimron, 1972;

Avigad, 1984; Katz et al., 2004) of the low, greenschist, metamorphic facies and with an age of 705 Ma (Morag, et al, 2011a) mark the end of the metamorphic events.

3.1.2 The calc-alkaline intrusions, the Shahmon Metabasite in the Elat block 640-644 Ma (Kroner et el., 1990; Morag et al., 2011a), Roded Granite Porphyry, 642 Ma (Morag et al., 2011a), Roded Quartz Diorite, 634 Ma (Stein and Goldstein, 1996; Katz et al., 1998) and Elat Granite, 630 Ma (Be'eri-Shlevin et al., 2009) in the Elat and Roded blocks mark the post-collision cratonization phase of the orogen. Some foliation was observed in the Shahmon Metabasite, Roded Quartz Diorite and in the Elat Granite. Eyal et al., (2004) suggested that the Elat Granite consists of two plutons, with the one on the eastern margins of Mt. Shahmon is foliated, metamorphic, and is therefore distinguished as the Shahmon Granitic Gneiss.

The intrusions of the alkaline granites such as the Amram, Shahmon and Yehoshafat granites, 608 Ma (Be'eri-Shelvin et al., 2009; Morag et al., 2011a), are accompanied by rhyolite dykes, 609 Ma (Morag and Avigad, 2010), andesite and composite dykes which mark the extension phase (Beyth et al., 1994). Occasionally such as in the "Dyke Country" at Mt. Shelomo the dykes form 85% of the outcrop (Gutkin and Eyal, 1998). The Shahmon Granite intrudes the Roded Quartz Diorite in numerous small intrusions (Bentor, 1961).

3.1.3 The volcano-conglomeratic event is the final major magmatic event in the Elat area, represented by the Amram Rhyolites, basalts, andesits and conglomerates of the Mapalim Formation in the Roded block (Paz, 1997, Weissbrod, 1965), andesites and trachytes at Gevaot Shehoret (Peltz and Eyal, 1995), acid volcanic rocks at the Yotam Caldera (Eyal and Peltz, 1994). The basalt and andesite volcanic rocks in Mt. Shelomo, hypabyssal shallow intrusions of the Amram Monzonite and Amram Quartz Syenite are also part of this event (Mushkin et al., 2003).
The Roded Conglomerate, the Mapalim Formation and the Elat Conglomerate in Mt. Shelomo (Gutkin and Eyal, 1998), dated at about 590 Ma (Morag et al., 2011b), are the products of a major erosion phase in which 12,000 m. of the section were removed (Garfunkel, 1999). Garfunkel (1970) interpreted this outcrop at N. Shelomo with the far travelled origin of the sediment and absence of local detritus as a graben because of the knife-sharp contact between the coglomerats and enclosing granites. The Elat Conglomerates are a product of cohesive debris flows whereas the Roded Conglomerate and the Mapalim Formation are fluviatile sediments (Kagan et al., 2010). Rhyolite, andesite and composite dykes 585 Ma. of age (Katzir et al., 2007) intrude these conglomerates. A petrologic study of these dykes that intruded the Elat Granite at Mt. Shahmon was conducted by Kessel et al. (1998). The Neoproterozoic basement is truncated by a peneplain and the youngest dolerite dyke below it is of 532 Ma age (Beyth and Heimann, 1999) and was mapped in the Elat Sheet at the southern part of Mt. Amram. Identical ages were reported from the dolerite intrusions in the Zenifim Formation (Weissbrod, 2005). This Early Cambrian peneplain was formed by erosion of 2,000 m. of the section (Garfunkel, 1999) and by chemical weathering (Sandler et al., 2011). At the junction of Nahal Amir and Nahal Shehoret the Roded Granite Porphyry was altered to kaolinite, suggested by Sandler et al., (2011) to be a relict of a thick lateritic section that was removed before the sedimentation of the conglomerates of the Early Cambrian Amudei Shelomo Formation. Avigad and Gvirtzman (2009) suggested that the lowering of the Arabian-Nubian Shield to sea level at Early Cambrian was

significantly accelerated by post-delamination cooling and thermal subsidence during the last stages of "down wear" when erosion usually slows down.

The result of the geochronological studies indicate two possible major breaks in the Neoproterozoic magmatic activity: ~60 million years hiatus is between the metamorphic rocks and the calc-alkaline intrusions and the ~55 million years hiatus between the rhyolite, andesite and composite dykes and the dolerite dyke.

3.2 The sedimentary rocks. The pre-Dead Sea Transform sediments, from Cambrian to Eocene, consist in the Elat area of five groups: Yam Suf, Kurnub, Judea, Mount Scopus and Avedat (Fig. 5).

3.2.1 Yam Suf Group: The lower, Cambrian part of the sedimentary section consistss four formations: Amudei Shelomo, Timna, Shehoret and Netafim, described by Weissbrod (1969, 2005) and Segev (1986). They onlap the Early Cambrian peneplain for example, at Mt. Amram. A paraconformity, a stratigraphic gap, of 380 million years separates between the Aptian Amir Formation and the Cambrian Netafim Formation. This gap is the result of three uplift events that led to the erosion of approximately 2,500 m. of mainly lower Paleozoic and less upper Paleozoic and lower Mesozoic (Weissbrod, 2005; Kohn et al., 1992; Vermeesch et al., 2009). This paraconformity is well exposed in the north at Givat Yokheved and at the southwest margins of Mt. Amir syncline. The sand of the Yam Suf Group must have been transported several thousand kilometers from south to north Gondwana before deposition (Morag et al., 2011c). Avigad et al., (2005) suggested that the vast sheet of mature Cambro-Ordovician sand blanket of north Africa and Arabia are essentially first order cycle sediments derived from the Neoproterozoic basement. The **Amudei Shelomo Formation** of Early Cambrian age is consists of sub-arkosic sandstones and conglomerates filling a moderate relief, which was formed along a drainage system towards north and northwest (Karcz and Key, 1966). The base of this formation around Nahal Shehoret and Nahal Gishron is a dark-brown silty-clay bed a few meters thick. The Amudei Shelomo Formation was mapped at the southern margins of Mt. Amram, at the southeast margins of the Mt. Amir syncline, south-east of Nahal Shehoret, at Nahal Shani the Red Canyon and at Nahal Gishron. The **Timna Formation** is exposed in the Timna basin to the north and in the Elat basin to the south, which are separated by the east-west trending Mt. Amram and Mt. Neshef ridges (Segev, 1984). This formation is divided into the Hakhlil and Sasgon members. The lower Hakhlil Member consists of silt and sandstone with rhyolitic breccia at the base, whereas the upper, Sasgon Member consists of three lithofacies: dolomite, sand and clay (Segev, 1986). The dolomite at the Elat basin is dolomitic thrombolite. The sand is sub-arkosic with sandy columnar stromatolites (Soudry and Weissbrod, 1995). The age of the Timna Formation is Early Cambrian (Parnes, 1971) forming in a transgressive-regressive cycle along the coast of a pre-tethys sea. This formation is exposed at the Netafim pass, at the northern margins of Mt. Amram overlaying the Amudei Shelomo Formation. A full section of the Timna Formation with dolomite and limestone beds, manganese nodules and mud cracks occurs in Nahal Amir close to its junction with Nahal Shehoret. The **Shehoret Formation** consists of silt and sandstone deposited in a coastal environment. The formation was divided into three members along the margins of the Mt. Amir syncline: the lower sub-arkosic multicolored Member, 30-40 m. thick, the White Member of sub-arkosic sandstones with *Skolithus* with a maximum thickness of 52 m, and an upper Variegated Member up to 60 m thick consisting of red to brown clay alternating with white sub-arkosic to silt beds (Weissbrod, 2005). The **Netafim Formation**, 20 m.

thick consists of fine-grained sandstone deposited in a tidal environment, unconformably overlying the Shehoret Formation. The upper members of the Shehoret Formation and the Netafim Formation are missing in the Timna Valley (Segev et al., 1992). The dark-brown color, which is very distinctive on the airphotos, is typical for the Yam Suf Group.

3.2.2 The **Kurnub Group** (previously called the Hatira Formation) of the Lower Cretaceous consists of Amir, Avrona and Samar formations (Weissbrod 2005). The **Amir Formation** is a white friable, fine to mediun-grain quartz kaolinitic sandstone with recumbent cross-bedding, trace fossils and tidal channels (Weissbrod and Sneh, 1997) covered by a typical yellow-brown patina. The age of the Amir Formation is between Late Barremian to Early Aptian and its thickness is approximately 50 m. The **Avrona Formation** medium to coarse-grained sandstones with quartz pebbles of 5-10 cm in diameter and is up to 70 m thick. It is characterized by rounded cliffs, caves and large-scale cross bedding. The age 0f this formation is Aptian to Albian. Nodules of sulfidic copper mineralization with secondary green mineralization coating are common at the top of the Amir Formation and at the base of the Avrona Formation. Copper mineralization was also found along fractures and was mined in ancient times at Amudei Amram. The **Samar Formation** of middle Albian to Late Albian age is 80 to 130 m thick and consists of fine to medium grain- size of quartz sandstone, with lateritic beds. The age of this Formation is Albian. The Kurnub Group is of alluvial origin and forms the soft geomorphological unit below the carbonate cliffs of the Judea Group. The Kurnub Group outcrops along the margins of Mt. Amram, Nahal Netafim and Nahal Shani, in the southern cliff of Mt. Shehoret and north and south of Nahal Gishron.

During Late Barremian-Albian the southern margins of the Tethys Sea transgressed over the Arabian-Nubian continent in pulses evidenced by shallow marine sediments in between terrestrial clastics. Since the Early Cenomanian the sea covered the Elat region and gradually progressed southwards into Sinai (Egypt).

3.2.3 The **Judea Group** consist of four Cenomanian-Coniacian marine formations: Hazera, Ora, Gerofit and Zihor which were described by Bartov et al. (1972). The 120 m. thick **Hazera Formation,** is divided into four members, which are well observed at the Mt. Amir syncline. The lower one is the Hevyon Member that forms a 30 m. thick light brown dolomite cliff with up to 10 m. thick yellow glauconitic-dolomitic- sandstone bed at its base, unconformably overlying the Samar Formation. The next member is En Yorqe'am, that is 30 m. thick consist of green marl and clayey limestone rich in bivalves, gastropods and echinoderms. The gray limestone with chert nodules and *Nerinea* of the Zafit Member forms a 30 m high cliff. The “double cliff” of the lower Hevyon Member and the upper Zafit Member with the marly En Yorqe'am Member in between, is an important marker for geological mapping. The assignment of the members of the Hazera Formation described above and shown on the map, assumes a particular correlation with the type section of this formation. However, another correlation is also possible (Arkin et al., 1967). The section in the Elat area may also be interpreted to comprise only the Zafit, Avnon and Tamar members (i.e what is shown as Hevyon may actually be the Zafit member, etc.). More studies are needed to resolve this uncertainty.
The upper part of the Hazera Formation, the Yotvata Member is white to gray well-bedded limestone at its lower parts, paper limestone at the middle and white limestone with the ammonite *Neolobites Vibrayeanus* indicative of the Late Cenomanian at its upper part. A thin red-brown limonitic-dolomite bed at the very top of the Yotvata Member marks the top Hazera Formation. During the Late Cenomanian-Early Turonian

elongated shallow basins striking northeast-southwest developed in the Negev (Freund, 1962). In the Elat area the largest basin of this type was with a water depth of 50 to 100 m. where the **Ora Formation** (previously called Ora Shales) was deposited. The basin was situated between its coast to the south and the elevated carbonate platform belt (Ramon-Judea) to the north. Relative sea-level fluctuations temporarily turned the basin into a lagoon with brackish-water during influx of runoff water with plants, or hypersaline conditions depositing dolomite and gypsum. The Ora Formation is up to 108 m thick and is divided to three members: The lower member is mainly green to gray shales with gypsum veins and thin beds of yellow nodular limestone with Early Turonian ammonites. The middle member is known as the Vroman Bank (named at Makhtesh Ramon basin) consists of fossiliferous dolostone with the Turonian ammonite genus *Choffaticeras* and the gastropod *Tylostoma Cossoni* of Early and Middle Turonian. The upper member of the Ora Formation is red and green beds of shale, a 5 m thick massive gypsum bed and thin beds of limestone and dolostone. The soft morphology and the red and green shales with the gypsum bed are useful mapping markers. Complete sections of the Ora Formation are found at Nahal Shelalgon, the eastern part of Nahal Shani, at the axis of the Mt. Amir syncline and north of Maale Elat. The shales of the Ora Formation along some of the marginal faults of the Dead Sea Transform and the Themed Fault are folded into diapir like structures e.g at upper Nahal Shelomo Syncline, Nahal Shani and between Nahal Gishron and Nahal Yehoshafat. West of Mt. Amram the shale of the Ora Formation is the lubricant for the eastward sliding of a large massive block of the Grofit Formation. The **Gerofit Formation** of Late Turonian age is 130 m thick and consists of gray, finely crystallized limestone precipitated in a shallow sea. The lower part is limestone interbedded with green clay. Disharmonic structure and block rotation such as are found at Mt. Yoachaz, attest to horizontal shearing along the rift margins. The middle part of the formation is a white chalky limestone rich in ostracoda and foraminifera. The upper part consists of well-bedded limestone and dolostone with thin beds of chert and chert nodules and crustaceae burrows. The upper part forms a brown distinct cliff above the soft white carbonate. The *Hippurites* rudist of Turonian age found on the top of the Grofit Formation at the upper part of Nahal Shehoret indicating upward shallowing during the deposition of this formation. The Gerofit Formation forms planes at the northern parts of the Shelomo Graben, at Mt. Shehoret, at the structures along the Shelomo, Gishron and Yotam faults and at the Mt. Amir syncline. Inclined blocks of the Gerofit Formation are often obrerved to slide over the shale of the Ora Formation, which tend to cover the exact contact between these two formations and therefore inferred contact are used on the map. The **Zihor Formation** of Late Turonian-Coniacian age was mapped by Bartov (1967) as the Eteq Formation. It forms a light red-brown distinctive unite, up to 30 m thick, overlying the light brown-grayish limestone of top Gerofit Formation. It consists of limestone, marl and dolostone rich in fossils such as stromatoporoids and oysters. A one meter thick massive brown bed of clastic dolomite forms the base of the Zihor Formation at the upper part of Nahal Shehoret. In the same location at the top of the formation underlying the chalk of the Menuha Formation marl with *oncolites* (Lewy, 1972) of about 1 cm in diameter and the Coniacian ammonite *Heterotissotia neoceratites* were found. The Zihor Formation is mapped in the Taba, Rehav'am, Shelomo and Mt. Amir synclines and at Nahal Raham and in the upper part of Nahal Shehoret.

3.2.4 Mount Scopus Group consists of four formations: Menuha, Mishash, Gareb and Taqiye. The Menuha and Mishash formations were integrated by Bartov et al. (1967) into the Sayyarim Formation. The **Menuha Formation** is built of two chalk units, the lower

one is 20 m. thick and the upper 25 m. thick. Between them are (from bottom to top) sandstone beds, 10 m. of dolostone beds and 20 m, and occasionally of marl and in chert beds with phosphorite. The sandstone unit thins northward from 45 m. at the Taba syncline, to 25 m. at the Shelomo Syncline and to 10 m. at Nahal Raham (Bartov et al., 1972; Eyal, 1967). This sandstone bed was previously described as the Sand Member which changes northward to a shaly–marly member, in which the big oyster *Pycnodonte vesicularis* is common. The sandstone bed was also mapped at the axis of the Mt. Amir syncline close to the Arava Fault. Chalks of marine pelagic origin are typical of the Menuha Formation in central and northern Israel and are enriched in clastic sediments from continental origin southward in the Elat area. In the Raham Syncline the Menuha Formation consist of white chalk at its lower part and yellow marl at the upper part, and in total ~ 20 m. thick. The late Santonian Ostracoda *Limburgina miarensis* of biozone S3 (Lifshitz et al., 1985) was identified (A. Honigstein per. Com.) and also fish tooth and phosphatic bones (?). The overall thickness of this formation ranges from 80 to 100 m. The boundary between the Late Coniacian-earliest Campanian Menuha Fm. and the Campanian Mishash Fm. is at the contact between the second chalk bed and the main chert of the Sayarim Formation of Bartov et al. (1972). The **Mishash Formation** consists of three units: The lower the main chert bed, 25 m. thick, the middle soft carbonate rock with phosphorite, 20 m. thick and the upper porcelanite with phosphorite on top, 30 m. thick. The upper part of the Mishash Formation is marked by concretions of chert and limestone >1 m diameter. These two formations were mapped in the Taba, Rehavam, Shelomo, Shehoret west, Mt. Amir and Raham synclines and as small blocks along the north-south faults at the northern part of the Shelomo Graben. At the Raham Syncline in the white chalk of the Mishash Fm (third chalk (?)) the Ostracoda *Brachycythere beershavansis* and *Ventrocythereis rotunda* of biozone S-5a, early Late Campanian were identified (A. Honigstein per. Com., Lifshitz et al., 1985). Two chert beds with many concretions are exposed at the Rehavam and Shehoret west synclines. These two formations Menuha and Mishash were deposited in very different environment than those of the Judea Group. Sedimentation of the Mt. Scopus Group occured in an unstable shelf rich in nutrients and organic material while the Judea Group was deposited in a shallow sea poor in nutrients and tectonically stable. The **Gareb Formation** of Maastrichian age is built of well-bedded yellow-reddish marly chalk with gypsum veins and is up to 70 m thick. It is exposed in the Taba, Rehavam, Shelomo and Shehoret west synclines and in small outcrop at Nahal Netafim at the northern terminus of the Yotam Graben. The **Taqiye Formation** is built of green clay and marl with limonitic nodules with pyrite at the center. The Taqiye Formation was mostly mapped in association with the Gareb Formation. The thickness of both formations ranges from a few meters to a few tens of meters. The boundary between the Gareb and Taqiye formations is the base of the Cenozoic Era and Tertiary System which is characterized by a biological turnover such as the extinction of the dinosaurs.
Correlation, isopach and facies maps for the formations of the Judea and Mount Scopus groups for the northern Negev and Sinai are presented by Bartov and Steinitz (1977).

3.2.5 Avedat Group of Eocene age is divided in the Negev to four formations: Mor, Nizana, Horsha and Matred. In the Elat Sheet most probably the equivalent of the Mor Formation of Early to Middle Eocene are exposed. These rocks were mapped in the Nahal Shelomo, Nahal Rehavam and Taba synclines and consist of well bedded white chalk with chert interbeds and limestone concretions up to 1 m. in diameter. In Nahal Taba the Eocene rocks are up to 100 m thick (Eyal, 1967) and are most probably of Early

to Middle Eocene. At the Nahal Shelomo Syncline the top of the Mor formation is truncated by the Raham Conglomerate.

3.3 The **young clastic rocks** (previously called the Upper Clastic Unit) of Miocene-Pliocene-Pleistocene age were deposited as a result of the rifting. At the northwest margins of the rift at the Shaham planes and Nahal Shani the Arava Formation (Avni et al., 2001) and the Zehiha Formation (Ginat, 1997; Ginat et al. 2001) are overlying the Oligocene peneplain. The **Arava Formation** is a fluvio-lacustrine formation consisting of Pliocene conglomerates. They were deposited along the margins of the rift between 4-2 Ma at a relatively stable tectonic phase after the end of the main rifting phase that controlled the Miocene-Pliocene drainage pattern (Avni et al., 2001). The Sagi Member of the Arava Formation is up to 30 m. thick and was mapped in the Elat Sheet as a conglomerate consisting of up to 3 meters in diameter of well rounded boulders of local origin mainly carbonates and less chert and rhyolite. The average imbrication of the boulders indicate westward flow direction. The Arava Formation unconformably overlays the Mt. Neshef rhyolites and the Judea and Mount Scopus groups. The **Zhiha Formation** of Pleistocene age consist of fine-grained sandstone and red clayey-silt that unconformably overlies the Arava Formation (Ginat et al., 2001). Beds of calcitic paleosoils with carbonate concretions formed by pedogenic processes are common in the Zhiha Formation in contrast to more recent gypsiferous soils. These soils of the Zhiha Formation were developed in closed basins along the Pleistocene major rift fault systems when the flow direction in the rivers changed from westward to eastward. The calcitic paleosole is likely to suggest a more humid, semi-arid, climate than the present extreme-arid climate. The thickness of the Zhiha Formation is around 10 meters.
In the rift zone west of Elat at Nahal Shelomo Syncline the Miocene **Raham Conglomerate** was mapped (Garfunkel et al., 1974) and north and south of Elat the Elot and Garof formations (Ginat et al., 1994). The Raham Conglomerate is a poorly sorted, coarse conglomerate in which the boulders are rounded to angular and mainly consisting of the Avdat Group with nummulites and without magmatic and metamorphic boulders. Avni et al., (2011) suggested the Raham Conglomerate to be of the Eocene age. The Pliocene **Elot Formation** is up to 20 m. thick and is divided of two units: The lower brown-light red and in places green, well-bedded clayey sandstone with carbonate concretions and an upper unit of medium size-grained sandstone with fossil flora roots and pebble beds of magmatic origin. The **Garof Formation** of Pleistocene age is up to 20 meters thick and overlies the Elot Formation with an angular unconformity at the Holand Forest, north of Elat. At its lower part pebbles up to 50 centimeter in diameter are embedded in a sandy matrix. In its upper part conglomerates with a bed of large boulder up to 3 meters in diameter are observed. A white colored desert pavement developed at the top of the Grof Formation. Old **river terraces** (Q_1) were mapped east of Nahal Gishron and around Nahal Shelomo which, contain diorite boulders transported from an intrusion west of Nahal Gishron. These terraces represent a pre-Nahal Gishron drainage pattern and are of Early pleistocene age. The young terraces (Q_2) are part of the recent drainage system and is dated as Middle Pleistocene to Recent. The dating of six levels of Q_2 terraces at Nahal Shehoret alluvial fan east of Gevaot Shehoret was carried out by Porat et. Al., (2010) using the OSL method. The oldest age was >231,000 and the youngest 14,000 years. The accurate definition of the stratigraphy, dating the river terraces, in the Elat area needs additional research.

4. Structure

The structures of the Elat Sheet were classified into three types: 1) The ancient Neoproterozoic metamorphic/magmatic, 2) the young Dead Sea Transform and it's margins, and 3) the structures related to the Themed east-west dextral fault system.

4.1 The **ancient Neoproterozoic structures** are expressed by the metamorphic fabric and the dyke directions, which are all parts of the evolution of the East African Orogen and the Arabian-Nubian Shield. This tectonic event was terminated by extension, exhumation and peneplanation.
The structure of the metamorphic rocks in the **Elat block** is characterized by southward dipping foliation with east-west striking isoclinal folds (Shimron, 1972). These folds vary from isoclinal to kink folds and their size ranges from a few centimeters to a few meters as observed in Nahal Shelomo. The total thickness of the schists is approximately 10 Km. It was suggested that they constitute the northern flank of the east-west striking Murach Syncline, the axis of which lies along Wadi Murach 20 Km south of Elat (Eyal, 1980). At Nahal Yael a tectonic contact (thrust?), was mapped between the Elat Schist and the Elat Granitic Gneiss (Avigad, 1984). The foliation of the metamorphic rocks of the **Roded block** is vertical and its strike is north-south with isoclinal folding of a few tens of centimeters (Katz et al., 1998).
The Schist dykes intruding the Elat Granitic Gneiss at the Elat Block strike east-west (Shimron, 1972) and thus indicate a north-south extention during the intrusion and subsequent parallel shearing. The dominant direction of the rhyolite, andesite and composite dykes in the Elat and Roded blocks is north-south whereas in the **Amram block** it is east-west. These directions suggest perpendicular extention in the Late Neoproterozoic. Some of the Volcano-Conglomeratic complex at the Roded Block is preserved in east-west striking grabens (Garfunkel, 1999).
The pink, thick and morphologically positive rhyolite dykes are a useful marker of horizontal faults, such as the sinistral faults at Mt. Tzefahot, where these dykes intrude the grey Taba Gneiss.

4.2 The **young faults** (Figs. 2, 6, 7, 8): The major structures in the Elat area developed as part of the young tectonic activity associated with the Dead Sea Transform. These structures are the Gulf of Elat, the Elat Sabkha, Avrona Playa and the Yotam and Shelomo grabens. The grabens and the step faulting along the margins of the rift are controlled by north-north-east sinistral faults which also have a vertical component. The major faults at the south and central parts of the Elat Sheet are from west to east: the Gishron, Shelomo, Tzefahot, Yotam, Roded, Mahzevot and Elat faults (Eyal, Y., 1967). In the subsurface the Yotam, Tzefahot and Mahzevot faults coalesce north of the Yotam Graben, with the north-east striking Arava Fault. (Frieslender, 2000, Fig 2). West of the Gishron Fault the cumulative sinistral diaplacement of the Elat and Roded blocks with respect to the Sinai Block is 8 and 2.5 kilometers respectively (Garfunkel, 1980). Along the Roded Fault and the northern part of Shelomo Fault, northeast plunging synclines and anticline oblique to the faults were mapped, such as the Shehoret Syncline East and Shehoret Sycline West. Similar structures were mapped along the southwest margines of the Shelomo Fault in the Shelomo Graben: Taba, Rehavam and Shelomo synclines and a series of small tight folds along Nahal Yehoshafat (Eyal, Y., 1967). The axes of these folds are also trending north-east oblique to the Shelomo Fault. Along Nahal Gishron half domes such as the one north of upper Nahal Yehoshafat are observed deflecting the

direction of the stream. Most probably, both the folds and the faults were developed contemporaneously, in response to a northwest southeast stress field. Whereas the Shehoret synclines are broad, the folds of the southern parts of the Shelomo Syncline are asymmetric with up to vertical dips of the northern flanks. The reason for this difference is that the Shehoret synclines were developed in an extension environment whereas the folds south of Nahal Yehoshafat express shortening for up to 30%. Sub-horizontal slickensides, such as along the Tzefahot, Shelomo and Roded fault planes, are common and in the upper Nahal Shelomo with rhomb structures indicating sinistral movement. Sub-vertical slickensides are common such as at the fault planes of Yotam and Gishron faults. The east-northeast striking Mt. Amir Syncline and Nahal Raham Syncline (Bartov, 1967) are the largest mapped in the Elat Sheet. The Mt. Amir Syncline, between the Roded and Amram blocks plunges eastward and in it's north-eastern edge is a recumbent syncline where the dips of both flanks reach 80º.

The young-recent faults were first mapped by Quennel (1958) The active faults along the Dead Sea Transform mostly cross the Arava alluvial fans, the Avrona Playa and the Elat Sabkha (Garfunkel et al.(1981). These faults displace the Elot and Garof formations (Ginat et al., 1994) and were occasionally active during the last 10,000 years. It is possible to connect some of this activity to historical events (Amit et al., 1999). Amit et al. (1999) concluded that at the Avrona Playa there were at least six earthquakes of magnitude 6 or higher during the last 14,000 years. During the last 1,000 years a relief inversion occurred in the Avrona Playa as a result of an uplift by 1 meter due to a 6.1 magnitude earthquake. This event opened the previously closed drainage system of the Avrona Playa and is presently drained by Nahal Avrona to the Elat Sabkha. Presently the active faults which can create large earthquakes, such as Nuweiba 22.11.1995 earthquake, are the Elat Fault and the Avrona Fault (Tahal Engineering, 2002). These two active fault systems were defined in detailed geotechnical studies of Tahal Engineers and the Geological Survey along the alluvial fans of Nahal Roded and southern part of the city of Elat, between Nahal Garof and Nahal Shachmon (Israeli and Harash, 1990; Tahal Engineers, 2002; Zilberman et al., 2001). They suggested that the youngest one, striking north-east, was active during the Holocene (year>11,000) and the Late Pleistocene, and the oldest one striking northwest, was active from the Pliocene-Middle Pliestocene to Late Pleistocene. In the city of Elat the Shahamon Fault was mapped in detail with a fault plane of ~$80^0/300^0$ and a down throw of 7-10 meters of the western block (Israeli and Harash, 1990). This fault was also detected in the alluvium and was defined by them as an active fault. South-west of Gevaot Shehoret, the river terraces and the Garof Formation are cut by a north-west striking fault (the "Roded Fault"), which was active from Late Pliocene, during the sedimentation of the Garof Formation, to Late Pliestocene (?). Two additional faults, which displace the Garof Formation, were mapped west of Gevaot Shehoret. The entire area between Gevaot Shehoret at the north and the city of Elat at the south is crossed by numerous short faults and lineaments (Zilberman et al., 2001).

The direction of the Amram Block is east-west whereas the Elat and Roded blocks are elongated in the north-east direction. The boundary faults of the Amram Block are: The Arava Fault in the east, the Roded Fault in the west, Avrona Fault in the north and Amram Fault in the south. At the center the Amram Block is separated into two sub-blocks by the Zefunot Fault. Arava and Roded faults are sinistral faults striking north-east and Avrona, Amram and Zefunot faults are dextral faults striking east-west. Part of these faults are reactivated Neoproterozoic faults, such as the Zefunot Fault, where the north block of Amram Granite Porphyry faces the Amram Rhyolite south block below the Early Cambrian peneplain. These east-west striking faults such as the Amram and

Zefunot faults, are shear zones rather than distinctive single faults. These shear zones are most apparent when they crosses the Multicolored Member of the Shehoret Formation at the Amram Pillars, or north of Giv'at Bahat. The Avrona Fault is cut at the northwest corner of Mt. Amram by a north-south sinistral fault with a horizontal displacement of 120 m. Geophysical mapping indicates that the Arava Fault at the north-east corner of Mt. Amram sinistraly offsets the Avrona Fault by 1,138 meters assuming that the Be'er Ora Fault of (Frieslender, 2000) is the continuation of the Avrona Fault. The sub-surface saddle between the Avrona and Yaalon basins is most probably the sub-surface eastward continuation of the Amram Block. The Amram Block is an ancient reactivated east-west block, adjacent to the major regional Themed Fault. The Mt. Amir Syncline was formed along the tectonic junction of the Roded Block, moving northeastward and the east-west trending Amram Block. Change of flow directions of Nahal Amram and it's tributaries is an indication for recent activity of the Arava Fault (Beyth and Mushkin, 2010). The Nizoz Fault (Bartov, 1967) north-east of Mt. Amram displaces the Shehoret Formation and Amram Rhyolite on the east block, and places them opposite to the Judea Group on the west block.

4.3 The dextral **Themed Fault** which is part of the Sinai-Negev Shear Zone (Bartov, 1967) strikes west-northeast and extends from Nahal Shani at the west to Be'er Ora at the Arava at the east (Elat and Be'er Ora Sheets). Garfunkel (1970) suggested that it is a reactivated pre-rift marginal Neoproterozoic fault. The Themed Fault in the Elat sheet is accompanied by marginal grabens with blocks of Zihor, Menuha and Mishash formations, as well as synclines and anticlines parallel to the main fault few hundreds meters in size. The biggest structure is the Raham Syncline south of the Themed Fault. Faults striking north-south such as the Nizoz Fault at the south-eastern part of Be'er Ora Sheet or Neshef Fault at the west of it are cutcrossed by the Themed Fault. The Late Pleistocene Zhiha Formation at Nahal Shani is not affected by the Themed Fault.

5. Landslides and rock collapse

Landslides along the slopes of the rift margins are common as a result of the tectonic activity associated with the Dead Sea Transform and the stratigraphy where rigid dolomite and limestone beds overlie clay units that serve as the lubricant for sliding. The more common ones are blocks of the Gerofit Formation that slide on top of the Ora Formation shales, for example along the Mt. Amram cliffs and the basal clays of the Gerofit Formation at the upper Nahal Shehoret. Here a series of deep fractures striking northeast and cutting the Gerofit Formation parallel to the cliffs of Nahal Shehoret tributaries were mapped. A massive landslide was also observed here at the stream bed. Overlaying the limestone of the Gerofit Formation, dipping 10^0 to southeast, two large slided blocks of Zihor Formation were mapped. Rock collapse are common in the Elat area for example at the upper part of Nahal Netafim, in Nahal Raham and in Nahal Shani where large boulders of the Zafit Member limestone, originally overlaying the marly beds of the En Yorqe'am Member are observed along the creek. Blocks weighting more than 10 tons of the Amudei Shelomo and Shehoret formations were mapped along Nahal Amir.

6. Economic aspects

Geological mapping is a major tool for the sustainable use of natural resources. At the Elat region where desert tourism has a major economic impact detailed geological map is an important asset for tour guides. The map is also important for planning infrastructure and future development and to estimate and mitigate the high seismic risk of this area related to the Dead Sea Transform. Typical examples are the studies of Tahal Engineers (Tahal Engineers, 2002; Israeli and Harash, 1990) and of the Geological Survey (Zilberman et al., 2001) of the Roded and Shahmon sites. The intense solar radiation and the flat empty plains make the area also an ideal location for the production of solar energy. The elevated topography of the rift margins adjacent to the Elat/Aqaba Gulf, is ideal for pump storage that is essential for solar energy and electrical net end users. At the Amram Pillars mainly in the Amir Formation ancient copper mines of the Egyptian and Muslim periods were excavated (Willies, 1991) and traces of gold were found in the rhyolite dykes of Nahal Shehoret and Nahal Roded (Bogosh et al., 1993). The potential of raw materials for the construction industry was summarized by Shirav and Segev (1995). Twelve million m^3 of brackish water are pumped annually and are desalinized for the use of the local population. This brackish water is a mix of the fossil saline water from the sandstone aquifer of the Yam Suf and Kurnub groups with fresh renewable water from the alluvial fans (Bein et al., 2001).

7. Previous studies

Numerous geological studies were carried out in the Elat area and not all of them are included here. We refer mainly to those that directly contribute to the map and the explanatory notes. The Elat area was previously mapped by Bentor and Vroman (1955) at 1:100,000 scale; Garfunkel (1970) at 1:50,000 scale; Druckman et al. (1993) at 1:100,000 scale and Garfunkel et al. (2000) at 1:100,000 scale. Specific areas previously mapped in more detail and compiled into the present map are: Eyal, Y., (1967), Bartov (1967), Shimron (1972), Mushkin et al. (2003), Amit et al. (1999), Gutkin and Eyal, y. (1998), Avigad (1990), Katz et al. (2002), Katzir et al. (2007), Paz (1997), Peltz and Eyal, M. (1995), Eyal, M. and Peltz (1994), Ginat et al. (1994), Bartov et al. (2002), Weissbrod (1961) and Kagan (2006). Key studies for the understanding of the general structural geology are those of Garfunkel (1970), Y. Eyal (1967, 1973; Fig 6) focusing on the structural map of the Yotam and Shelomo grabens and Bartov (1967; Fig. 7) for the structural map of the Be'er Ora area and Themed Fault. The study by Frieslander (2000; Fig. 2) is important for the subsurface geology along the Dead Sea Transform and the structural map included. Mushkin et al. (2003) mapped the Amram block. Amit et al. (1999) and Zilberman et al. (2001) mapped the recent faults along the Dead Sea Transform.

Dating of the Neoproterozoic metamorphic and magmatic rocks was done by: Kroner et al. (1990), Stein and Goldstein (1996), Katz et al. (1998), Garfunkel (1999), Beyth and Heimann (!999), Kolodner (2007), Katzir et al. (2007), Be'eri-Shlevin et al.(2009) and Morag et al. (2010, 2011 a.b.c).

The maps by Shaw (1947) of Southern Palestine and by Bentor and Vroman (1955) of the Elat Area served as a base map for the subsequent mapping. The study by Bentor (1961) was the pioneering work on the Neoproterozoic metamorphic and magmatic complex.

Shimron (1972) presented a structural framework of the metamorphic complex. Garfunkel (1980, 1999) analyzed in detail the petrology of the Neoproterozoic rocks and the erosion phases at the Late Neoproterozoic Early Cambrian transition. M. Eyal and Peltz (1994 and 1995) described the Late Neoproterozoic volcanic rocks. Weissbrod (1969, 2005) described the stratigraphy of Yam Suf and Kurnub groups and Bartov et al. (1972) summarized the stratigraphy of the Judea and Mt. Scopus groups. Regional magnetic and gravimetric data is presented in Segev et al. (1999).

Acknowledgment

Fieldwork: Shelomo Ashkenazi, Hanan Ginat, Oded Katz, Amit Mushkin, Yoav Avni, Amihai Sneh, Amit Segev, Dov Avigad, Rivka Amit, Ezra Zilberman, Hallel Lutzki and Raanan Budzin.Editing: Amihai Sneh, Zeev Lewy, Tuvia Weissbrod, Beverly Katz and also David Soudry, Rami Weinberger, Yhudit Harlavan, Uli Wetzel, Avi Honigstein and Moshe Eyal.GIS: Alexiy Borshevsky, Rani Calbo, Onn Crouvi, Alexander Varshavsky and Marcelo Rosensaft.This mapping was carried out as project no. 40236-Elat Sheet geological mapping of the Geological Survey of Israel.

References

Amit, R., Zilberman, E., Porat, N. and Enzel, Y., 1999, Relief Inversion in the Avrona playa as evidence of large-magnitude historical earthquakes, southern Arava Valley, Dead Sea Rift: Qurternary Research 52:76-91.

Angerer, T., Greilling, R. O. and Avigad, D., 2011, Fabric development in the weathering profile at a basement-cover interface, the sub-Cambrian peneplain, Israel: Implications for decollement tectonics: J. Structural Geol. 33:819-832.

Arkin, Y., Braun, M. and Itzhaki, y., 1967, Cenomanian mapping units and their correlation in the Negev (South Israel): Geol. Surv. Israel, Bull. 43:15-20.

Avigad, D., 1984. The deformation and metamorphism of the schistose dikes in the Elat area (NE Sinai). M.Sc. thesis, Hebrew University, Jerusalem, 85 pp.

Avigad, D., 1990, Geological map of the east-central part of the Roded area, 1:2500: Geol. Surv. Isr.

Avigad, D., Sandler, A., Kolodner, K., Stern, R. J., McWilliams, M., Miller, N. and Beyth, M., 2005, Mass-production of Cambro-Ordovician quartz-rich sandstone as a consequence of chemical weathering of Pan-African terranes: Environmental implications: Earth Planet Sci. Lett. 240:818-826.

Avigad, D. and Gvirtzman, Z., 2009, Late Neoproterozoic rise and fall of the northern Arabian-Nubian shield: The role of lithospheric mantle delamination and subsequent thermal subsidence: Tectonophysics 477:217-228.

Avni, Y., Bartov, Y., Garfunkel, Z. and Ginat, H., 2001. The Arava Formation - A Pliocene sequence in the Arava Valley and its western margin, southern Israel. Isr. J. Earth Sci. 50: 101-120

Avni, Y., Segev, A. and Ginat. H., 2011a, Oligocene peneplain in south Israel: Documentation of a major phase in the formation of the tectonic structure of the margins of the Dead Sea Transform: , Isr. Geol. Soc. Ann. Meeting, Mitzpe Ramon, Field Trips .

Avni, Y., Segev, A. and Ginat. H., 2011b, Oligocene regional denudation of the northern Red Sea and Levant areas: early breakup stages of the Afro-Arabian plate and early activation of the Dead Sea Fault: Isr. Geol. Soc., Mitzpe Ramon, 2011, abstract p. 33.

Bartov, Y., 1967, The geology of Beer Ora area, unpublished M.Sc. thesis, Hebrew University, Jerusalem (in Hebrew), 39 pp.

Bartov, Y., Eyal, Y., Garfunkel, Z. and Steinitz, 1972, Late Cretaceous and Tertiary stratigraphy and paleogeography of southern Israel: Isr. J. Earth Sci. 21:69-97.

Bartov, Y. and Steinitz, G., 1977, The Judea and Mount Scopus groups in the Negev and Sinai with trend surface analysis of the thickness data: Isr. J. Earth Sci. 26:119-148.

Bartov, Y., Sneh, A., Fleischer, L., Arad, V. and Rosensaft, M., 2002. Potentially active faults in Israel. Geol. Surv. Isr., Rep. GSI/29/2002.

Basson, U., Ben-Avraham, Z., Garfunkel, Z. and Lyakhovsky, V., 2002, Development of recent faulting in the southern Dead Sea Rift according to GPR imaging. In: Cloetingh S. A. P. L. and Ben –Avraham, Z. (eds). From continental extension to collision: Africa-Europe interaction, the Dead Sea and analogue natural laboratories. Stephan Mueller Spec. Publ. Series, Volume 2.

Be`eri-Shlevin, Y., Katzir, Y. and Whitehouse, M., 2009, Post collisional tectonomagmatic evolution in the northern Arabian-Nubian Shield: time constraints from ion-probe U-Pb dating of zircon: J. Geol. Soc. 166:71-85.

Bein, A., Yechieli, Y. and Bensabat, J., 2001, Quatifying the groundwater resources of the southern Arava Rift Valley: A confined desert system recharged laterally by external sources: Isr. J. Earth Sci. 50:217-236.

Bentor, Y. K., 1961, Petrographical outline of the Precambrian in Israel: Bul. Research Counc. Isr. 10G:19-63.

Bentor, Y. K. and Vroman, A., 1955, The geological map of Israel. Series A. The Negev. Sheet 24: Elat. Geol. Surv. Isr.

Beyth, M., Stern, R., J., Altherr, R. and Kroner, A., 1994, The Late Precambrian Timna Igneous Complex, southern Israel: Evidence for comagmatic type Sanukitoid monsodiorite and alkali granite magma: Lithos 31:103-124.

Beyth, M. and Heimann, A., 1999, The youngest igneous event in the crystalline basement of the Arabian-Nubian Shield, Timna igneous complex: Isr. J. Earth Sci.: 48:113-120.

Beyth, M. and Mushkin, A., 2010, Mt. Amram, an E-W striking Neogene-Quarternary rejuvenated Early Cambrian structure: Isr. Geol. Soc. Ann. Meeting, Elot p. 37 (abstract).

Bogoch, R. and Weissbrod, T., 1986, Barite-flourite-calcite veins in the Precambrian Roded Block, southern Israel: Geol. Surv. Isr., report No. GSI/24/86 pp. 20.

Bogoch, R., Shirav, M., Beyth, M. and Halicz, L., 1993, Geochemistry of ephemeral stream sediments in the Precambrian mountainous arid terrain of southern Israel: J. Geochem. Explor.: 46:349-364.

Collins, A. S. and Pisarevsky, S., A., 2005, Amalgamating eastern Gondwana: the evolution of the Circum-Indian Orogens. Earth-Science Reviews. 71:229-270.

Druckman, Y., Weissbrod, T. and Garfunkel, Z., 1993, Geological map of Israel, 1:100,000, Yotvata and Elat: Geol. Surv. Israel.

Eyal, M. and Peltz, S., 1994, The structure of Ramat Yotam Caldera, southern Israel: A deeply eroded Late Precambrian ash-flow caldera: Isr. J. Earth Sci.: 43:81-90.

Eyal, M., Litvinovsky, B.A., Katzir, Y. and Zanvilevich, A N., 2004, The Pan-African high- K calc-alkaline peraluminous Elat Granite from southern Israel: geology, geochemistry and petrogenesis: J. Afric. Earth Sci. 40:115-136.

Eyal, Y., 1967, The geology of the sedimentary rocks at Nahal Shelomo-Nahal Netafim region, M.Sc. thesis, Hebrew University, Jerusalem, 38 pp. (in Hebrew).

Eyal, Y., 1973, The tectonics of the Shelomo and Yotam grabens, Elat, Israel: Isr. J. Earth Sci.: 22:165-184.

Eyal, Y., 1980, The geological history of the Precambrian metamorphic rocks between Wadi Twaiba and Wadi Um-Mara, NE Sinai: Isr. J. Earth Sci., 29:53-66.

Eyal, Y., Eyal, M. and Kroner, A., 1991, Geochronology of the Elat terrain, metamorphic basement and its implication for crustal evolution of the NE part of the Arabian-Nubian Shield: Isr. J. Earth Sci. 40:5-16.

Fleischer, L., 2002, Stratigraphic Table of Israel, outcrops and subsurface, October 2002 (compilation): Geophy. Inst. Isr.

Freund, R., 1962, Problems in the stratigraphy of the Cenomanian-Turonian in Israel. Unpub. Ph.D. thesis: Hebrew University, Jerusalem (in Hebrew, English abstract).

Freund, R., 1961, Distribution of Lower Turonian ammonites in Israel and the neighbouring countries. Bull. Res. Council Isr. 10:79-100.

Frieslander, U., 2000, The structure of the Dead Sea Transform emphasizing the Arava using new geophysical data: Ph.D. thesis, Hebrew University, Jerusalem; 101 pp. (in Hebrew, English abstract)

Garfunkel, Z., 1970, The tectonics of the western margin of the southern Arava: Ph.D. thesis, Hebrew University, Jerusalem, 204 pp. (In Hebrew, English abstract)

Garfunkel, Z., 1980, Contribution to the geology of the Precambrian of the Elat area; Is. J. Earth Sci. 20:25-40.

Garfunkel, Z., 1999, History and paleogeography during the Pan-African orogen to stable platform transition: Reappraisal of the evidence from the Elat area and the northern Arabian-Nubian Shield: Isr. J. Earth Sci.: 48:135-157.

Garfunkel, Z., Bartov, J., Eyal, Y. and Steinitz, G., 1974, Raham Conglomerate-new evidence for Neogene tectonism in the southern part of the Dead Sea Rift: Geol. Mag. 111:55-64.

Garfunkel, Z., Zak,. I. and Freund, R., 1981, Active faulting in the Dead Sea Rift. Tectonophysics 80:1-26.

Garfunkel, Z., Eyal, Y., Eyal, M., Weissbrod, T., Shimron, A., Peltz, S., Gutkin, V., Bartov, J., Druckman, Y., Rosensaft, M. and Sneh, A., 2000, Geological map of the northern Gulf of Elat area, 1:100,000: The Geol. Surv. Isr.

Ginat, H., 1997, The geology and landscape evolution of the Hiyyon and Zihor valleys: Ph.D thesis, Hebrew University, Jerusalem, 115 pp. (in Hebrew, English abstract).

Ginat, H., Enzel, Y., Bartov, J. and Zilbermann, E., 1994, Mapping of young faults in alluvial fans in the city of Eilat. Geol. Surv. Isr. Rep. GSI/14/94, 11 pp. (in Hebrew)

Ginat, H., Zilberman, E. and Amit, R., 2001, Red sedimentary unit as indicators for Early Pleistocene tectonic activity in the southern Negev desert, Israel. Geomorphology 1146: 127-146. .

Gutkin, V. and Eyal, Y., 1998, Geology and evolution of Precambrian rocks, Mt. Shelomo, Elat area: Isr. J. Earth Sci.: 47:1-17.

Gvirtzman, G. and Weissbrod, T., 1984, The Hercynian geanticline of Helez and the Late Paleozoic history of the Levant. In: Dixon, J. E. and Robertson, A. H. F. (eds.), The Geological Evol;ution of the Eastern Mediterranean. Geol. Soc. London, Spec. Publ. No. 17, pp. 177-186.

Israeli, A. and Harash, A., 1990, Shahmon area, Eilat, a geotechnical report for the master plane; Tahal Engineering, Rep. 04/90/10, 20 pp. (in Hebrew, an English appendix)

Kagan, R., 2006, The development of the Elat Conglomerate in the Elat Massif: M.Sc. thesis, Ben- Gurion University, 79 pp.

Kagan, R., Eyal, M. and Eyal, Y., 2010, The Elat Conglomerate and the adjacent volcanic rocks: Isr. Geol. Soc. Ann. Meeting, Field Trip, Elot, 60-68 pp. (in Hebrew).

Karcz, I. and Key, C. A., 1966, Note on the pre-Paleozoic morphology of the basement in the Timna area (southern Israel): Isr. J. Earth Sci. 15:47-56.

Karcz, I., Weiler, Y. and Key, C.A., 1971, Lithology and environment of deposition of the Amudei Shelomo Sandstone ("NSP") in Nahal Shani, Elat. Isr. J. Earth Sci. 20:119-124.

Katz, O., 1997, The Metamorphism and the structure of the southeastern Roded block, Contribution to the Precambrian basement evolution research: Geol. Surv. Isr. Rep. GSI/4/97, 97 pp. (in Hebrew, English abstract).

Katz, O., Avigad, D., Matthews, A. and Heimann, A., 1998, Precambrian metamorphic evolution of the Arabian-Nubian Shield in the Roded area, southern Israel: Isr. J. Earth Sci.:47:93-110.

Katz, O, Beyth, M., Miller, N., Stern, R., Avigad, D., Basu, A. and Anbar, A., 2004, Late Neoproterozoic (~630 Ma) high-magnesium andesite suit from southern Israel: implications for consolidation of Gondvanaland: Earth Planet Sci. Lett. 218:475-490.

Katz, Y., Weinberger, R., and Starinsky, A. 2002. Faulting in porous sandstones, Amir Mountain, southern Israel. Isr. Geol. Surv. Isr. Current Res. 13:59-63.

Katzir, Y., Litvinovsky, B.A., Jahn, B. M., Eyal, M., Zanvilevich, A.N., Valley, J. W., Vapnik, Ye., Beeri, Y. and Spicuzza, M.J., 2007, Interrelations between coeval mafic and A-type silicic magmas from composite dykes in a bimodal suite of southern Israel, northernmost Arabian-Nubian Shield: Geochemical and isotope constraints: Lithos, 97:336-364.

Kessel, R., Stein, M.and Navon, O., 1998, Petrogenesis of Late Neoproterozoic dikes in the northern Arabian-Nubian Shield. Implications for the origin of A-type granites. Precambrian Res. 92:195-213.

Kohn, B. P., Eyal, M. and Feinstein, S., 1992, A major Late Devonian-Early Carboniferous (Hercynian) thermotectonic event at the NW margin of the Arabian-Nubian Shield: Evidence from zircon fission-track dating. Tectonics 11:1018-1027.

Kolodner, K., 2007, The provenance of the siliciclastic section in Israel and Jordan: U-Pb dating of detrital zircons. Ph.D. thesis, Hebrew University, Jerusalem, 133 pp.

Kroner, A., Eyal, M. and Eyal, Y., 1990, Early Pan-African evolution of the basement around Elat, Israel, and the Sinai Peninsula revealed by single-zircon evaporation dating, and implications for crustal accretion rates: Geology 18:545-548.

Lewy, Z., 1972, Recent and Senonian oncolites from Sinai and southern Israel: Isr. J. Earth Sci. 21: 193-199.

Lifshitz, A., Honigstein, A., Livnat, A., Roded, R. and Flexer, A., 1985, The Sayyarim Formation, Nahal Ya'alon area, southern Arava Valley: Lithostratigraphy, Ostracode biostratigraphy and paleoenvironmental implications: Isr. J. Earth Sci. 34:193-204.

Matthews, A., Reymer, A. P. S., Avigad, D., Cochin, J. and Marco, S., 1989, Pressures and temperatures of Pan-African high-grade metamorphism in Elat Association, NE Sinai: Isr. J. Earth Sci. 38:1-17.

Miller, N. R., Avigad, D., Stern, R., J. and Beyth, M., 2011, The Tambien Group, Northern Ethiopia (Tigre): Arnaud, E., Halverson, G., P. and Shields-Zhou, G. (eds) The Geological Record of Neoproterozoic Glaciations. Geol. Soc. London, Memoirs 36:263-276.

Morag, N. and Avigad, D., 2010, Crustal evolution of the continental crust in the Arabian Nubian Shield in the Elat Area: Isr. Geol. Soc. Ann. Meeting, Eilot, Field Trip. pp. 49-57 (in Hebrew).

Morag, N., Avigad, D., Gerdes, A., Belousova, E. and Harlavan, Y., 2011 a, Crustal evolution and recycling in the northern Arabian-Nubian Shield: new perspectives from zircon Lu-Hf and U-Pb systematics, Precambrian Res. 186:101-116..

Morag, N., Avigad, D., Gerdes, A. and Harlavan, Y., 2011 b, Crustal evolution in the northern Arabian-Nubian Shield revealed by the Elat Conglomerate detrital zircon archive. Isr. Geol. Soc. Ann Meet. Mitzpe Ramon, abstract p. 111.

Morag, N., Avigad, D., Gerdes, A., Belousova, E. and Harlavan, Y., 2011 c, Detrital zircon Hf isotopic composition indicates long-distance transport of North Gondwana Cambrian-Ordovician sandstones: Geology 39/955-958.

Morag, N., Avigad, D., Gerdes, A. and Harlavan, Y., 2012, 1000-580 Ma crustal evolution in the northern Arabian-Nubian Shield revealed by U-Pb-Hf of detrital zircons from Late Neoproterozoic sediments: Precambrian Res. 197-212.

Mushkin, A., Navon, O., Halicz, L., Hartmann, G. and Stein, M., 2003, The petrogenesis of A-type magmas from the Amram Massif, southern Israel. J. Petrol.: 44:815-832.

Parnes, A., 1971, Late Lower Cambrian trilobites from the Timna area and Har Amram (southern Negev, Israel): Isr. J. Earth Sci. 20:179-205.

Paz, Y., 1997, The geology and the stratigraphy of the volcano-sedimentary units in Nahal Netafim and Nahal Roded in the Elat area: Implications for the history of the Late Precambrian in the Elat region: Unpubl. M.Sc. thesis, Ben –Gurion University (in Hebrew, English abstract): 121 pp.

Peltz, S. and Eyal, M., 1995, Lithology and volcanic stratigraphy of Givot Shehoret, Elat region, 1995, Geol. Sur. Isr. Rep. GSI/10/95, 16 pp.

Porat, N., Amit, R., Enzel, Y., Zilberman, E., Avni, Y., Ginat, H. and Gluck, D., 2010, Abandonment ages of alluvial landforms in the hyperarid Negev determined by luminescence dating. J. Arid Environ., 74:861-869.

Quennel, A. M., 1958, The structural and geomorphic evolution of the Dead Sea rift. Quater. J. Geol. Soc. 114:1-24.

Sade, A.R., Hall, J., K., Tibor, G., Niemi, T., M., Ben-Avraham, Z., Hartman, G., Akawwi, F., Alueladas, A. and Amit, G., 2008, Multibeam bathymetry of the northern Gulf of Aqaba/Elat. Geol. Surv. Isr. Rep. GSI/03/2008.

Sandler, A., Teutsch, N. and Avigad, D., 2011, A sub-Cambrian pedogenesis recorded in weathering profiles of the Arabian-Nubian Shield: Sedimentology 50: 1305-1320.

Segev, A., 1984, Lithostratigraphy and Paleogeography of the marine Cambrian sequence in southern Israel and southwestern Jordan: Isr. J. Earth Sci. 33:26-33.

Segev, A., 1986, Lithofacies relations and mineralization occurrences in the Timna Formation, Timna Valley. Geol. Sur. Isr. Rep. GSI/7/86, 131 pp. (in Hebrew, English abstract).

Segev, A., Beyth, M. and Bar-Matthews, 1992, The geology of the Timna Valley with emphasis on copper and manganese mineralization-updating and correlation with the eastern margins of the Dead Sea: Geol. Surv. Isr. Rep. GSI/14/92 30 pp.

Segev, A., Rybakov, M., Weissbrod, T. and Beyth, M., 1995, Lower Cretaceous gabbroic intrusion at shallow depth in the Timna Valley, southern Israel. Isr. J. Earth Sci. 44:137-148.

Segev, A., Goldshmidt, V. and Rybakov, M., 1999, Late Precambrian-Cambrian tectonic setting of the crystalline basement in the northern Arabian-Nubian Shield as derived from gravity and magnetic data: Basin-and-Range characteristics: Isr. J. Earth Sci. 48:159-178.

Shaw, S. H., 1947, Southern Palestine, Geological map on a scale of 1:250,000 with explanatory Notes: Government of Palestine, Government Printer, Jerusalem 42 pp.

Shimron, A.E., 1972, The Precambrian Structural and Metamorphic History of the Elat Area: Ph.D. Thesis, Hebrew University, Jerusalem: 244 pp.

Shirav, M. and Segev, A., 1995, Raw materials for construction in sheets, Mt. Seguv (25-III), south Beer Ora (25-IV) and Elat (26-I, II): Geol. Surv. Isr. Rep. GSI/37/95, 18 pp. (In Hebrew).

Soudry, D. and Weissbrod, T., 1995, Morphogenesis and facies relationships of thombolites and siliciclastic stromatolites in a Cambrian tidal sequence (Elat area southern Israel). Palaeogeogr., Paleoclim., Paleoecol. 114:339-355.

Stein, M. and Goldstein, S.L., 1996, From plum head to continental lithosphere in the Arabian-Nubian Shield: Nature 382:773-778

Tahal Engineering, 2002, Study of the geotechnical aspects; faults; and earthquakes: Elat north-Roded site, for the detailed master plan: 15 pp. (in Hebrew).

Vapnik, Y., 1993, Fluid inclusions in metamorphic rocks of the Elat area. Isr. J. Earth Sci. 42:71-84.

Vermeesch, P., Avigad, D. and McWilliams, O., 2009, 500 m.y. of thermal history elucidatedby multi-method detrital thermochronology of North Gondvana Cambrian sandstone (Eilat area, Israel): GSA Bull. 121:1204-1216.

Weissbrod, T., 1961, The geology and petrography of the Roded Massif: unpubl. M.Sc. thesis Hebrew University, Jerusalem (in Hebrew), 64 pp.

Weissbrod, T., 1965, Precambrian volcanism at Roded Massif, Elat area: Isr. Geol. Soc. Ann Meet., abstract p. 11 (in Hebrew).

Weissbrod, T., 1969, The Paleozoic of Israel and adjacent countries, part II. Geol. Surv. Isr. Bull. 48, 32 pp.

Weissbrod, T., 1980, The Paleozoic of Israel and adjacent countries (lithospheric study). unpubl. Ph.D. thesis, Hebrew University, Jerusalem, 275 pp. (In Hebrew, English abstract).

Weissbrod, 2002, Stratigraphy and correlation of the Lower Cretaceous exposures across the Dead Sea Transform with emphasis on tracing the Amir Formation in Jordan: Isr. J. Earth Sci. 51:55-78.

Weissbrod, T., 2005, The Paleozoic in Israel and Environs. In: Hall et al., (Eds), Geological Framework of the Levant Volume II: The Levantine Basin and Israel, Historical Production Hall, p. 283-316.

Weissbrod, T. and Nachmias, J., 1986, Stratigraphic significance of heavy minerals in the Late Precambrian-Mesozoic clastic sequence ("Nubian Sandstone") in the near east. Sediment. Geol. 47:263-291.

Weissbrod, T. and Sneh, A., 1990, Capturing of streams in the Roded area- an indication for young tectonic activity along the rift margins: Isr. Geol. Soc. Ann. Meet., Field Trip, Elat, p. 25-26 (in Hebrew).

Weissbrod, T. and Sneh, A., 1997, Stratigraphy and sedimentology of the Lower Cretaceous Amir Formation in Israel and Sinai: A marine clastic deposit with tidal channels. Isr. J. Earth Sci. 46:79-93.

Weissbrod, T. and Barthel, W. K., 1998, An Early Aptian ichnofossil assemblage-zone in southern Israel and Sinai (Egypt): An ichnofauna habitat in a chanelled tidal flat. J. Afr. Earth Sci. 26:225-239.

Weissbrod, T. and Sneh, A., 2002, Sedimentology and paleogeography of the Late Precambrian- Early Cambrian arkosic and conglomeratic facies in the northern margins of the Arabo-Nubian Shield. Isr. Geol. Surv., Bull., No. 87, 44 p.

Weissbrod, T. and Segev, A., 2003, The Lower Cretaceous volcanic activity in the Timna Valley geological setting and $^{39}Ar/^{40}Ar$ dating. Isr. J. Earth Sci. 52:77-96.

Weissbrod, T. and Bogoch, R., 2007, Distribution pattern and provenance implications of the heavy minerals in Neproterozoic to Mesozoic siliciclastic successions in the Arabo-

Nubian Shield and its northern periphery: A review. In: Mange, M. A. and Wright, D. T. (eds.), Heavy Minerals in Use. Developments in Sedimentology, 58, pp. 647-676. Elsevier.

Willies, L., 1991, Ancient copper mining at Wadi Amram, Israel, an archaeological survey: Bull. Peak District Mines Historical Soc., 11:109-138.

Wurtzburger, U., 1959, The geology and petrography of the Amram mountains: M. Sc. Thesis, Hebrew university, Jerusalem (in Hebrew).

Zilberman, E., Amit, R. and Nachmias, Y. 2001, Mapping fault systems around Nahal Roded and Gevaot Shehoret : Israel Geol. Surv. Isr. Rep. GSI/25/2001, 14 pp. (in Hebrew).

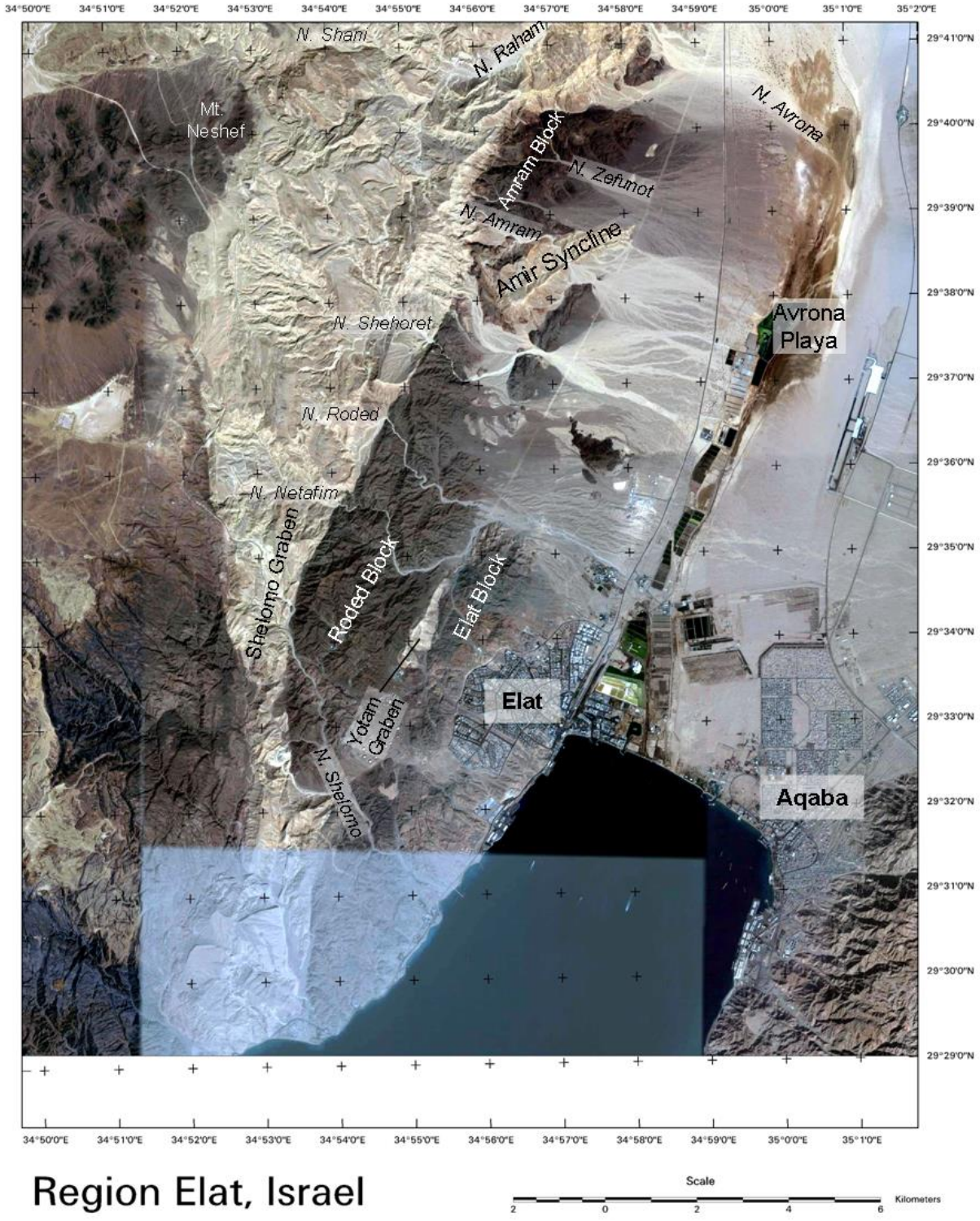

Fig. 1-Location map.

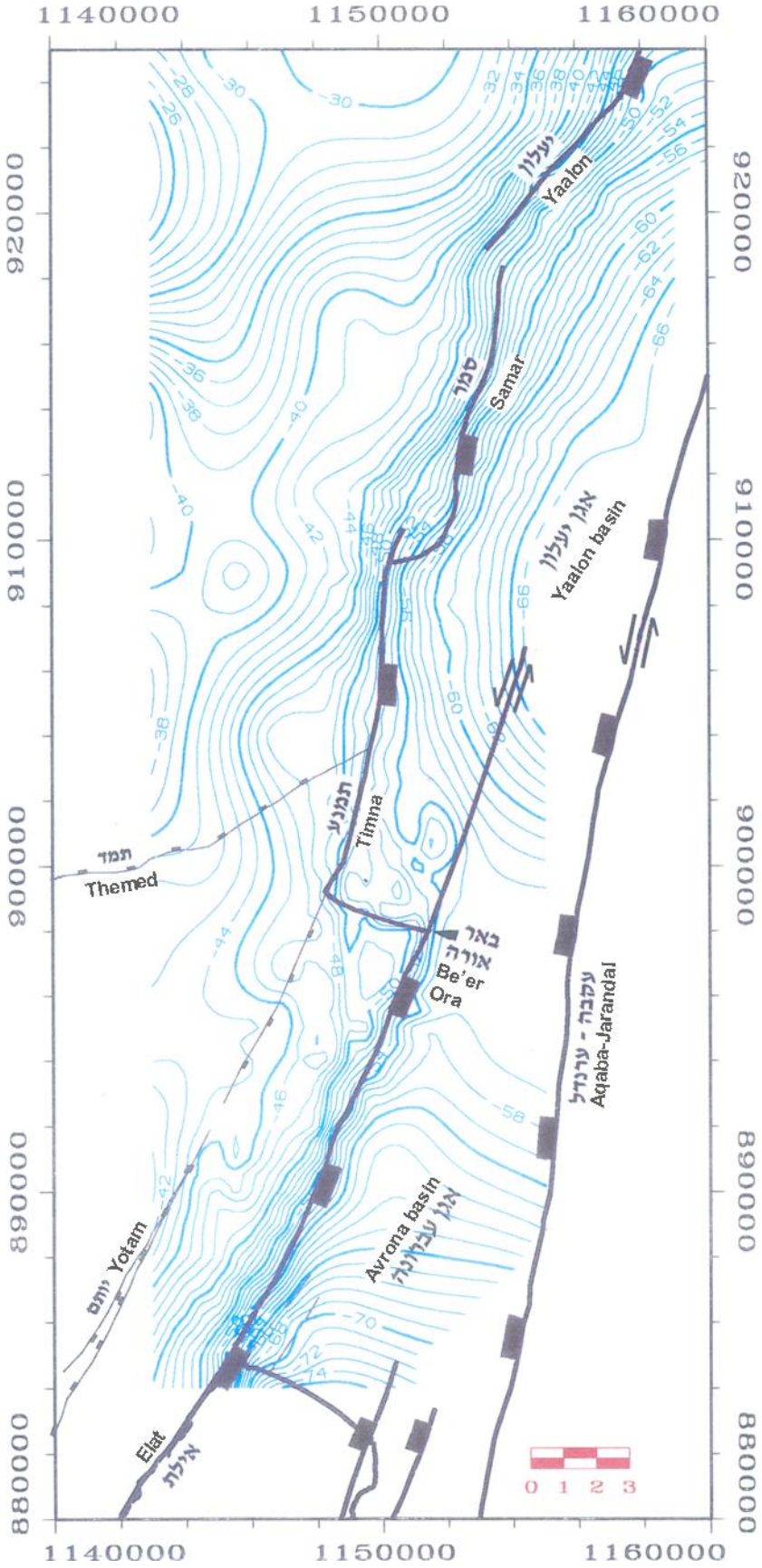

Fig. 2 -Map of Bouguer anomalies in the southern Arava and its margins (Frieslander, 2000). Main faults and basins are emphasized

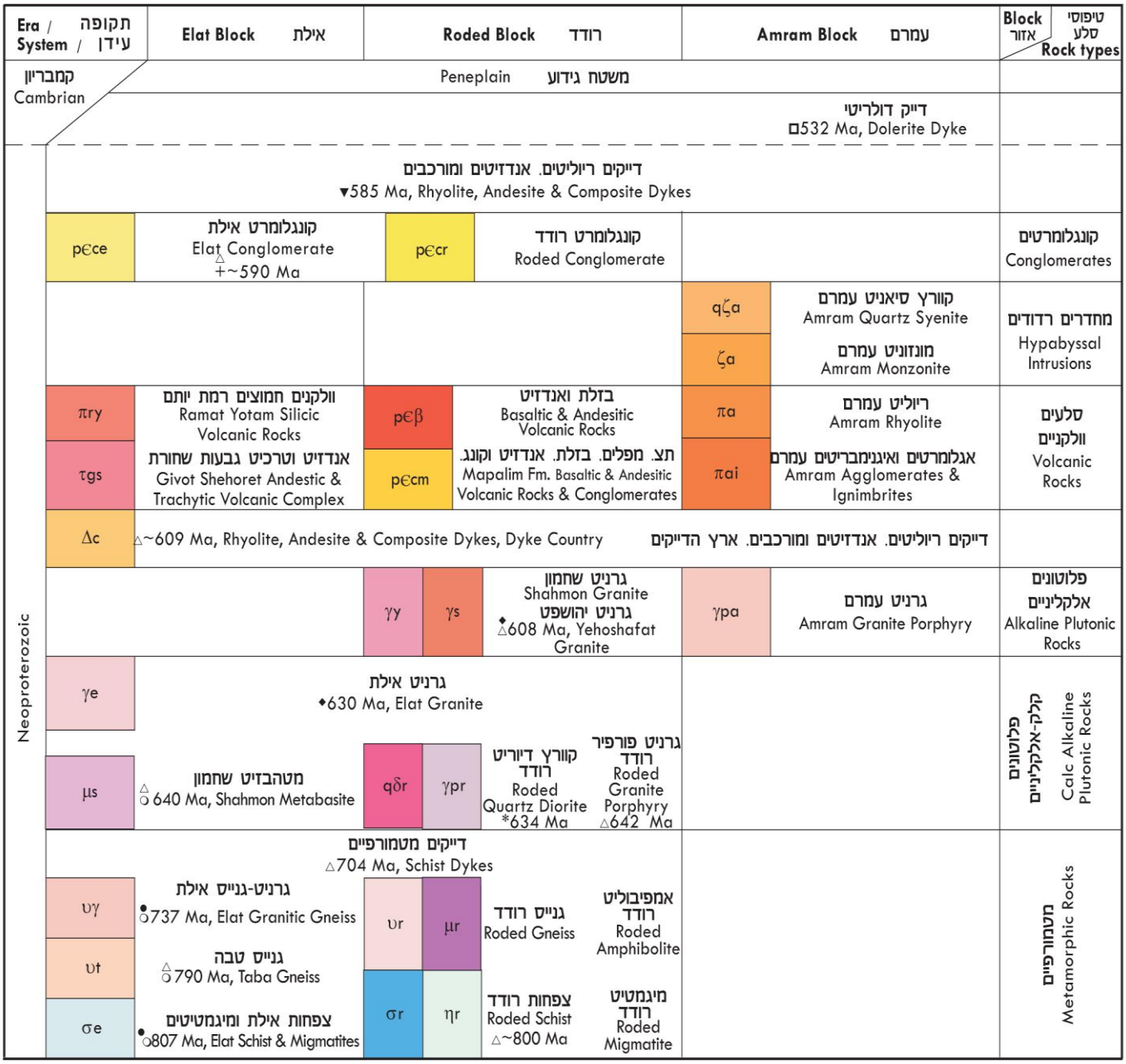

Radiometric ages:
Be'eri-Shelvin et al., 2009 ♦
Beyth and Heimann, 1999 ◘
Garfunkel, 1999 +
Katz et al., 1998 *
Katzir et al., 2007 ▼
Kolodner, K., 2007 ●
Kroner et al., 1990 ○
Morag and Avigad, 2010, Morag et al., 2011a, b. △
Stein and Goldstein, 1996 *

Fig. 3- Neoproterozoic basement

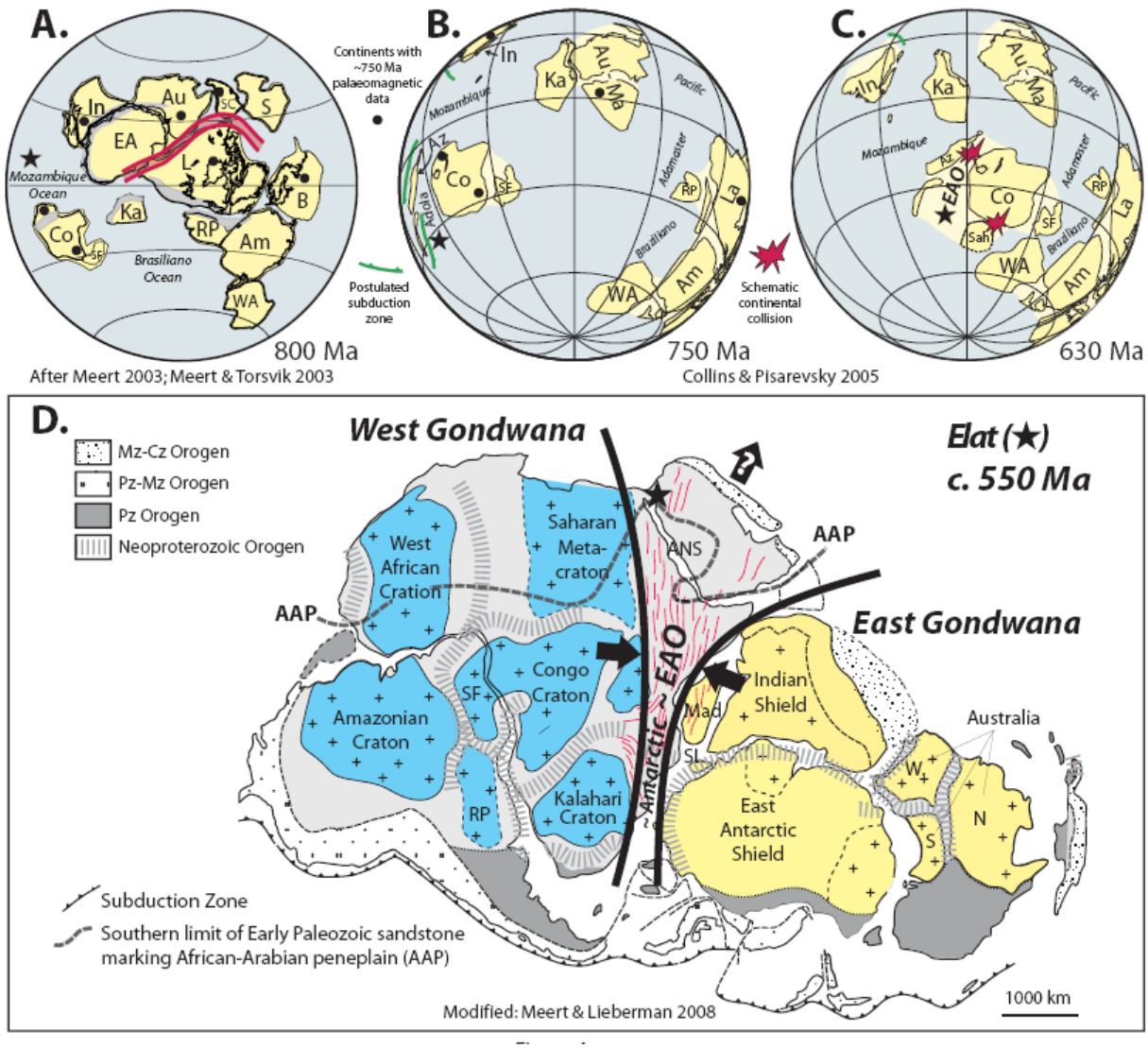

Fig. 4 - World Paleogeography of the Neoproterozoic. (Miller et al., 2011)

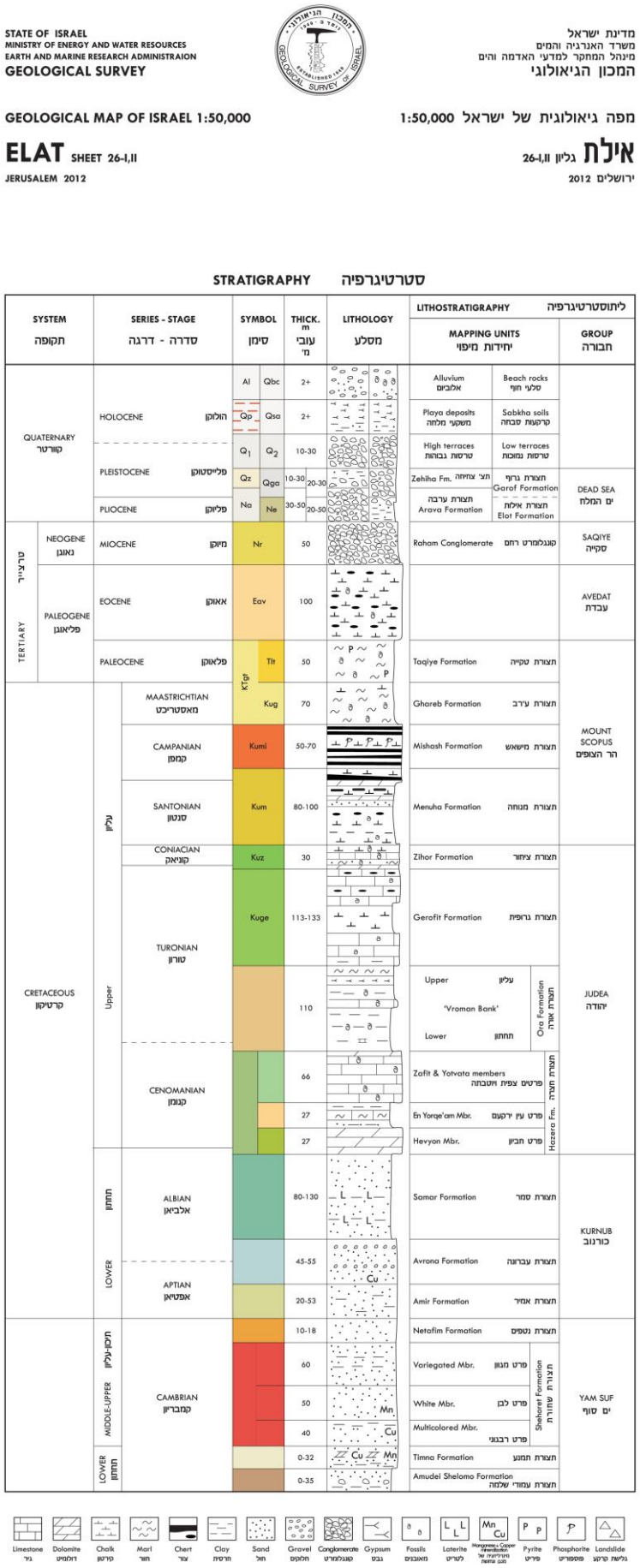

Fig. 5 - Stratigraphic column of the sedimentary rocks.

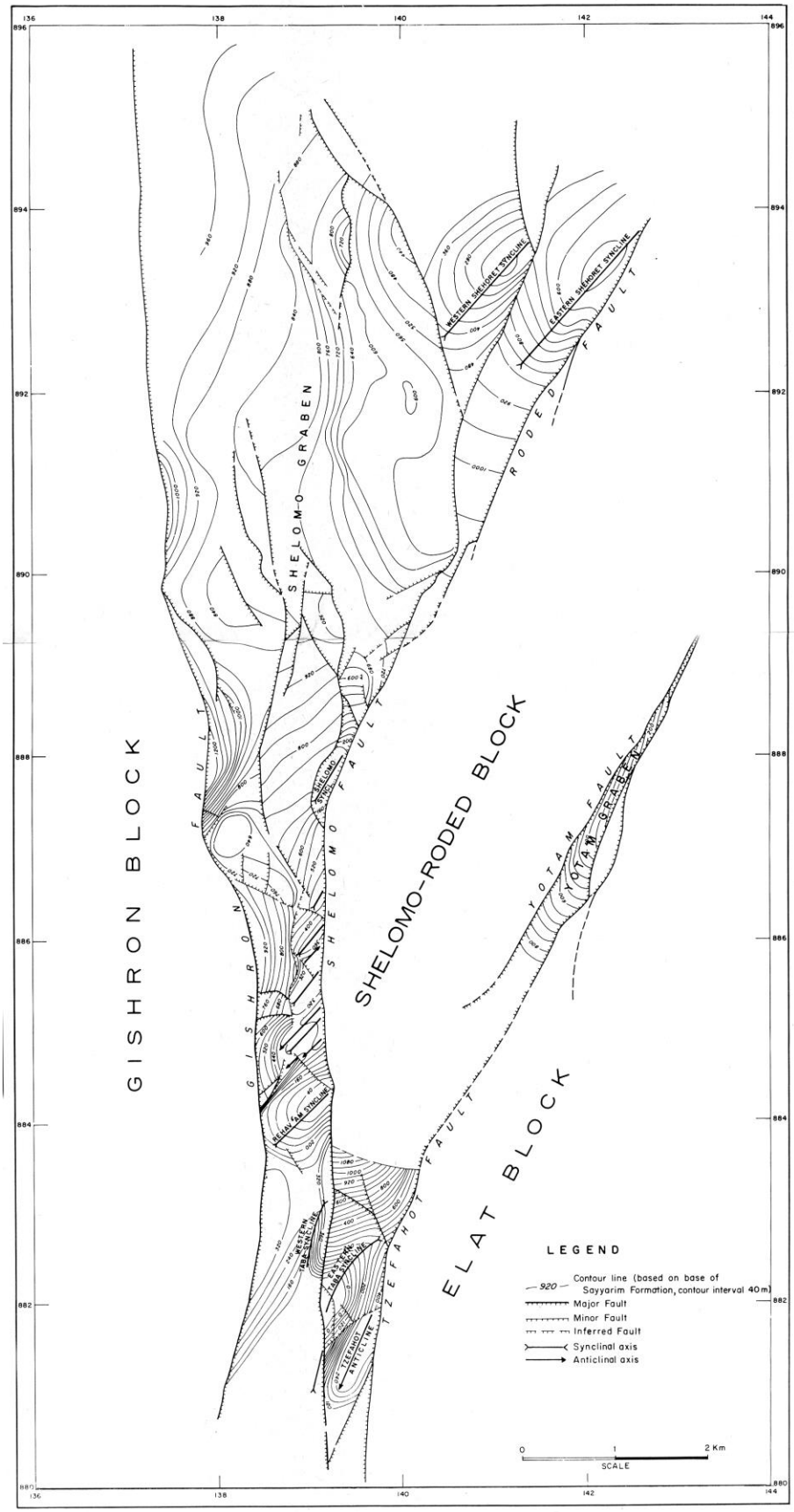

Fig. 6-Structural map, top Judea, Shelomo and Yotam grabens (Y. Eyal, 1973)

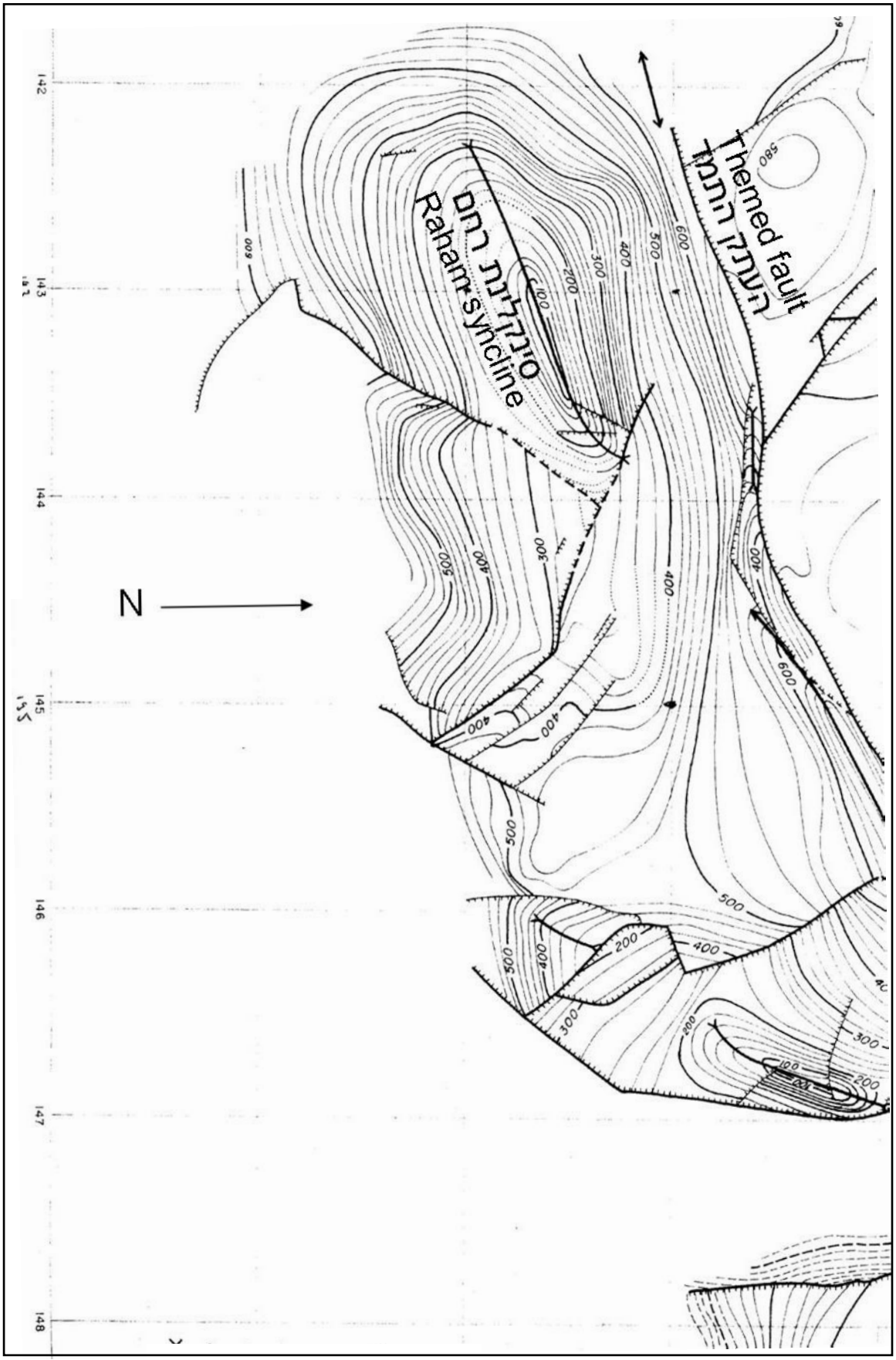

Fig. 7- Structural map, top Judea, Nahal Raham. Prominent are the Themed Fault and Raham syncline (Bartov, 1967).

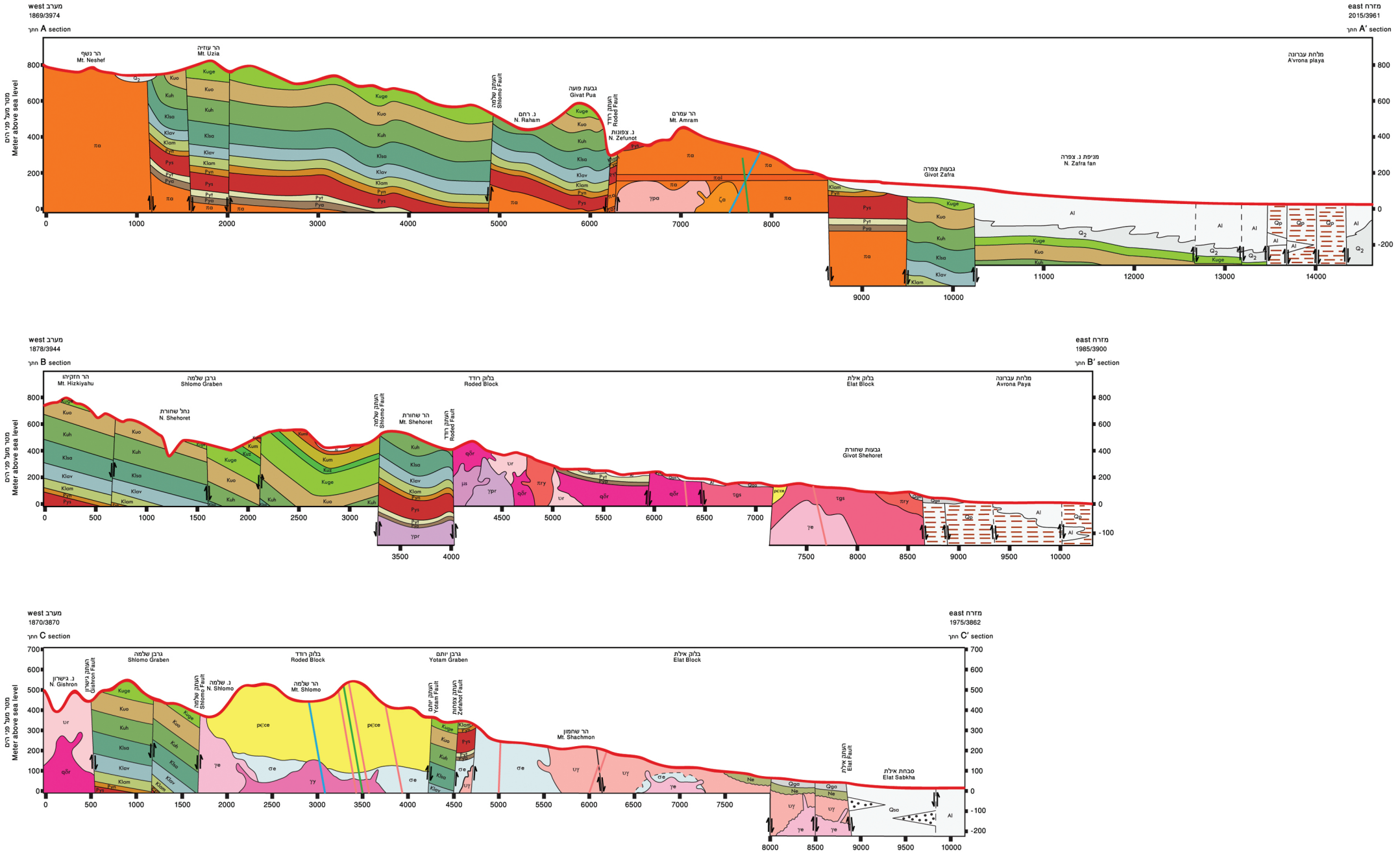

Fig. 8 - Geological cross sections

II

The Timna Valley as a Geological Park

Michael Beyth and Ran Calvo

Geological Survey of Israel, 30 Malkhe Israel, Jerusalem 95501, Israel

Timna Park is a major tourist attraction in the southern Arava and of major scientific archeological and geological interest (Ben Yosef et al., 2012; Beyth et al., 2013). The goal of the presented initiative is to make the unique geology of the Timna Valley and its surrounding more attractive to the tourist, amateur geologist and students based on the up-to-date research and recent mapping. This project is carried out by the Geological Survey in cooperation with the Dead Sea and Arava Science Center and the Timna Park Development Company. 62 stations mainly along the Israel National Trail, where the detailed geological description presented is supported by drafts, maps and photos. The hard-copy report is available to download at the Geological Survey web-site. The final goal is to make it accessible to each visitor through a mobile multi-sensory cellular application (like "Maslulari" developed by the Dead Sea and Arava Science Center) which will be available to iPhone and Android users.

The stratigraphy and structure of the Timna Valley is summarized by Beyth et al., (2013 available in www.gsi.gov.il). The present project was published as a report of the Geological Survey (Beyth and Calvo, 2014, in Hebrew, available in www.gsi.gov.il). Timna geological park was divided into three areas: (A) The Timna Valley; (B) The north-westeren highlands; and (C) The southern margins. The stations, roads and trails, including the Israel National Trail, were marked on the very recent geological maps of each area. An up-to-date reference list is attached to the reports and a list of the GPS locations of all the stations.

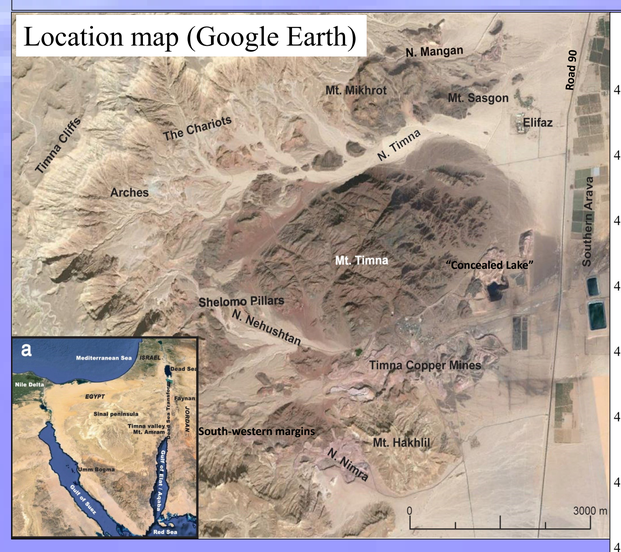

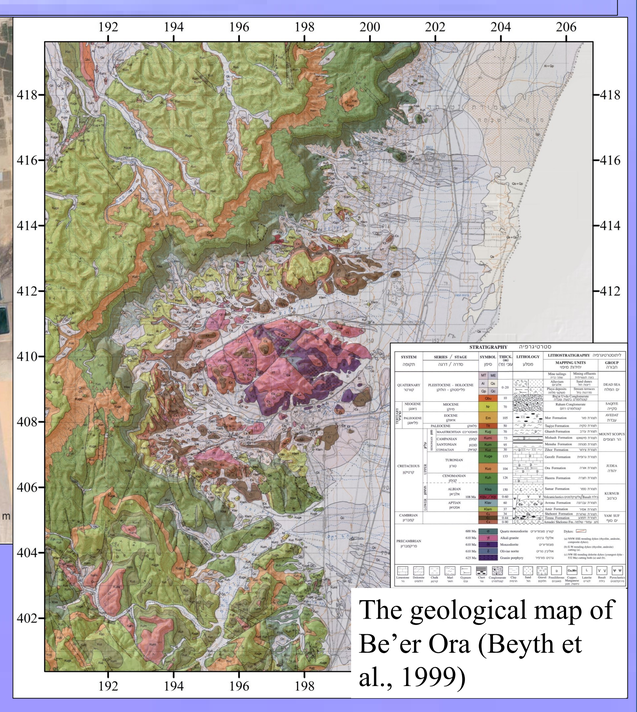

The geological map of Be'er Ora (Beyth et al., 1999)

Bartov, Y., 1967, The geology of Be'er Ora region. M.Sc. thesis, The Hebrew University of Jerusalem, 64 p. (in Hebrew with English abstract).

Ben-Yosef, E., Shaar, R., Tauxe, L., and Ron, H., 2012, A new chronological framework for Iron Age copper production in Timna (Israel), Bulletin of the American Schools of Oriental Research 367:31-71.

Beyth, M. and Calvo, R., 2014, The Timna Valley as a Geological Park. Geological Survey of Israel, Report GSI/09/2014, 69 p.

Beyth, M., Segev A., and Bartov, Y., 1999, The geological map of Be'er Ora,1:50,000, Sheet 25-IV. Geological Survey of Israel.

Beyth, M., Segev, A., and Ginat, H., 2013, Stratigraphy and structure of the Timna Valley and adjacent ancient mining areas. Geological Survey of Israel, Report GSI/15/2013, 28 p.

Steinitz, G., Shalmon, M., Ginat, H., Eyal, Y., and Bartov, Y., 2010, The geology of the Be'er Ora area. Israel Geological Society, Explanatory notes excursion, p. 7-13.

The Timna Valley

Station #26: Burrows at top Amir Formation at the Arches site.

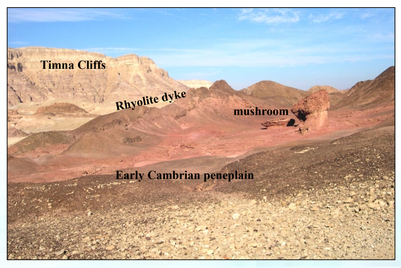

Station #29: The Early Cambrian peneplain at the "Petria"(mushroom) which is build of the conglomerates and sandstones of Amudei Shelomo Formation.

Station #28: The stratigraphic section at the Chariots site.

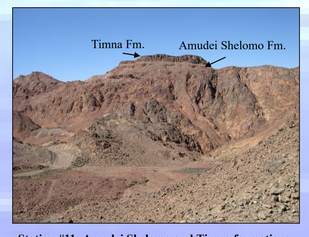

Station #11: Amudei Shelomo and Timna formations at the top of Mount Timna.

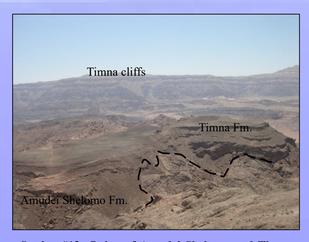

Station #13: Onlap of Amudei Shelomo and Timna formations on the Early Cambrian peneplain.

Station #25a: Halite pseudomorphs in sandy dolomite of Timna Formation, Step Faults.

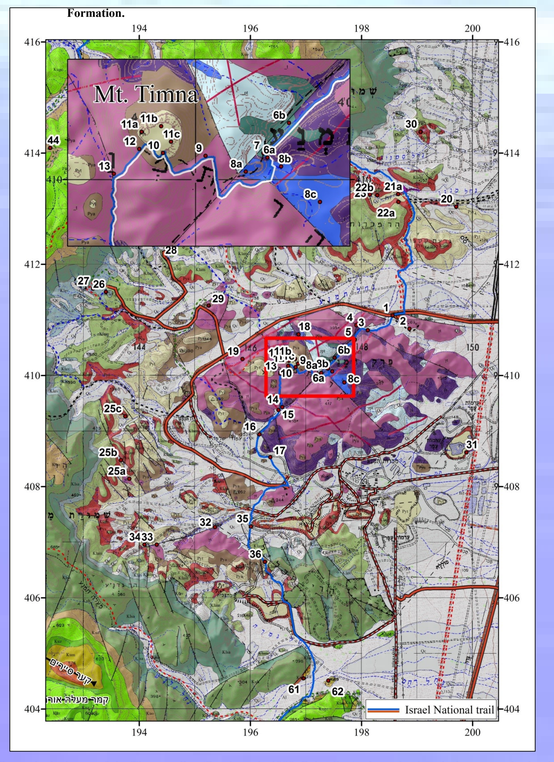

The geological map of the Timna valley (Beyth et al., 1999, Be'er Ora) where the descriptions are submitted in the framework of the following sub-areas: The Timna Igneous Complex (TIC) of Mount Timna (#2-17): The Arches (#26-27) and the Chariots (#28) sites where the ancient cooper mines were found; The Early Cretaceous volcanic activity along Nahal Mangan (#20-23); The Step Faults (#25); "Small Timna" (#30); The "Concealed Lake" (#31); The south-western margins of the Timna Valley (#32-36).

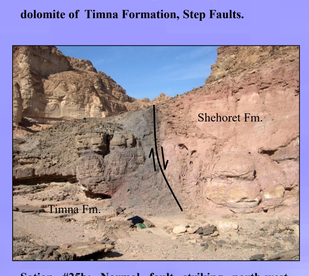

Sation #25b: Normal fault striking north-west-north, Step Faults.

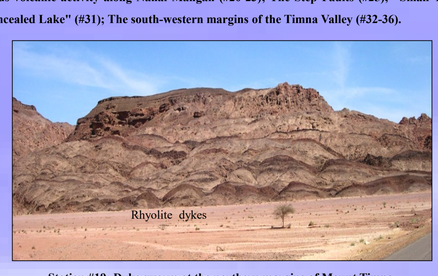

Station #19: Dyke swarm at the northern margins of Mount Timna.

Station #20: Basaltic plug, 100 Ma age, intruding the Timna Formation, Nahal Mangan.

Station #8b: Partly altered olivine-norite.

Station #17: Composite dyke, rhyolite at the center, andesite at both margins.

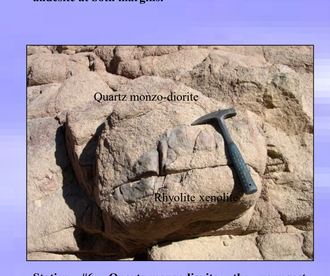

Station #6: Quartz-monzodiorite, the youngest igneous intrusion in the TIC, 600 Ma, with rhyolite xenolith.

The north-westeren highlands

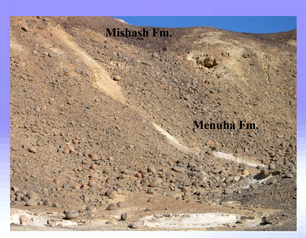

Station #38: Talus of chert and limestone concretions, Sayarim Valley.

Station #39: Limestone concretion vertically tilted along the Milhan Fault.

Station #40: Bir Milhan.

Station #41: Ammonites, mainly *Choffaticeras* and *Vascoceras*, Ora Formation.

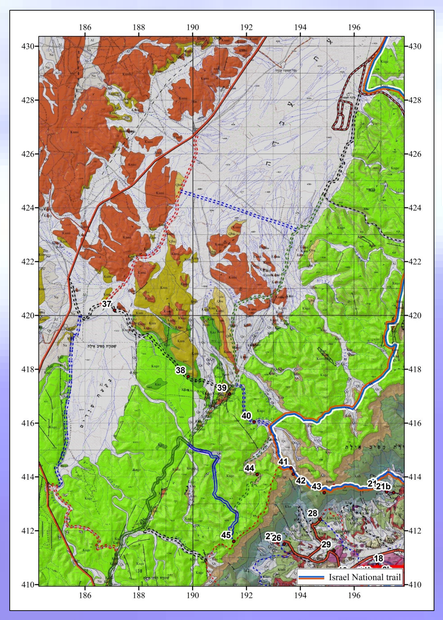

The geological map of the north-western highlands (Ginat, 1991, Yotvata and 2001, Mitzpe Sayyarim; Beyth et al., 1999, Be'er Ora; Segev and Beyth, 2000, Har Seguv). The major subareas are N. Milhan and Mt. Berech.

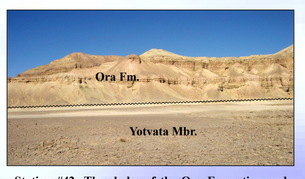

Station #42: The shales of the Ora Formation and the limestone of the Yotvata Member.

Station #43: A view of the Timna Valley from top Yotvata Member, "Zukei Timna" (Timna Cliffs).

Station #44: Well bedded shale, gypsum and sandstone, Ora Formation, Nahal Metek.

Station #45: View of the Timna Valley, the Arava Valley and Edom Mountains from Mount Berech.

Station #43: A view of "Zukei Timna" (Timna Cliffs).

The southern margins

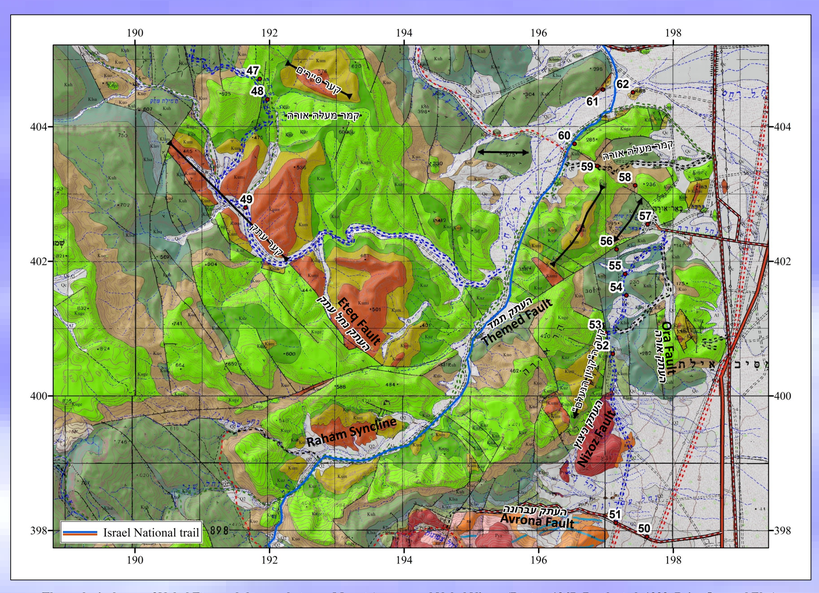

The geological map of Nahal Eteq and the area between Mount Amram and Nahal Nimra (Bartov, 1967; Beyth et al, 1999, Be'er Ora and Elat).

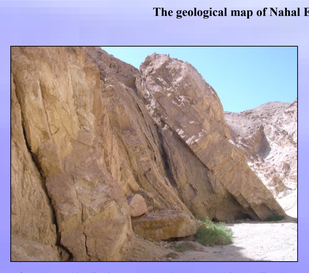

Station #53: Deformation along the Nizoz Fault, Avrona cliffs.

Station #47: Folding of Gerofit limestone beds, "Ezba Elohim", Nahal Eteq.

Station #61: Northern margins of Raham Graben, Nahal Raham.

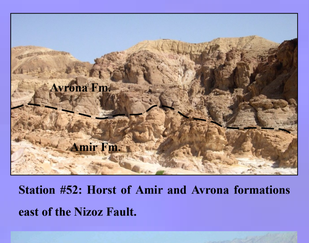

Station #52: Horst of Amir and Avrona formations east of the Nizoz Fault.

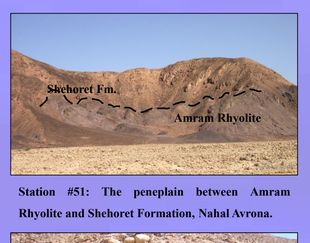

Station #51: The peneplain between Amram Rhyolite and Shehoret Formation, Nahal Avrona.

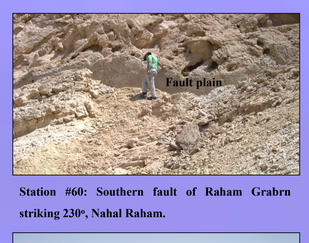

Station #60: Southern fault of Raham Grabrn striking 230º, Nahal Raham.

Station #50: The Givat Zafra syncline formed along the westeren mariginal faults of the DST east of Mt. Amram.

Station #62: Raham Conglomerate, Nahal Raham.

Station #58: Ora anticline, direction of axis east-west.

Station#	Station name:
1	View of Timna Valley from east.
2	Abandoned taluses.
3	River terraces, Nahal Alachson.
4	Sinistral displacement of dykes along a north-west striking fault.
5	Igneous boulders, Nahal Alachson.
6a	Quartz-monzodiorite, the youngest intrusive rock in the TIC.
6b	Xenoliths in the quartz-monzodiorite.
7	Rhyolite dyke with copper mineralization.
8a	Trench in the "Deshe"-altered norite.
8b	Altered norite.
8c	The "Deshe"-altered norite, along a normal fault.
9	Junction of the Israel National Trail and Nahal Alachzon.
10	Mineralization of copper in the Timna Formation.
11	View point from top Mount Timna.
12	West decline from Mount Timna.
13	Early Cambrian peneplain, onlap of Amudei Shelomo and Timna formations.
14	Granodiorite and alkali granite.
15	The dolerite dyke.
16	Junction of Nahal Alachson and Nahal Nehushtan.
17	The composite dyke.
18	Olivine norite.
19	Swarm of dykes.
20	Basaltic plug.
21	The volcanic vents.
22	Prospection pit for manganese.
23	Karstification of the Cambrian dolomite.
24	Avrona Formation.
25	The Step Faults.
26	Burrows, top Amir Formation.
27	The Arches.
28	The Chariots.
29	The Early Cambrian peneplain.
30	"Small Timna".
31	The "concealed Lake".
32	The Alkali granite.
33	Reverse fault.
34	Karstification stripe.
35	Copper quarry.
36	South view point.
37	Bikat Sayarim.
38	Talus of chert concretions.
39	Milhan Fault.
40	Bir Milhan.
41	Ammonites of Ora Formation.
42	Unconformity at the top of Hazera
43	View to Zukei Timna-Timna Cliffs.
44	Nahal Metek.
45	Mount Berech.
46	Maale Sayarim.
47	"Ezba Elohim".
48	Gevei Etek.
49	Etek Syncline.
50	View on Mount Amram from east.
51	Junction of red and black trails.
52	Horst of Amir Formation.
53	Nizoz Fault.
54	Sandstones of Samar Formation.
55	A geological profile from Ora through Mishash formations.
56	The Themed Fault.
57	The evacuated camp of Be'er Ora.
58	Ora anticline.
59	Top Ora Formation.
60	South mariginal fault of Nahal Raham
61	Northern margins of Nahal Raham Graben.
62	Raham Conglomerate.